



UNIVERSITY OF  
BIRMINGHAM

DYNAMIC SIMULATIONS OF CARBON DIOXIDE PIPELINE TRANSPORTATION FOR  
THE PURPOSE OF CARBON CAPTURE AND STORAGE

By

BILAAL YUSUF HUSSAIN

A thesis submitted to the University of Birmingham

For the degree of

ENGINEERING DOCTORATE

Efficient Fossil Energy Technologies Centre

School of Metallurgy and Materials

College of Engineering and Physical Sciences

University of Birmingham

September 2017

UNIVERSITY OF  
BIRMINGHAM

**University of Birmingham Research Archive**

**e-theses repository**

This unpublished thesis/dissertation is copyright of the author and/or third parties. The intellectual property rights of the author or third parties in respect of this work are as defined by The Copyright Designs and Patents Act 1988 or as modified by any successor legislation.

Any use made of information contained in this thesis/dissertation must be in accordance with that legislation and must be properly acknowledged. Further distribution or reproduction in any format is prohibited without the permission of the copyright holder.

## **Abstract**

This Engineering Doctorate project aimed to study the effects of varying flowrates on the flow dynamics of carbon dioxide within a pipeline for the purposes of carbon capture and storage. Understanding the flow dynamics of the carbon dioxide within a pipeline when there are varying inlet flowrates is important in establishing the most appropriate method to operate such a system.

The researched utilised the software tool gCCS to develop models in which three different transport systems were simulated. The first scenario looked at the effects of transporting pure carbon dioxide in both the supercritical phase and the sub-cooled liquid phase. The outputs from the model showed that when the inlet flowrate is decreased, the outlet flowrate responds in three distinct phases. The first phase that occurs has been referred to as the 'delayed response phase', the second phase is the 'offset phase' and the final phase is the 'reduction phase'. The simulations showed that the flowrate difference between the inlet and the outlet of the pipeline during the 'offset phase' was greater when transporting carbon dioxide in the supercritical phase when compared to the sub cooled liquid phase.

The second scenario looked at comparing the effects of three different impurities; hydrogen, nitrogen and oxygen, in the carbon dioxide on the flow response when the inlet flowrate is decreased. It was found that all three impurities caused an increase in the offset between the inlet and outlet flowrate during the 'offset phase'. The largest difference in the flowrates was observed when hydrogen was present.

The third case that was investigated looked at how multiple sources of carbon dioxide effected the flowrate within the main trunk pipeline when the flowrate of one

of the sources was reduced. It was found that multiple sources of carbon dioxide do not affect the flow of within the pipeline beyond that of the base case.

The final part of the research compared real pipeline data from the Shell QUEST pipeline to the model, this enabled validation of the model. It was found that the model was able to predict the flowrate and pressure of the carbon dioxide with good accuracy. Temperature predictions were significantly different from the data and it has been suggested this is due to the restrictions of the thermal conductivity of the surrounding pipeline material in the model.

## **Acknowledgements**

This EngD could not have been done without the help and support of numerous people who provided me with all that I needed to complete the research.

I would firstly like to give greatest thanks to both of my supervisors. My academic supervisor, Professor Joe Wood who helped drive me to do the best that I could do and gave me guidance throughout the project. My Industrial supervisor Den Gammer who is the reason I have had the opportunity to do this project and who I am indebted to for all the help and support he has provided.

Thank you to the Efficient Fossil Energy Technologies doctoral centre, the EPSRC and the Energy Technologies Institute who provided the funding to allow this project to be done. I would also like to thank Andrew Green, Shell Canada and the Canadian Foreign and Commonwealth Office for allowing me to undertake an 8 month placement which enabled the research to reach new heights that would otherwise not have been possible. I would specifically like to thank Stephen Tessarolo at Shell for supporting me while I was undertaking my research in Canada.

All the people at the Energy Technologies Institute for making the entire experience enjoyable.

A special thank you to Shamal Crowther, for always being there for me during the difficult times and uplifting my spirits when I needed it the most and my cousin Hassan who provided me with the support I needed through the most difficult times.

The most important people in allowing me be able to achieve all that I have, my parents, who gave me the love and support I needed to be able to get through my EngD and I will always be grateful to them for all they have given me. My sisters who have always been there for me when I needed them and my nephews and niece who always made me smile when I needed it.

## Table of Contents

Chapter 1	- Introduction.....	1
1.1	Background .....	2
1.2	Research Aims .....	2
1.3	Thesis Outline.....	3
Chapter 2	– Literature Review.....	6
2.1	Introduction.....	7
2.2	Green House Gasses and Global Warming .....	7
2.3	Carbon Capture and Storage.....	8
2.3.1	What is Carbon Capture and Storage? .....	8
2.3.2	Global CCS Projects.....	10
2.4	How CO <sub>2</sub> is Transported .....	11
2.4.1	Methods of Transporting CO <sub>2</sub> .....	11
2.4.2	Vessel VS Pipeline Transport .....	11
2.5	CO <sub>2</sub> Pipeline Modelling .....	16
2.5.1	Economic Modelling of CO <sub>2</sub> Pipelines.....	16
2.5.2	Technical Modelling of CO <sub>2</sub> Pipelines .....	19
2.6	Modelling Tools Evaluation .....	25
2.6.1	Model Requirements.....	25
2.6.2	OLGA .....	28
2.6.3	Aspen HYSYS .....	31
2.6.4	gCCS.....	33
2.7	Conclusion.....	35
Chapter 3	– Comparing Variable Flows For Liquid and Supercritical Phase Carbon Dioxide 39	
3.1	Introduction.....	40
3.2	Hypothesis.....	40
3.3	gCCS Transport Models .....	40
3.3.1	Carbon Dioxide Source Model .....	41
3.3.2	Pipeline and Well Models.....	42
3.3.3	Valve Model.....	46
3.3.4	Distribution Header Model .....	47

3.3.5	Reservoir .....	48
3.4	Carbon Dioxide Pipeline Model Development .....	50
3.5	Simulation Output Analysis .....	54
3.5.1	Liquid Phase Transport.....	54
3.5.2	Supercritical Phase Transport.....	61
3.5.3	Carbon Dioxide Phase Evaluation .....	67
3.6	Conclusion .....	72
Chapter 4	– Effects of Impurities and Multiple Sources of CO <sub>2</sub> on Pipeline Flow .....	75
4.1	Introduction.....	76
4.2	Hypothesis.....	77
4.3	CO <sub>2</sub> with Impurities Case Model Development.....	77
4.3.1	Impurities.....	78
4.4	Results .....	79
4.4.1	Nitrogen Case.....	79
4.4.2	Hydrogen Case.....	83
4.4.3	Oxygen Case.....	85
4.5	Analysis .....	88
4.6	Multiple Sources of CO <sub>2</sub> Model Development .....	89
4.6.1	Pipeline Dimensions .....	89
4.6.2	Pipeline Flows .....	90
4.7	Results .....	91
4.7.1	Flowrate analysis.....	91
4.7.2	Pressure Analysis.....	92
4.7.3	Temperature Analysis.....	93
4.8	Conclusion.....	94
Chapter 5	– Modelling of Shell QUEST CO <sub>2</sub> Pipeline .....	96
5.1	Introduction.....	97
5.1.1	Overview .....	97
5.1.2	The QUEST Carbon Capture Facility.....	98
5.2	Methodology .....	99
5.2.1	Pipeline Details.....	100
5.2.2	Pipeline Operation .....	106
5.2.3	Simulation details .....	107
5.2.4	Data Analysis.....	109



5.2.5	Measurement Devices .....	109
5.2.6	Simulation Periods.....	112
5.3	Initial Model Development.....	116
5.3.1	Topology.....	116
5.3.2	Control Schemes .....	117
5.3.3	Schedule .....	117
5.3.4	Initial Model Analysis .....	120
5.3.5	Secondary Model Development.....	120
5.4	Comparison Between Model and QUEST Data .....	123
5.4.1	Flowrate.....	123
5.4.2	Pressure .....	128
5.4.3	Temperature .....	134
5.5	Determining 'Goodness of Fit' .....	137
5.5.1	Coefficient of Efficiency .....	137
5.5.2	Index of Agreement .....	138
5.6	Conclusion.....	140
Chapter 6	– Conclusions and Future Work.....	142
6.1	Conclusions.....	143
6.2	Future Work .....	149
Appendix A	Simulation Code.....	152
A.1	Code for Base Case and Impurities Case .....	152
Appendix B	Simulation Code.....	153
B.1	Code for Multiple CO <sub>2</sub> Sources Case .....	153
Appendix C	Simulation Code.....	154
C.1	Code for Shell QUEST Simulation for Time Period 24/10/15 – 28/10/15.....	154
C.2	Code for Shell QUEST Simulation for Time Period 31/10/15 – 04/11/15.....	155
C.3	Code for Shell QUEST Simulation for Time Period 08/11/15 – 11/11/15.....	156
References	.....	157

## List of Figures

Figure 2-1: CO <sub>2</sub> Phase Diagram .....	13
Figure 3-1: CO <sub>2</sub> Source Variables .....	41
Figure 3-2: Pipeline Segment Design Variables .....	43
Figure 3-3: Pipeline Segment Heat Transfer Variables .....	45
Figure 3-4: Well Heat Transfer Variables .....	46
Figure 3-5: ESD Valve Configuration .....	47
Figure 3-6: Distribution Header Configuration .....	48
Figure 3-7: Reservoir Configuration .....	49
Figure 3-8: Model Pipeline Topology.....	51
Figure 3-9: Inlet and Outlet Flowrate Profile for Pipeline 1 and 2 .....	56
Figure 3-10: Inlet and Outlet Flowrate Profile for Pipeline 1 and 2.....	57
Figure 3-11: Flowrate Profile along Pipeline001.....	57
Figure 3-12: Inlet and Outlet Pressure for Pipeline 001.....	59
Figure 3-13: Inlet and Outlet Temperature for Pipeline 001.....	60
Figure 3-14: Outlet Flowrate and Outlet Temperature for Pipeline 001 .....	61
Figure 3-15: Inlet and Outlet Flowrate for Pipeline 001 and 002.....	63
Figure 3-16: Inlet and Outlet Flowrate for Pipeline 001 and 002.....	64
Figure 3-17: Flowrate Profile along Pipeline001.....	64
Figure 3-18: Inlet and Outlet Pressure for Pipeline 001.....	65
Figure 3-19: Inlet and Outlet Temperature for Pipeline 001.....	66
Figure 3-20: Inlet and Outlet Flowrate for Liquid and Supercritical CO <sub>2</sub> .....	69
Figure 3-21: Flowrate profile along Pipeline001 for Supercritical and Liquid CO <sub>2</sub> .....	69
Figure 3-22: Inlet and Outlet Pressure for Liquid and Supercritical CO <sub>2</sub> .....	71
Figure 3-23: Inlet and Outlet Temperature for Liquid and Supercritical CO <sub>2</sub> .....	72
Figure 4-1: Pipeline Inlet and Outlet Flowrate (CO <sub>2</sub> + N <sub>2</sub> ).....	80
Figure 4-2: Pipeline Inlet and Outlet Pressure (CO <sub>2</sub> + N <sub>2</sub> ).....	81
Figure 4-3: Pipeline Inlet and Outlet Temperature (CO <sub>2</sub> + N <sub>2</sub> ).....	82
Figure 4-4: Pipeline Inlet and Outlet Flowrate (Pure CO <sub>2</sub> & CO <sub>2</sub> + N <sub>2</sub> ) .....	82
Figure 4-5: Pipeline Inlet and Outlet Flowrate (CO <sub>2</sub> + H <sub>2</sub> ).....	83
Figure 4-6: Pipeline Inlet and Outlet Pressure (CO <sub>2</sub> + H <sub>2</sub> ).....	84
Figure 4-7: Pipeline Inlet and Outlet Temperature (CO <sub>2</sub> + H <sub>2</sub> ).....	84
Figure 4-8: Pipeline Inlet and Outlet Flowrate (Pure CO <sub>2</sub> & CO <sub>2</sub> + H <sub>2</sub> ) .....	85
Figure 4-9: Pipeline Inlet and Outlet Flowrate (CO <sub>2</sub> + O <sub>2</sub> ) .....	86
Figure 4-10: Pipeline Inlet and Outlet Pressure (CO <sub>2</sub> + O <sub>2</sub> ).....	86
Figure 4-11: Pipeline Inlet and Outlet Temperature (CO <sub>2</sub> + O <sub>2</sub> ).....	87
Figure 4-12: Pipeline Inlet and Outlet Flowrate (Pure CO <sub>2</sub> & CO <sub>2</sub> + O <sub>2</sub> ).....	87
Figure 4-13: Pipeline Topology with Multiple Sources of CO <sub>2</sub> .....	91
Figure 4-14: Inlet and Outlet Flowrate for Pipeline 001, Pipeline 002 and Pipeline 003...	92
Figure 4-15: Inlet and Outlet Pressure for Pipeline 001, Pipeline 002 and Pipeline 003 ..	93
Figure 4-16: Inlet and Outlet Temperature for Pipeline 001, Pipeline 002 and Pipeline 003 .....	94
Figure 5-1: QUEST pipeline topography .....	101
Figure 5-2: Pressure sensor.....	111

<i>Figure 5-3: Inlet and Outlet mass flowrate of the Quest pipeline between 07/10/15 and 28/11/15.....</i>	113
<i>Figure 5-4: QUEST pipeline inlet mass flowrate data from 25/10/15 to 28/10/15.....</i>	114
<i>Figure 5-5: QUEST pipeline inlet mass flowrate data from 31/10/15 to 04/11/15.....</i>	115
<i>Figure 5-6: QUEST pipeline inlet mass flowrate data from 08/11/15 to 11/10/15.....</i>	116
<i>Figure 5-7: Initial pipeline model .....</i>	119
<i>Figure 5-8: Simplified QUEST pipeline model .....</i>	122
<i>Figure 5-9: Model and QUEST pipeline inlet and outlet flowrates 24/10/15 – 28/10/15. ....</i>	124
<i>Figure 5-10: Model and QUEST pipeline inlet and outlet flowrates 31/10/15 – 04/11/15.....</i>	124
<i>Figure 5-11: Model and QUEST pipeline inlet and outlet flowrates 08/11/15 – 11/11/15.....</i>	125
<i>Figure 5-12: Quest pipeline inlet and outlet flowrate 24/10/15 - 28/10/15.....</i>	126
<i>Figure 5-13: Quest pipeline inlet and outlet flowrate 31/10/15 - 04/11/15.....</i>	127
<i>Figure 5-14: Quest pipeline inlet and outlet flowrate 08/11/15 - 11/11/15.....</i>	127
<i>Figure 5-15: Model and QUEST pipeline pressures 24/10/15 – 28/10/15.....</i>	129
<i>Figure 5-16: Model and QUEST pipeline pressures 25/10/15 09:00 - 25/10/15 10:30 ...</i>	130
<i>Figure 5-17: Model and QUEST pipeline pressures 26/10/15 12:00 - 27/10/15 12:00 ...</i>	130
<i>Figure 5-18: Model and QUEST pipeline pressures 31/10/15 – 04/11/15.....</i>	131
<i>Figure 5-19: Model and QUEST pipeline pressures 01/11/15 05:00 – 01/11/15 06:30 ..</i>	131
<i>Figure 5-20: Model and QUEST pipeline pressures 02/10/15 14:00 – 02/11/15 21:00 ..</i>	132
<i>Figure 5-21: Model and QUEST pipeline pressures 08/11/15 – 11/11/15.....</i>	132
<i>Figure 5-22: Model and QUEST pipeline pressures 08/11/15 13:30 – 08/11/15 15:00 ..</i>	133
<i>Figure 5-23: Model and QUEST pipeline pressures 09/11/15 14:00 – 10/11/15 00:00 .</i>	133
<i>Figure 5-24: Model and QUEST pipeline inlet and outlet temperatures 24/10/15 – 28/10/15.....</i>	136
<i>Figure 5-25: Model and QUEST pipeline inlet and outlet temperatures 31/10/15 – 04/11/15.....</i>	136
<i>Figure 5-26: Model and QUEST pipeline inlet and outlet temperatures 08/11/15 – 11/11/15.....</i>	137

## List of Tables

<i>Table 2-1: Cost estimates (€/t CO<sub>2</sub>) for commercial natural gas-fired power plants with CCS or coal-based CCS demonstration projects with transported volume of 2.5 Mtpa ...</i>	14
<i>Table 2-2: Cost estimate for large scale networks of 20 Mtpa (€/tonne CO<sub>2</sub>).....</i>	15
<i>Table 2-3: Pre-combustion CO<sub>2</sub> impurities from pulverised coal.....</i>	26
<i>Table 2-4: Post-combustion CO<sub>2</sub> impurities from pulverised coal.....</i>	27
<i>Table 2-5: Oxyfuel combustion CO<sub>2</sub> impurities.....</i>	27
<i>Table 3-1: CO<sub>2</sub> Source Parameters .....</i>	51
<i>Table 3-2: ESD Valve Design Parameters .....</i>	52
<i>Table 3-3: Pipeline Section Design .....</i>	52
<i>Table 3-4: Choke Valve Design .....</i>	52
<i>Table 3-5: Well Design.....</i>	52
<i>Table 3-6: Reservoir Parameters.....</i>	53
<i>Table 4-1: Common Impurities Found in Captured CO<sub>2</sub> .....</i>	79
<i>Table 4-2: Pipeline Dimensions .....</i>	90
<i>Table 5-1: QUEST pipeline details.....</i>	102
<i>Table 5-2: QUEST pipeline dimensions .....</i>	103
<i>Table 5-3: QUEST fluid composition .....</i>	104
<i>Table 5-4: Quest pipeline operating conditions .....</i>	105
<i>Table 5-5: Reservoir Operating Conditions .....</i>	106
<i>Table 5-6: Soil Material &amp; Thermal Conductivities.....</i>	135
<i>Table 5-7: Goodness of fit.....</i>	139

## List of Symbols

### Alphabetic Symbols

$A$	Helmholtz free energy	
$a_1, a_2, a_3$	Adjustable parameters	-
$a_c$	Acentric factor	-
$d$	Index of agreement	-
$D_o$	Outer pipeline diameter	m
$E$	Coefficient of Efficiency	-
$f_D$	Darcy friction factor	-
$F_L$	Location factor	-
$F_T$	Terrain factor	-
$L$	Pipeline length	m
$L_{offshore}$	Offshore pipe length	m
$L_{onshore}$	Onshore pipe length	m
$M$	Mass flowrate	kg s <sup>-1</sup>
$O_i$	Observed value	-
$P_c$	Critical pressure	MPa

$P_i$	Predicted value	-
$q$	Heat energy	J
$R$	Molar gas constant	J mol <sup>-1</sup> K <sup>-1</sup>
$T$	Temperature	K
$T_c$	Critical temperature	K
$T_f$	Fluid temperature	K
$T_o$	Soil temperature	K
$U_o$	Overall heat transfer coefficient	W m <sup>-2</sup> K <sup>-1</sup>
$V$	Volume	m <sup>3</sup>
$\Delta p$	Pressure drop	mPa
$\dot{V}$	Volumetric flowrate	m <sup>3</sup> s <sup>-1</sup>

## Greek Symbols

$\delta$	Reduced density
$\delta_{ij}$	Binary interaction coefficient
$\Theta$	Function
$\tau$	Inverse reduced temperature
$\phi$	Dimensionless Helmholtz free energy
$\phi^o$	Ideal gas behaviour
$\phi^r$	Reduced fluid behaviour

## **Chapter 1 - Introduction**



## **1.1 Background**

Carbon capture and storage (CCS) will be a critical greenhouse gas reduction technology for as long as fossil fuels are widely used [1]. Modelling by the Energy Technologies Institute has found that without CCS the cost of meeting the UK 2050 greenhouse gas targets will double [2]. The development of any CCS capture technology will require an understanding of how the CO<sub>2</sub> is transported. Transportation via pipeline is seen as the most viable option to transfer the CO<sub>2</sub> from the source to the site of sequestration. An awareness of the dynamics of the CO<sub>2</sub> fluid is necessary to ensure the pipeline can be operated in the most economical way.

To develop the knowledge base around CCS, the Efficient Fossil Energy Technologies (EFET) engineering doctorate centre was established, which is a collaboration between the University of Nottingham, Loughborough University and the University of Birmingham along with the Energy Technologies Institute and other industrial partners, with funding from the Engineering and Physical Sciences Research Council. The work presented in this thesis reports the application of a developed modelling tool to simulate a dynamic CO<sub>2</sub> pipeline, so as to represent a real CCS system that is connected to a combined cycle gas turbine power plant.

## **1.2 Research Aims**

The aim of the research is to investigate the effects of variable CO<sub>2</sub> flowrates on the dynamics of the fluid within a CO<sub>2</sub> pipeline used for CCS purposes. To carry out this research, a professionally developed piece of software (gCCS) has been used to simulate the pipeline dynamics. To validate the simulation outputs, industrial data obtained from the Shell Quest CO<sub>2</sub> pipeline has also been utilised.

The research was split into the simulation and then the validation. The simulation looked at three different scenarios, the first scenario examined a base case where pure CO<sub>2</sub> was transported via a single pipeline and investigated the difference between transporting in the supercritical phase and the subcooled liquid phase, the second scenario investigated transporting near pure CO<sub>2</sub> and compares the effects of different impurities on the dynamics of the fluid within the pipeline; the third scenario simulated multiple sources of CO<sub>2</sub> and understanding how changing the flowrate from one source effects the pipeline.

The validation part of the research involved collaboration with Shell Canada, via an eight month long placement at the QUEST project in Fort Saskatchewan, Alberta, with the aim of comparing real CO<sub>2</sub> pipeline data to the simulation outputs and evaluating the accuracy of these outputs.

For each scenario a hypothesis is presented which is either proven or disproven through the research.

### **1.3 Thesis Outline**

The thesis contains six chapters. The first chapter introduces the project and the background of the research along with the aims of the study and an overview of each of the chapters.

The second chapter reports a critical review of the literature and helps to inform the direction of the research and where there are knowledge gaps in the area. The literature covers the broader area of carbon capture and storage and then a more detailed investigation into the area of CO<sub>2</sub> transportation where all types of CO<sub>2</sub> transport are examined. The review then covers the current literature on CO<sub>2</sub>

pipelines, the most economical way of transportation and the modelling and simulation work that has been done which compares the technical differences between supercritical and the subcooled liquid phase in steady state operation. The final part of the literature review addresses which of the current commercially available modelling tools are the most appropriate for the research to be undertaken and is based upon the tools ability to predict the physical properties of CO<sub>2</sub> and near pure CO<sub>2</sub>.

The third chapter provides the details of the process simulation tool that is used and details specifically the units related to pipeline and CO<sub>2</sub> storage and what values are user defined. The development of the simulations of the scenario of a base case pipeline model comparing supercritical and subcooled liquid phase CO<sub>2</sub> are covered. The results from the simulations are then presented and analysed.

The fourth chapter covers two areas of the research, the impacts of impurities on the dynamics of CO<sub>2</sub> flow which looks at the main impurities found within CO<sub>2</sub> from different CCS technologies and the effects of multiple sources of CO<sub>2</sub> on pipeline dynamics. Each scenario is simulated and the results presented and analysed.

The fifth chapter covers the work carried out at the Shell QUEST facility in Canada. The Shell QUEST pipeline is modelled and historical input data from the pipeline is used to develop the simulation. The simulation and the pipeline outlet data are compared and a statistical analysis is carried out to measure the goodness of fit of the model. This chapter allows the model to be validated and identify whether the model produces any unrealistic results.

The sixth and final chapter is the conclusion to the research. This covers all the work in the other chapters and possible future work that can be carried out on CO<sub>2</sub> transportation. This chapter also investigates how the process simulation tool could be updated to give greater accuracy in predicting dynamic CO<sub>2</sub> flows.

## **Chapter 2 – Literature Review**

## **2.1 Introduction**

Carbon capture and storage has been reported to be a technology that will play a dominant role as a greenhouse gas reduction solution for as long as fossil fuels are used [1]. A major part of the technology is the transportation of carbon dioxide from a point source such as a fossil fuelled power station with CO<sub>2</sub> capture to the site of sequestration. This chapter will critically review the current literature on the different methods for CO<sub>2</sub> transportation, the different phases of CO<sub>2</sub>, how CO<sub>2</sub> behaves in pipelines and the current literature on the technical and economic modelling of CO<sub>2</sub> pipelines for the purpose of CCS. This chapter will also inform on the novel contribution of the work that was carried out and that is presented in this thesis.

## **2.2 Green House Gasses and Global Warming**

Carbon Dioxide is known to be a greenhouse gas as its increased concentration in the atmosphere has been found to be linked to an increase in radiative forcing [3], this is the difference between the energy absorbed by the earth and the energy reflected back out of the atmosphere. The increase of the earth's temperature by only a few degrees could have significant impacts on the planet through climate change. It has been found that since the industrial revolution there has been a significant increase in the atmospheric CO<sub>2</sub> concentration due to humans burning fossil fuels, this is known as anthropogenic CO<sub>2</sub> [4]. The United Nations Climate Conference in Paris that was held in 2015 concluded with 195 countries agreeing to a plan to reduce CO<sub>2</sub> and other greenhouse gas emissions, in order to limit the global temperature rise by 2°C [5].

Within the UK, energy supply has been the biggest contributor to greenhouse gas emissions where in 2015 29% of CO<sub>2</sub> emissions could be linked to the energy sector [6]. This therefore makes the energy sector one of the main areas in which greenhouse gas reduction has been targeted. Research carried out by the Energy Technologies Institute has found that Carbon Capture and Storage and Bioenergy are the two main technologies required to reduce the UK's CO<sub>2</sub> emissions from the energy sector [7]. Without either one of these technologies the cost of reaching the 2050 CO<sub>2</sub> reduction targets could increase by 1% GDP [8] which is equivalent to an extra £1000 on annual average household energy bills for energy and transport [2]. This shows that CCS is a crucial technology to ensure an affordable, reliable and low carbon energy system.

## **2.3 Carbon Capture and Storage**

### **2.3.1 What is Carbon Capture and Storage?**

Carbon Capture and Storage (CCS) is a technology that can remove and sequester up to 90% of the carbon dioxide emissions from large point sources, such as fossil fuelled power plants [9]. The CCS technology consists of three distinct processes. Firstly, the CO<sub>2</sub> is captured from the flue gasses that are produced during the burning of fossil fuels. The high purity CO<sub>2</sub> is then transported either via ship or pipeline to the storage location. Finally the CO<sub>2</sub> is then stored deep underground where it is sequestered [10]. The idea behind CCS technology is to prevent the CO<sub>2</sub> from the burning of fossil fuels from entering the atmosphere so that it does not contribute to global warming.

#### *2.3.1.1 CO<sub>2</sub> Capture and Compression*

The capture of CO<sub>2</sub> from large point sources is the first part of the CCS process. There are three main processes that are the main methods of CO<sub>2</sub> capture are, post-combustion capture, pre-combustion capture and oxyfuel combustion [11]. Post-combustion capture is a type of technology where the CO<sub>2</sub> is separated from the flue gasses after the fuel has been combusted. The most mature and economically viable post combustion capture technology is amine-based chemical absorption [12] which has a technology readiness level (TRL) of 9 [13] which indicates it is a mature technology. Other capture methods such as adsorption and membrane technologies have a lower TRL of around 6 [14] which indicates there is still development required to allow these technologies to be ready for industry. Amine based chemical absorption is the only one of the three that can be retrofitted to existing power plants [15]. Pre-combustion capture technology works by the production of syngas from the fuel and capturing the CO<sub>2</sub> from the syngas. After the CO<sub>2</sub> is captured the syngas contains a high concentration of hydrogen which can be used to produce electricity [16]. The most common pre-combustion capture technologies are physical and chemical absorption [16]. The third technology is oxyfuel combustion which is where the fuel is burned in oxygen instead of air, this produces a flue gas consisting mainly of CO<sub>2</sub> and H<sub>2</sub>O [17]. This allows for a less energy intensive separation process compared to the other two technologies.

After the capture process there is the purification of the CO<sub>2</sub> which is followed by the compression of the pure CO<sub>2</sub>. Compression of the carbon dioxide is necessary to enable it to be easily transported and stored in underground geological storage



sites [18]. There are different strategies for CO<sub>2</sub> compression with some of the major ones listed below [19];

- Intercooling compression
- Intercooling compression with subcritical liquefaction and pumping
- Intercooling compression with supercritical liquefaction and pumping
- Shockwave compression

The literature concerning CO<sub>2</sub> compression has reiterated how there has been extensive research and focus on the carbon capture process, as well as injection and monitoring in geological storage sites [18] [19]. This indicates that there has been less focus on CO<sub>2</sub> compression and CO<sub>2</sub> transportation and therefore there are greater opportunities to further the knowledge in these areas.

### 2.3.2 Global CCS Projects

There are currently 22 large-scale CCS projects around the world that are either in operation or under construction, with a combined CO<sub>2</sub> capture capacity of 40 million tonnes per annum [20]. However it should be noted that of the currently operating projects, only two of them are within the energy sector. These are the Boundary Dam project in Saskatchewan, Canada and the Petra Nova project in the United States. The Boundary Dam CCS project began operation in 2014, it is a 115MW power station with a CO<sub>2</sub> capture plant, that is capable of capturing 1.3 million tonnes of CO<sub>2</sub> per annum which is a CO<sub>2</sub> reduction of 90% [21]. The Petra Nova project became operational in January 2017. It is a 240MW power plant that will capture 1.4 million tonnes of CO<sub>2</sub> per annum [22]. There are currently no CCS

project in operation in the UK. In 2015 the UK government cancelled a £1 billion CCS commercialisation project and until 2017 there have been no new proposals for any large scale CCS projects.

## **2.4 How CO<sub>2</sub> is Transported**

### **2.4.1 Methods of Transporting CO<sub>2</sub>**

The method of transport for the captured CO<sub>2</sub> is an important choice when developing carbon capture and storage. There are different factors that need to be considered when deciding on the optimal method of transport. There are two methods in which the pure CO<sub>2</sub> can be transferred to the storage site. The first is through vessels which are filled at the capture facility and then transported through a mixture of land vehicles, barges and ships. The second method of CO<sub>2</sub> transport is via pipeline. There have been numerous studies comparing these two methods from both a technical and economic standpoint. This has given greater knowledge on when and where each of the two transport options should be used as well as the technical aspects relation to each transport method.

### **2.4.2 Vessel VS Pipeline Transport**

#### *2.4.2.1 Technical Comparison*

From the literature there has been identified two parameters that effect which transport method should be used. These are; the volume of CO<sub>2</sub> that is to be transported which is based on an annual value and the distance from the capture facility to the site of sequestration. It should also be noted that the transport method chosen will influence the phase which the CO<sub>2</sub> is transported in. As can be seen in Figure 2-1[23], CO<sub>2</sub> that is transported by vessel should be transported in the

liquid phase. This is because the density is comparably higher in the liquid phase than in the gas phase and therefore a greater mass of CO<sub>2</sub> can be transported per vessel making it more economical than if it is in the gas phase. As a higher density of CO<sub>2</sub> is desirable when transporting via vessel it should be the case that CO<sub>2</sub> be transported in the solid phase, given the density is approximately 1500kg/m<sup>3</sup> and therefore smaller vessels would be required or more CO<sub>2</sub> could be transported. However given the complex loading and unloading procedures this method becomes uneconomical [24]. It has been found that the for economical large scale transport via shipping, the CO<sub>2</sub> should be in a phase close to the triple point of CO<sub>2</sub>, approximately 6.5 bar and -52°C [24]. Transporting CO<sub>2</sub> via pipeline can be done in either the liquid phase or the supercritical phase as can be seen in Figure 2-1 [23].

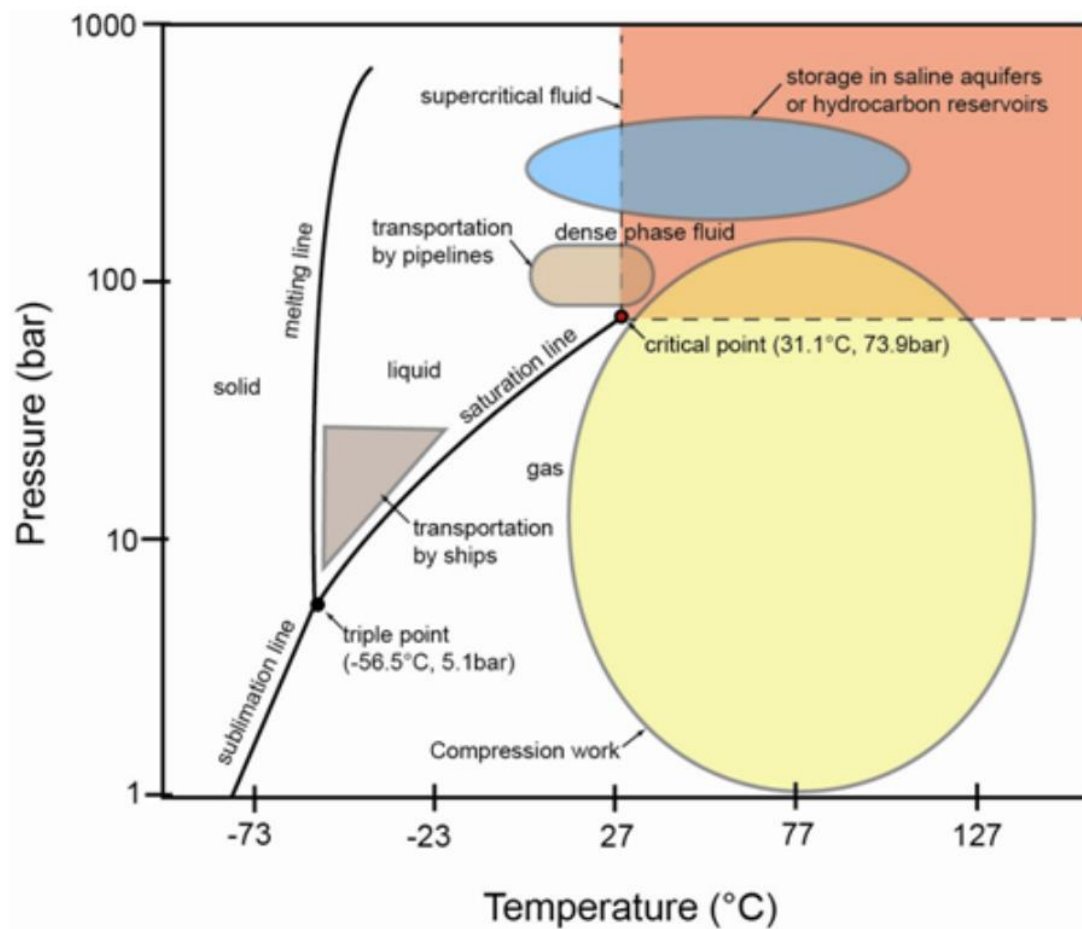


Figure 2-1: CO<sub>2</sub> Phase Diagram

In pipeline transport pressure losses need to be taken into account as this will affect the pumping requirements. Therefore the phase in which CO<sub>2</sub> is transported should be one that reduces pressure losses but also has a relatively high density.

#### 2.4.2.2 Cost Comparison

The deciding factor that dictates what transport option will be used is based around economics. There have been numerous studies comparing the costs of CO<sub>2</sub> transport via pipeline to that of shipping. A study conducted by the Zero Emissions Platform (ZEP) has compared the costs of different transportation methods. Table


2-1 [25] shows estimated costs of onshore pipelines, off shore pipelines and shipping for 2.5 Mtpa of CO<sub>2</sub> at varying distances.

*Table 2-1: Cost estimates (€/t CO<sub>2</sub>) for commercial natural gas-fired power plants with CCS or coal-based CCS demonstration projects with transported volume of 2.5 Mtpa*

Distance km	180	500	750	1500
 Onshore pipeline	5.4	n. a.	n. a.	n. a.
 Offshore pipeline	9.3	20.4	28.7	51.7
 Ship	8.2	9.5	10.6	14.5
 Liquefaction (for ship transport)	5.3	5.3	5.3	5.3

As can be seen in Table 2-1, for distances equal or greater than 500km shipping becomes more economical when compared to pipeline transport. The further the distance for transportation of CO<sub>2</sub> to the storage site, the more economical shipping becomes. The study carried out by ZEP also looked at the costs when transporting 20Mtpa of CO<sub>2</sub> as a comparison to understand how the mass of CO<sub>2</sub> to be transported effects the method which is the most economical. This is shown in Table 2-2.

Table 2-2: Cost estimate for large scale networks of 20 Mtpa (€/tonne CO<sub>2</sub>)

Spine Distance km	180	500	750	1500
 Onshore pipeline	1.5	3.7	5.3	n. a.
 Offshore pipeline	3.4	6.0	8.2	16.3
 Ship (including liquefaction)	11.1	12.2	13.2	16.1

It can be seen that for large masses of CO<sub>2</sub> pipeline transport is the most economical and shipping only becomes the preferable choice when transport distances are equal or greater than 1500km. What can also be seen in Tables 2-1 and 2-2 is that distance has a greater impact on pipeline transport than for shipping.

Other studies have also made similar conclusions in which CO<sub>2</sub> transport via ship is preferable when transporting relatively low volumes across long distances and transport via pipeline is more economical when transporting large volumes over shorter distances [25]. The reasons behind this difference in costs is because developing new pipeline infrastructure comes with high capital costs which can be as much as 90% of the cost of transport whereas capital costs for shipping are approximately 50% of the cost of transportation [26].

Other studies have suggested a strategy for the development of CCS in which transportation will initially be carried out by shipping when the volumes of CO<sub>2</sub> being transported are relatively low. When CCS uptake increase then there will be a switch to pipelines due to the greater volumes of CO<sub>2</sub> [25]. This strategy however is

not one that has been proposed in many CCS projects. Both CCS projects that were proposed in the UK for the CCS competition used onshore and offshore pipelines for CCS transport. The Peterhead project that was proposed by Shell suggested that current pipeline infrastructure that has until recently been used for natural gas could be reused for CO<sub>2</sub> transport [27]. The theory behind developing single pipelines for single source to storage usage is that the pipelines would be oversized. This would then promote the further development of CCS in the area which would lead to the creation of CCS 'hubs' as the oversized pipeline can be used by multiple users and hence reduce the cost of transportation.

## **2.5 CO<sub>2</sub> Pipeline Modelling**

From the analysis of the literature comparing CO<sub>2</sub> transport by vessel to that of pipeline it can be clearly seen that pipeline transport is the preferred choice for CCS both in the short term, shown by the current projects in operation and the long term, shown by the economic benefits of pipeline transport when large volumes of CO<sub>2</sub> are transported. Given this evaluation it is therefore necessary to have a comprehensive understanding of CO<sub>2</sub> pipeline transport for the purposes of CCS. This is crucial knowledge in developing safe and economic CO<sub>2</sub> pipelines which can also be operated efficiently. The analysis of the current literature on CO<sub>2</sub> pipelines can be separated into economic analysis and technical analysis.

### **2.5.1 Economic Modelling of CO<sub>2</sub> Pipelines**

Economic modelling of CO<sub>2</sub> pipelines is necessary to understand costs and how these costs compare with the rest of the CCS process. Economic models can also inform investment decisions and the economic viability of a project. The cost of a

CO<sub>2</sub> pipeline has been found to be highly dependent on the design capacity of the pipeline and the pipe length. This is shown in one study in which the model simulation results showed an increase in costs from US \$1.16/tonne to US\$2.23/tonne of CO<sub>2</sub> when the design capacity was reduced from 5 million tonnes per year to 2 million tonnes per year [28]. The same study also showed that an increase in the length of the pipeline from 100km to 200 km increases costs further to US\$ 4.06/tonne of CO<sub>2</sub>. A more detailed model developed by the IEA GHG found similar results which show that an increase in the diameter of the pipeline and hence an increase in the capacity, increases the overall capital cost of the pipeline but will decrease the cost of the pipeline per tonne CO<sub>2</sub> [29]. This study by the IEA GHG goes into further detail to look at the costs related to pumping stations. It found that for onshore pipelines it is more economic to use booster stations to maintain the pressure than to operate large low pressure drop pipelines. However when considering offshore pipelines it was found to be more economic to pressurise the CO<sub>2</sub> at the shore to the point where the pressure in the pipeline will not fall below 90 barg and then only pressurise again at the sequestration site.

There is limited cost data on CO<sub>2</sub> pipelines even though there are over 6500km of CO<sub>2</sub> pipelines in the united states alone [30] many of the pipeline developers keep such information out of the public domain. The models that predict pipeline costs, generally use diameter calculations which can be applied to various pipelines universally however developing a single cost equation to accurately evaluate pipeline costs for all locations and regulatory structures around the world is not practical [31].



This makes it difficult to validate the cost models that have been developed. However it has been argued that the available capital cost data for natural gas pipelines is valid for construction costs which is generally independent of the fluid being transported [31]. Using this data, simple regression analysis can be carried out to develop equations that can be used for CO<sub>2</sub> pipelines. Equation 2-1 was developed by the IEAGHG [32] for the onshore pipeline costs with the addition of the location factor  $F_L$ . The location factor is used to account for different economic locations while the terrain factor  $F_T$  allows for the equation to take into account cost inflation caused by complex terrains such as mountainous or populated areas[33]. The value of the location factor is assumed to be 1.00 for the USA, Canada and Europe while the value of 1.2 has been used for the UK. The terrain factor varies for different land types for instance a value of 1.00 is used for grassland, 1.05 for woodland and 1.10 for cultivated land[31]. The constants in equation 2-1 were developed through the use of a pipeline cost model[34];

$$\begin{aligned} \text{Pipeline Capital Cost}_{onshore} &= F_L \times F_T \times 10^6 \\ &\times \left[ (0.057 \times L_{onshore} + 1.8663) + (0.00129 \times L_{onshore}) \times D_o \right. \\ &\left. + (0.00486 \times L_{onshore} - 0.000007) \times D_o^2 \right] \end{aligned}$$

*Equation 2-1: Capital Cost Equation for Onshore Pipelines*

The IEAGHG also developed a formula for offshore pipeline costs;

$$\begin{aligned}
\text{Pipeline Capital Cost}_{offshore} &= F_L \times 10^6 \\
&\times [(0.4048 \times L_{offshore} + 4.6946) \\
&- (0.00153 \times L_{offshore} + 0.0113) \times D_o \\
&+ (0.000511 \times L_{onshore} + 0.00024) \times D_o^2]
\end{aligned}$$

*Equation 2-2: Capital Cost Equation for Offshore Pipelines*

These formula for pipeline costs have been said to be only useful for estimates for pipeline costs and should only be used in feasibility and possibly FEED studies [31].

### 2.5.2 Technical Modelling of CO<sub>2</sub> Pipelines

A greater understanding of the technical parameters of a CO<sub>2</sub> pipeline is necessary to ensure the safe operation of such a system. It has already been mentioned that there are thousands of kilometres of CO<sub>2</sub> pipelines in the USA however given the confidential information with regards to these pipelines their technical performance is not publicly available. Therefore there has been a development of CO<sub>2</sub> pipeline models to understand the performance of potential pipeline systems.

#### 2.5.2.1 Pipeline Depressurisation Modelling

Health and safety is of extreme importance when considering the development of a CO<sub>2</sub> pipeline system. An incident related to a pipeline in which there is loss of containment is extremely dangerous given that it could impact on the public, as CO<sub>2</sub> has a greater density than air, a release of CO<sub>2</sub> could cause a blanket effect with the potential to cause asphyxiation. Therefore, modelling to assess the consequences of a pipeline rupture will allow for improved safe operation and design of the pipeline. The modelling of the decompression and the discharge rate

of the CO<sub>2</sub> helps determine the minimum safe distance to populated areas, emergency response planning and optimum spacing of emergency shut down valves [35]. Some of the models developed to investigate the release of CO<sub>2</sub> have also been validated through experimental results [35] [36]. The validation of such models allows for greater accuracy of the outputs. One consideration that these models do not take into account is the presence of impurities in the CO<sub>2</sub>. It has been identified that there is insufficient knowledge to enable the correct predictions for depressurisation of CO<sub>2</sub> with impurities [37] however it has been argued that the inclusion of impurities is very important [38]. It has been found that concentrations of N<sub>2</sub> greater than 1 mole% have significant changes on the depressurisation thermodynamic trajectory [39].

#### *2.5.2.2 CO<sub>2</sub> Phase Modelling*

As previously mentioned, the phase of CO<sub>2</sub> when it is transported is important. There is agreement in the literature that CO<sub>2</sub> will be transported in either the subcooled liquid or the supercritical phase [40] given that transporting in the gas phase is less economic due to the large energy requirements for moving the fluid. There has been significant research into whether the liquid phase or the supercritical phase is the optimal for transportation of CO<sub>2</sub>. One such study used ASPEN PLUS 10.1 to simulate and compare the efficiency and costs of transport of CO<sub>2</sub> in the supercritical phase to the liquid phase [41]. It was found that CO<sub>2</sub> in the subcooled liquid phase is ideal for colder climates where energy savings of up to 9% are feasible. For warmer climates refrigeration units may be economical to ensure the temperature stays below the critical temperature. It is not only economic reasons that transporting in the subcooled liquid phase have been found to be

beneficial over the supercritical phase. One study which compared transporting CO<sub>2</sub> in the liquid phase to the supercritical phase used Aspen to model the safe distance before choked flow occurs, it found that the lower the inlet temperature to the pipeline the longer the distance before choking occurs and therefore a longer distance before recompression of the CO<sub>2</sub> is required. This indicates that the subcooled liquid phase provides greater safety in that choked flow occurs at longer distances than in the supercritical phase [42]. While these modelling and simulation studies have indicated that transporting CO<sub>2</sub> in the subcooled liquid phase has both economic and safety benefits, much of the research in the modelling of CO<sub>2</sub> pipelines has done so in the supercritical phase. This may be due to CO<sub>2</sub> being less likely to form bubbles in the supercritical phase, which minimises cavitation problems occurring in components such as booster stations and pumps [43]. There is also the benefit that if the pressure were to fall to the point where phase change were to occur in the pipeline, the change from supercritical phase to the gas phase is less extreme in that there is a smaller density change than from the liquid phase to the gas phase. This is because the supercritical phase is an intermediate phase between liquid and a gas.

#### *2.5.2.3 Steady State Transport Modelling*

Technical models of CO<sub>2</sub> can be separated into steady state and dynamic. Steady state models assess the technical parameters of a CO<sub>2</sub> pipeline with a steady flow of CO<sub>2</sub>. This would be the case when a power plant is operating at base load, where the power output from the plant is constant and therefore the CO<sub>2</sub> output from the plant would also be constant. Modelling of steady state CO<sub>2</sub> pipelines vary depending on the modelling tool used and the assumptions made around the design

and operation of the pipeline. Research has been carried out that looked at how the pressure, temperature, density and flow velocity changed along the length of a 150km pipeline for 5 different scenarios [44], these were simulated in the modelling tool MATLAB/Simulink where algorithms were developed for the simulation of the CCS system described, the scenarios looked at;

1. Transport and injection; maintaining minimum pressure at the end of the pipeline above 85 bar;
2. Transport and injection; ensuring the pressure at the bottom of the well is less than the maximum pressure;
3. Transport, pre-conditioning and injection; avoiding two-phase flow in pipeline and well;
4. Transport and injection, alternative conditioning measures;
5. Influence of impurities on transport and storage.

The results from scenario 1 show that the inlet pressure to the pipeline must be a minimum of 98 bar to ensure an exit pressure of 85 bar. The CO<sub>2</sub> temperature decreased along the length of the pipeline and as a result the density increased which meant that the flow velocity also decreased. These results were observed in all scenarios with slight variation of the inlet pressure and the profile of the observed variables along the length of the pipeline. It was found that for near pure CO<sub>2</sub> with impurities of O<sub>2</sub> and N<sub>2</sub> the density of the fluid is lower, where at 40°C the density is approximately 60% of pure CO<sub>2</sub> [45]. This therefore results in lower storage potential and higher pressure drops.

#### *2.5.2.4 Dynamic Transport Modelling*

Carbon capture and storage can also be applied to combined cycle gas turbine plants (CCGT's). These plants are mainly used as load following power plants. Therefore the output from these plants varies over time. These types of power plants are used for this application as they have relatively fast response times and therefore can provide power when the demand increases. As the load factor changes the emissions will also change, this means that the flow of CO<sub>2</sub> entering the pipeline will vary. It is therefore necessary to understand how the variability in flowrate will affect the operation within the pipeline and whether there are consequences which may require extra measures of control. Dynamic models are used to simulate how certain variables change over time. In the case of CO<sub>2</sub> pipelines, dynamic models simulate the change in the inlet flow of CO<sub>2</sub>. Simulations of dynamic CO<sub>2</sub> pipelines has been carried out using the software tool Modelica within the Dymola environment [46]. The researchers modelled a 30km pipeline transporting supercritical CO<sub>2</sub> to a 1.2km depth well. Simulations were developed to study the effect of load change in which the mass flow was varied to 90%, 15%, 105% and 50% of the nominal reference load of 100kg/s. The study concluded that there was considerable risk of the occurrence of two phase flow in the well and that preventative measures will be required to help avoid two phase flow. This study considered exclusively supercritical CO<sub>2</sub> therefore the results from sub-cooled liquid CO<sub>2</sub> could be drastically different, however such a study has not been found within the literature. This study also contained a flaw in that it did not allow the flowrate at the end of the pipeline to reach the setpoint before another change to the setpoint

was made, this means that a complete understanding of the impacts of making a change in the flowrate was not established.

#### *2.5.2.5 Multiple Sources of CO<sub>2</sub>*

As previously mentioned, the long term development of CO<sub>2</sub> pipeline transport is expected to form around CCS hubs. These hubs are expected to develop to allow the sharing of infrastructure between different sources of CO<sub>2</sub>. By doing this the cost of CCS can be reduced. The idea is that there will be a main trunk pipeline that is initially oversized and transports the CO<sub>2</sub> to the sequestration site. The producers of the CO<sub>2</sub> will each have smaller pipelines which connect them to the trunk pipeline. However the dynamics of such a system may be significantly different from a single source pipeline as the flowrate from one capture site may be constant while the other may vary. It will be necessary to understand how to operate the trunk pipeline where both these flows merge. One such study has considered steady state modelling of multiple sources of CO<sub>2</sub> [47]. The study was based on real proposals of two CCS projects in the Humber region. The first project is known as the Don Valley Power Project, which is a 650 MW Integrated Gasification Combined Cycle (IGCC) power plant [48]. The second proposal is known as the White Rose project, which is a 426 MW oxyfuel power plant [49]. This study used Aspen HYSYS to model a system with a collecting pipeline for each of the CO<sub>2</sub> sources which join onto an onshore trunk pipeline, which leads to an offshore pipeline. One of the main technical findings from the study was that as the higher the velocity of the CO<sub>2</sub> the higher the pressure drop along the pipeline and hence greater boosting pressure at the pump station before the off shore pipeline. The fluid within the pipeline is in the subcooled liquid phase. The study doesn't consider transportation within the

supercritical phase and doesn't consider dynamic flows of CO<sub>2</sub>, both of which are possible scenarios in the development of CCS hubs.

## **2.6 Modelling Tools Evaluation**

### **2.6.1 Model Requirements**

#### *2.6.1.1 Model Inputs and Outputs*

Before the analysis of the different software packages, it is necessary to make clear what is needed from the model. The tool should have the option to vary parameters with time. For this research the ability to vary the flowrate of CO<sub>2</sub> to the inlet of a pipeline is of crucial importance and is the basis of the work that is presented. For the design of the pipeline it is necessary to be able to define the pipeline geometry, heat transfer properties and the elevation. The output data from the simulations should show the fluid temperature, pressure, density and flowrate at any point within the pipeline. This allows for the phase of the fluid in the pipeline to be determined and hence whether any phase boundaries are crossed within the pipeline.

#### *2.6.1.2 Model Calculations*

Since the research is investigating CO<sub>2</sub> pipelines for CCS purposes it is important that the fluid entering the pipeline is equivalent to that which is expected from a CCS capture plant. There has been some experimental work carried out, which has considered the effects of impurities on the physical properties of CO<sub>2</sub>. The impurities that are of most concern for CO<sub>2</sub> transport and storage purposes are dependent on the technology used in the CO<sub>2</sub> capture process. For pre-combustion carbon capture the main impurities are nitrogen and hydrogen, due to the fact that pre



combustion is used for coal or biomass gasification which produces a stream comprising of mainly CO<sub>2</sub> and H<sub>2</sub>. Table 2-3 [50] shows the main components within a stream of gas captured using different pre-combustion technologies.

Table 2-3: Pre-combustion CO<sub>2</sub> impurities from pulverised coal

	[6] ‡	[7] Selexol	[8] Rectisol®	[9] SEWGS*	[10, 11-14] †
CO <sub>2</sub> % v/v	98	98.1	95-98.5	> 99	
N <sub>2</sub> % v/v	≤ 0.9	0.0195	< 1	< 1	0.0195
H <sub>2</sub> % v/v	≤ 1	1.5	0.002	< 1	2.4
Ar ppmv	≤ 300	178	150	< 1	1000
H <sub>2</sub> O ppmv	10 – 600	378	0.1 – 10	500	5.07
H <sub>2</sub> S/COS ppmv	≤ 100	1700	0.2 – 20	1 – 5000	5968
CH <sub>4</sub> ppmv	100	112	100	< 1	
CO ppmv	400	1300	400	< 1	1667
CH <sub>3</sub> OH ppmv	200	-	20 – 200		
Ash ppm		1.2			
NH <sub>3</sub> ppmv		38			
Cl ppmv		17.5			
Hg ppbv		0.068			1.1
As ppmv		0.0033			0.01
Se ppmv		0.01			0.017
NO ppmv					400
SO <sub>2</sub> ppmv					25
Ni ppmv					0.009
Pb ppmv					0.0045
Benzene ppmv					0.014
Napthalene ppmv					0.0008

For post combustion carbon capture technologies the main impurity is nitrogen, which is due to the burning of either coal or natural gas with excess air. The impurities in a stream of gas from a post combustion capture technologies can be seen in Table 2-4. Table 2-4 shows that for both amine PC plant and an MEA PC plant the amount of Nitrogen within the CO<sub>2</sub> stream is between 0.045 and 0.18 % v/v.

Table 2-4: Post-combustion CO<sub>2</sub> impurities from pulverised coal

	[6] Amine PC plant	[7] MEA PC plant	[10, 11-14] French CO <sub>2</sub> Club †
CO <sub>2</sub> % v/v	99.8	99.7	N.I.
N <sub>2</sub> % v/v	0.045 (+Ar)	0.18	N.I.
CO ppmv			10
Ar ppmv		22	210
H <sub>2</sub> O ppmv	100	640	N.I.
NO <sub>x</sub> ppmv	20	1.5 (NO <sub>2</sub> )	38.8
SO <sub>x</sub> ppmv	10	< 1 (SO <sub>2</sub> )	67.1 (SO <sub>2</sub> )
CO ppmv	10		10
O <sub>2</sub> ppmv	150	61	N.I.
Cl ppmv		0.85	
Ash ppm		11.5	
Hg ppmv		0.00069	0.0028
As ppmv		0.0055	0.0022
Se ppmv		0.017	0.0122
Mn ppmv			0.0309
Ni ppmv			0.002
Pb ppmv			0.0011
Benzene ppmv			0.019
Napthalene ppmv			0.0012

In oxyfuel combustion technology the main impurities are oxygen, nitrogen and argon. The presence of oxygen is due to the burning of the fuel in pure oxygen. The levels of these impurities can be seen in Table 2-5.

Table 2-5: Oxyfuel combustion CO<sub>2</sub> impurities

	Oxyfuel Combustion		
	Raw / dehumidified	Double flashing	Distillation
CO <sub>2</sub> % v/v	74.8-85.0	95.84-96.7	99.3-99.4
O <sub>2</sub> % v/v	3.21-6.0	1.05-1.2	0.01-0.4
N <sub>2</sub> % v/v	5.80-16.6	1.6-2.03	0.01-0.2
Ar % v/v	2.3-4.47	0.4-0.61	0.01-0.1
NO <sub>x</sub> ppmv	100-709	0-150	33-100
SO <sub>2</sub> ppmv	50-800	0-4500	37-50
SO <sub>3</sub> ppmv	20	-	20
H <sub>2</sub> O ppmv	100-1000	0	0-100
CO ppmv	50	-	50
H <sub>2</sub> S/COS ppmv			
H <sub>2</sub> ppmv			
CH <sub>4</sub> ppmv			

For the modelling of CO<sub>2</sub> streams it is important for the modelling tools underlying equations of state to be able to determine the physical properties of the following mixtures; CO<sub>2</sub>+N<sub>2</sub>, CO<sub>2</sub>+O<sub>2</sub> and CO<sub>2</sub>+H<sub>2</sub>. This is necessary, to ensure that modelling of CO<sub>2</sub> streams from the different capture technologies is possible with a high degree of accuracy, as it is known that the presence of these impurities has significant impact upon the physical properties of a CO<sub>2</sub> rich stream. Experimental studies to determine the physical properties of a CO<sub>2</sub> rich stream containing O<sub>2</sub>, Ar and N<sub>2</sub> have shown that there is an increase in pressure of 3000-5000 kPa for the single liquid phase region. This is accompanied by an increase in density of as much as 35% at the same temperature and pressure of pure CO<sub>2</sub> [50].

Other impurities which are found in CO<sub>2</sub> from different capture technologies and are in lower quantities include SO<sub>x</sub>, NO<sub>x</sub> and H<sub>2</sub>O which can be seen in tables 2-3, 2-4 and 2-5, these impurities are present in quantities of PPM. Some studies have suggested that because these impurities are significantly low especially when the water content is below the solubility limit for pure CO<sub>2</sub> the corrosion rates are likely to be sufficiently low[51, 52].

## 2.6.2 OLGA

### 2.6.2.1 Software Background

OLGA is a tool that is traditionally used to simulate the transport of oil, water and gas as well as mixtures of these components. [53]. It is used for simulating multiphase systems and has the ability to model a pipeline system from reservoir pore to process facility [54]. OLGA has been used extensively in the petrochemical industry by companies such as British Petroleum. One case study using OLGA resulted in BP saving 12 days of downtime and 6000m<sup>3</sup> of diesel, this was done by

conducting a scenario in OLGA to identify alternative restarting methods for the pipeline that uses less diesel. [55]. This shows the impact that simulation tools can have on the decisions made by large organisations and the economic benefits that modelling can provide.

#### 2.6.2.2 Equations of State

For CO<sub>2</sub> transport OLGA uses the Span and Wagner equations of state to determine the thermodynamic properties of CO<sub>2</sub> at different temperatures and pressures [56]. The Span and Wagner equation of state has been developed for pure CO<sub>2</sub> and has the ability to determine thermodynamic properties up to 30MPa and 523K. This covers the range in which normal transportation of CO<sub>2</sub> occurs so is therefore valid to use for CO<sub>2</sub> pipeline modelling. Within this temperature and pressure region the uncertainty of the equation ranges from  $\pm 0.03\%$  to  $\pm 0.05\%$  for the density,  $\pm 0.03\%$  to  $1\%$  in the speed of sound and  $\pm 0.15\%$  to  $1.5\%$  in the isobaric heat capacity.

The Span and Wagner equation of state is expressed as the dimensionless Helmholtz free energy as shown by equation 2-3. If an expression for the Helmholtz free energy and its derivatives are known then all other thermodynamic properties can be derived from the expression [57].

$$\phi(\tau, \delta) = \phi^0(\delta, \tau) + \phi^r(\delta, \tau)$$

*Equation 2-3: Dimensionless Helmholtz Energy*

The Helmholtz function  $\phi = A/(RT)$  is split into an ideal gas part  $\phi^0$ , and a residual part  $\phi^r$ .

The Span and Wagner equation of state expresses the ideal part of the equation as;

$$\phi^0(\tau, \delta) = \ln(\delta) + a_1^0 + a_2^0 \tau + a_3^0 \ln(\tau) + \sum_{i=4}^8 a_i^0 \ln[1 - e^{(-\tau \theta_i^0)}]$$

*Equation 2-4: Helmholtz Energy Ideal Gas Property*

The residual part is expressed in equation 2-5 and represents the compressibility of the fluid[58];

$$\begin{aligned} \phi^r(\tau, \delta) = & \sum_{i=1}^7 n_i \delta^{d_i} \tau^{t_i} + \sum_{i=8}^{34} n_i \delta^{d_i} \tau^{t_i} e^{-\delta^{c_i}} + \sum_{i=35}^{39} n_i \delta^{d_i} \tau^{t_i} e^{(-\alpha_i(\delta-\varepsilon_i)^2 - \beta_i(\tau-\gamma_i)^2)} \\ & + \sum_{i=35}^{39} n_i \Delta^{b_i} \delta e^{(-C_i(\delta-1)^2 - D_i(\tau-1)^2)} \end{aligned}$$

*Equation 2-5: Helmholtz Energy Residual*

#### 2.6.2.3 Modelling of CO<sub>2</sub> Rich Mixtures

The Span and Wagner equation of state was developed specifically for determining the thermodynamic properties of pure CO<sub>2</sub>. There have been found to be no studies on the use of the Span and Wagner equation of state for CO<sub>2</sub> rich mixtures. Its use in this way would be inappropriate given that the properties of CO<sub>2</sub> rich mixtures are different from just pure CO<sub>2</sub>. Because of this, the use of OLGA for these types of systems would give inaccurate results and hence not be sensible to use for the modelling of CO<sub>2</sub> pipelines.

### 2.6.3 Aspen HYSYS

#### 2.6.3.1 Equations of State

For CO<sub>2</sub> pipeline modelling Aspen HYSYS has numerous different packages using various equations of state. Previous studies have decided on using the cubic equations of state, Peng Robinson as the method of determining the thermodynamic properties of CO<sub>2</sub> within the pipeline [59]. The P-R equation of state is given by equation 2-6.

$$P = \frac{RT}{V - b} - \frac{a(T)}{V(V + b) + b(V - b)}$$

Equation 2-6: Peng-Robinson Equation of State

For pure components, the terms a and b are expressed using critical properties and acentric factors;

$$a(T) = a_c \alpha$$

$$a_c = 0.45724 \frac{R^2 T_c^2}{P_c}$$

$$\alpha^{1/2} = 1 + \kappa \left( 1 - T_r^{1/2} \right)$$

$$\kappa = 0.32464 + 1.54226\omega - 0.26992\omega^2$$

$$b = 0.07780 \frac{RT_c}{P_c}$$

For mixtures of components the terms a and b are expressed as follows

$$a = \sum_i \sum_j x_i x_j (1 - \delta_{ij}) a_i^{1/2} a_j^{1/2}$$

$$b = \sum_i x_i b_i$$

The term  $\delta_{ij}$  is the binary interaction coefficient and is determined experimentally.

#### 2.6.3.2 Pure CO<sub>2</sub>

A study investigated the accuracy of different models at predicting the vapour-liquid equilibrium of CO<sub>2</sub> found that the Peng-Robinson Equation of state was capable of predicting the VLE data accurately. However this study also shows that there is deviation of the model when the temperature approaches the critical pressure.

A study simulated a scenario in which pure CO<sub>2</sub> within a pipeline enters the gas-liquid two phase region in which liquid hold-up occurs [60]. It was found that the Peng-Robinson equation of state diverged from the actual values of pressure, temperature and hold-up at the outlet of the pipeline, indicating that for pure CO<sub>2</sub> there are situations in which Peng-Robinson cannot be used. It has been explicitly written that the poor agreement of the Peng Robinson equation of state with the density measurements of pure CO<sub>2</sub> near the critical pressure is unacceptable and that variants of the Peng-Robinson model also suffer the same limitations. The explanation behind this is due to the model being developed for separation of mixtures of natural gas where CO<sub>2</sub> is a minor additive [61].

#### 2.6.3.3 CO<sub>2</sub>-rich Mixtures

Studies have been carried out to determine the accuracy of the Peng-Robinson equation of state for some of these mixtures. A study that investigated the ability of the Peng-Robinson equation of state to predict the phase behaviour of both a CO<sub>2</sub>-N<sub>2</sub> and a CO<sub>2</sub>-H<sub>2</sub> mixture found that there is good agreement between the model with the experimental data. However this study also found that the model failed

marginally in the critical region [62]. This finding is crucial in determining which software is most appropriate to use for the research, as the transportation of CO<sub>2</sub> can occur in the supercritical phase so there are possibilities that the CO<sub>2</sub> could approach the critical region within the pipeline.

#### 2.6.4 gCCS

##### *2.6.4.1 Software Background*

gCCS is the newest of the three modelling tools to be evaluated for the use of the research. It was developed by Process Systems Enterprise for the specific purpose of modelling a full chain CCS system, from power plant all the way through to sequestration. It is based upon the gPROMS platform and uses the gSAFT tool to calculate the properties of CO<sub>2</sub>. gSAFT uses statistical associating fluid theory (SAFT) as the method to determine the thermodynamic and the phase equilibrium properties of fluids.

##### *2.6.4.2 Equations of State*

SAFT is based upon Wertheim's theory of Helmholtz energy expansion. It is known as thermodynamic perturbation theory. In this method the Helmholtz free energy is calculated from graphical summation of interactions of different species [63]. The SAFT equation of state can also be developed for determining the properties for mixtures of fluids, through a simple extension of the model. Unlike cubic equations of state e.g. Peng-Robinson, SAFT does not require experimental data to produce good approximations of fluid properties of mixtures.

##### *2.6.4.3 Pure CO<sub>2</sub>*

Previous research on the ability of SAFT equations of state to determine CO<sub>2</sub> properties has been carried out. One such study looked at the ability of SAFT EoS



to determine the vapour liquid equilibrium data and the second derivative thermodynamic properties of various components related to carbon capture and storage. These components included  $\text{CO}_2$ ,  $\text{H}_2\text{S}$ ,  $\text{N}_2$ ,  $\text{H}_2\text{O}$ ,  $\text{O}_2$  and  $\text{CH}_4$ . The properties that were calculated within this study include the isobaric and isochoric heat capacity, speed of sound, Joule-Thomson coefficient and isothermal compressibility. It was found that the model is able to calculate the vapour pressure and the liquid density of pure  $\text{CO}_2$  with good accuracy in both the sub-critical and the super critical regions, however similar to the Peng-Robinson the accuracy of the model decreases closer to the critical region. This again could pose some problems when modelling CCS processes as there is possibility that the fluid may approach the critical region [64].

#### *2.6.4.4 $\text{CO}_2$ Mixtures*

There is currently limited literature on the use of SAFT equations of state for predicting the fluid properties of  $\text{CO}_2$  rich mixtures that include the components that are expected in CCS processes. Research carried out on using SAFT equations to predict the phase equilibrium of  $\text{CO}_2$ - $\text{H}_2\text{O}$  mixtures concluded that there was satisfactory agreement between the calculated and the experimental values [65]. There was found to be no literature on the ability of SAFT equations to accurately determine the fluid properties of mixtures of  $\text{CO}_2$ - $\text{H}_2$ ,  $\text{CO}_2$ - $\text{O}_2$  and  $\text{CO}_2$ - $\text{N}_2$ . This limits the ability to critically evaluate the gCCS modelling tool for  $\text{CO}_2$  pipeline transport, however in comparison to the Span and Wagner and Peng-Robinson equations of state SAFT is known to have a greater accuracy in modelling fluid mixtures [66], especially when there is an absence of experimental data which is required for the Peng-Robinson equation of state.

## 2.7 Conclusion

A review of the literature on the transportation of CO<sub>2</sub> for the purpose of CCS has given an understanding of the areas that still need to be researched or where more detailed analysis can take place. From the literature it has become apparent that CO<sub>2</sub> pipelines will be the preferred method of transportation given the greater economic benefit when transporting large volumes of CO<sub>2</sub>. This is backed up with the current CCS projects in Canada also using pipelines compared to vessels. The financial modelling of pipeline transport is well developed and understood. However given that pipeline costs are highly dependent on the length, diameter and the operation of the pipeline the models can only give a rough approximation of the costs which can be used in the preferred study but would need to be modified for each CCS project to give greater accuracy. Detailed technical information on CO<sub>2</sub> pipelines is not publicly available given that there are operational pipelines in the USA. This may be due to intellectual property issues with the organisations operating the pipelines not wanting to share the data publicly. This means that the current modelling of CO<sub>2</sub> pipelines has not been validated alongside actual pipeline data.

An area within CO<sub>2</sub> pipeline modelling which has been the main focus of the research is in the depressurisation of pipelines in the case of pipeline ruptures. This is understood to be an extremely important area of research given the health and safety implications of such a hazard occurring. This area of research also includes experimental data of pipeline ruptures which allows for more detailed models and hence is believed to be an area which is well understood. Given that CO<sub>2</sub> can be

transported in different phases, modelling has been carried out to understand the optimum phase of the CO<sub>2</sub>. Given the research there was no definitive answer on whether the sub cooled liquid phase or the supercritical phase should be used and this will be decided for each CCS project separately. Unless there is the option of reusing pipelines which will provide an economic benefit, gas phase transport was concluded to be undesirable for pipeline transport given the low density.

In the modelling of CO<sub>2</sub> transport there are two main types of models that have been developed. The first are steady state models, these are simpler and represent the flow of CO<sub>2</sub> from base load power plants where there is a constant supply of CO<sub>2</sub> to the pipeline. The results from these models allow understanding of pressure profiles along the pipeline and whether phase change occurs for specific inlet conditions. There has also been the development of steady state models which also take into consideration near pure CO<sub>2</sub> with N<sub>2</sub> and O<sub>2</sub> as impurities.

Simulations studying dynamic flows of CO<sub>2</sub> have been used to determine whether two phase flow will occur when there is a change in flowrate at the inlet of the pipeline. This allows the simulation of a pipeline which transports CO<sub>2</sub> from a load following power plant such as a CCGT. These models however do not show how the flowrate changes throughout the pipeline, therefore they do not indicate at what point along the pipeline phase change occurs. The models developed for dynamic flows also do not compare the difference between transporting in the sub cooled liquid phase and the supercritical phase. There has also been no research on the effects of impurities within the CO<sub>2</sub> on the dynamics. These areas show that there is empty space within the research that require to be filled and are areas of novelty.

Models simulating multiple sources of CO<sub>2</sub> have been developed, these models have given technical insight into steady state flows of CO<sub>2</sub>. While these models have been comprehensive by modelling real proposed projects and taking into account impurities within the CO<sub>2</sub>. There is still novel research to be carried out looking at the effects of dynamic flows from multiple sources of CO<sub>2</sub> on the fluid within the pipeline.

Through the literature review it has been possible to understand what research has been carried out and what research is still needed, to enable a more comprehensive understanding of CO<sub>2</sub> transport within pipelines. There are key areas of novel research particularly looking at dynamic flows of both sub cooled and supercritical CO<sub>2</sub>. These are the areas in which the research has expanded and developed on. To carry out the research an analysis of three different modelling tools was carried out OLGA, Aspen HYSYS and gCCS. The approach taken to evaluate the most appropriate tool was to assess the equations of state each one uses to determine the properties of CO<sub>2</sub> and of CO<sub>2</sub> rich fluids. For pure CO<sub>2</sub> the Span and Wagner equation of state used in OLGA is deemed to be the most accurate, as it was specifically developed for CO<sub>2</sub>. Peng-Robinson which is used in Aspen HYSYS was seen to be the least accurate, especially around the critical region and was considered by some researchers to be not good enough to model CO<sub>2</sub> for CCS purposes. The SAFT equation of state was said to have good agreement with experimental data for CO<sub>2</sub> in the sub critical and supercritical region with deviation occurring closer to the critical point. It was concluded however that it was still appropriate to use for CO<sub>2</sub> modelling.

The modelling of CO<sub>2</sub> mixtures containing H<sub>2</sub>, N<sub>2</sub> and O<sub>2</sub> is important when looking at CO<sub>2</sub> from different capture technologies, as even small amounts of these impurities can affect the properties of the fluid. The Span and Wagner equation of state was not developed for CO<sub>2</sub> rich fluids and therefore is not capable of modelling these types of systems. Peng-Robinson uses binary interaction coefficients for fluid mixtures, which rely on the availability of experimental data. The literature found that for CO<sub>2</sub>-H<sub>2</sub> and CO<sub>2</sub>-N<sub>2</sub> systems there was good agreement with the experimental data except around the critical region as with pure CO<sub>2</sub>. For the SAFT equation of state there was found to be very limited literature on the modelling of CO<sub>2</sub> and therefore a full analysis of the model was not possible.

Through the analysis carried out, it was decided that given the specific application of gCCS it was the most appropriate tool of choice for the modelling of dynamic flows in pipelines of CO<sub>2</sub> and CO<sub>2</sub> rich fluids and allowed for another layer of novelty of the research, in the use SAFT equations of state for CO<sub>2</sub> pipeline modelling. It was preferred over OLGA because the Span and Wagner equation of state is not applicable for CO<sub>2</sub> rich systems, while it was the greater accuracy compared to the Peng-Robinson equation of state that was the reason it was chosen over Aspen HYSYS.

## **Chapter 3 – Comparing Variable Flows For Liquid and Supercritical Phase Carbon Dioxide**

### **3.1 Introduction**

Transporting carbon dioxide via pipeline is a part of the process that enables the sequestration of CO<sub>2</sub> from large point sources, including power stations. This can include both coal fired power stations as well as natural gas combined cycle power (NGCC) stations. Within the UK NGCCs are operated as load following power plants. This means that an NGCC with CCS will produce variable flowrates of CO<sub>2</sub>. The purpose of this chapter is to report the effects of reducing the inlet flowrate of CO<sub>2</sub> into the pipeline and comparing the outputs when CO<sub>2</sub> is transported in the liquid phase and the supercritical phase. Understanding the effects of changing flowrates within a CO<sub>2</sub> pipeline could help indicate which phase of CO<sub>2</sub> would be the most beneficial and inform the development of transporting CO<sub>2</sub> in the most efficient way.

### **3.2 Hypothesis**

For this chapter the following statement presents the hypothesis that will either be proved or disproved through the modelling and simulations that will be carried out.

“The gCCS model will show that the rate of change in the outlet flowrate of a CO<sub>2</sub> pipeline when the inlet flowrate is reduced, will be greater when the CO<sub>2</sub> is transported in the subcooled liquid phase compared to the supercritical phase”.

### **3.3 gCCS Transport Models**

A CO<sub>2</sub> transport system is constructed within gCCS through the connections of single models. Each model has specific variables that can either be chosen or defined; these allow the system to be designed to a certain specification. It is

necessary to understand the degrees of freedom within the system to ensure the simulation will complete. Over specifying or underspecifying a variable will result in the simulation returning an error message indicating a problem, however it will not inform the user which variable has been over or under specified.

### 3.3.1 Carbon Dioxide Source Model

In the case of modelling the transport and storage of CO<sub>2</sub> separately from the rest of the system, for example without including the capture process itself, a source of CO<sub>2</sub> is specified using the CO<sub>2</sub> Source model within gCCS. This model allows for a user to define the flowrate specifications of CO<sub>2</sub> that enters the pipeline. The manipulated variables for this model can be seen in Figure 3-1.

Source\_CO2001 (Source\_CO2)

Cumulative flow: Don't track cumulative flow

Physical properties: gCCS standard

Phase: Gas

Composition: Mass fractions

Pressure: Not specified

Flowrate: Not specified

Specify

☒ Temperature: 298.15 K

☒ Mass fraction: ☐ Uniform for entire array ☒ Per element

Components	kg/kg
CO2	
H2O	
H2	
H2S	
CO	
Ar	
O2	
SO2	
N2	

OK Cancel Reset all Help

Figure 3-1: CO<sub>2</sub> Source Variables

Within the CO<sub>2</sub> source model the thermodynamic properties of the fluid are defined by specifying the temperature and the pressure if it is not specified anywhere else



within the system. For a transport system the CO<sub>2</sub> flowrate must be defined here. The model also allows the composition of the fluid to be specified, giving the choice of 9 of the most common components that are to be found in captured CO<sub>2</sub>, for example impurity gases. There are two ways in which the components can be specified; firstly through the 'gCCS standard' tab which requires a mass fraction to be entered for each of the 9 components, even if the value is zero. This however causes the model to run through every calculation for even those which have a mass fraction of zero and increases the time it takes for the simulation to complete. The second way in which the components can be specified is through the 'user defined' option which is available in the drop down list of the 'physical properties' tab. This method produces a separate dialogue box in which the desired components of non-zero mass fractions can be specified. Only those components will require a mass flowrate to be defined. This therefore reduces the time for the simulation to complete.

### 3.3.2 Pipeline and Well Models

To build a full CO<sub>2</sub> transport system gCCS has within it, a 'pipeline' model and a separate 'well' model. The pipeline model represents a pipeline segment whereas the well model represents the entire well. Figure 3-2 shows the configuration tab for the pipeline model which is identical to the well model. This allows specification of the pipeline design. It allows the user to manipulate the pipe length, elevation changes, internal diameter, pipe thickness and pipe roughness. These variables are necessary to calculate important parameters for the fluid flowing in the pipeline.

- The pipe roughness is required to obtain the Darcy friction factor which then allows for the frictional pressure losses to be calculated.

- The internal diameter is required to determine the flow regime i.e. Reynolds number, which is also used to determine the pressure drop in the pipeline.
- The pipe length and elevation are also used in determining the pressure drop along the pipe length.

There is also a choice of material for the pipeline, carbon steel and stainless steel are the options available within the model and are the most common materials for pipe construction.

The screenshot shows a software dialog box titled "PipeSegment001 (PipeSegment)". It contains several configuration options for a pipeline segment. The "Specify" section includes dropdown menus for "Same diameter as upstream pipe?" (set to "Yes"), "Pipe material" (set to "Carbon steel"), and "Pipe schedule" (set to "none"). There are checkboxes for "Maximum allowable operating pressure" (153 bar), "Pipe wall roughness" (4.57E-5 m), "Erosional velocity margin" (70 %), "Number of pipe sections" (1), "Pipe section length" (with radio buttons for "Uniform for entire array" and "Per element"), "Elevation change" (with radio buttons for "Uniform for entire array" and "Per element"), "Pipe internal diameter" (0.254 m), and "Pipe thickness" (10 mm). At the bottom, there are tabs for "Configuration", "Heat Transfer", "Methods", "Fittings", and "Costing", and buttons for "OK", "Cancel", "Reset all", and "Help".

Figure 3-2: Pipeline Segment Design Variables

The heat transfer tab for the pipeline model can be seen in Figure 3-3. The factors that affect heat transfer of the fluid in the pipeline which can be defined include, the ambient temperature  $T_a$ , which effects the soil temperature  $T_s$  and hence the temperature gradient between the fluid and the surrounding material. Further factors to be taken into consideration are:

#### *3.3.2.1 Burial Depth of the Pipeline*

The burial depth plays a significant factor in determining the temperature change in the pipeline. Studies have shown that the effect of the ambient temperature on the soil temperature changes with burial depth. The deeper the soil the smaller the effect of the ambient temperature on the soil temperature [67].

#### *3.3.2.2 Material the Pipeline is Buried in*

The choices for the surrounding material includes soil, air and water. These choices are available to simulate buried pipes, above ground pipes and offshore pipelines. A further choice is available for the type of soil that the pipeline is buried in, this includes dry sandy soil, soaked sandy soil, dry clay soil or soaked clay soil. The soil type affects the heat transfer as different soils will have different thermal properties and therefore affect the soil heat transfer coefficient  $h_s$  which in turn will affect the overall heat transfer coefficient  $U$ . It has been found that wet soils have a greater thermal conductivity compared to dry soils and therefore will have a greater heat transfer coefficient [68]. This will affect the heat losses from the pipeline in two ways, firstly the effect of the ambient temperature on the ground temperature will be greater for wet soils and secondly the heat transfer between the pipe wall and the soil will be greater for wet soils.

— PipeSegment001 (PipeSegment)

Specify

Heat transfer option: Specify ambient conditions

Pipe segment surrounding material: Soil (Buried pipeline)

Soil types: Sandy soil (dry)

Initial Conditions: Steady state

☒ Ambient temperature specification in: 278.15 K

☒ Ambient temperature specification out: 278.15 K

☒ Pipe centreline depth below surface: 1 m

☒ Initial inlet fluid temperature guess: 300 K

☒ Initial outlet fluid temperature guess: 300 K

Configuration | **Heat Transfer** | Methods | Fittings | Costing

OK Cancel Reset all Help

Figure 3-3: Pipeline Segment Heat Transfer Variables

The heat transfer tab for the well model is different from that of the pipeline model. In exchange for a choice of the surrounding pipeline material, the well model instead allows for a value for the overall heat transfer coefficient to be specified. The heat transfer tab for the well model is shown in Figure 3-4.

Parameter	Value	Unit
Ambient temperature specification in	278.15	K
Ambient temperature specification out	278.15	K
Initial inlet fluid temperature guess	300	K
Initial outlet fluid temperature guess	300	K
Overall heat transfer coefficient	11	W/(m² K)

Figure 3-4: Well Heat Transfer Variables

### 3.3.3 Valve Model

As part of a CO<sub>2</sub> pipeline system it is necessary to have Line Block Valves (LBV) along the pipeline as a safety feature. If a leak occurs anywhere along the pipeline the valves can be quickly closed to limit the release of CO<sub>2</sub> to the atmosphere.

The LBV valve acts as a safety valve and is not optimised for tight control of the flow. The addition of the valve allows a system to be modelled that is closer to what is seen in real CO<sub>2</sub> pipelines. The valve model takes into account the pressure and temperature changes that occur through the valves. While the temperature changes across the valve may be relatively small, depending on the liquid flow coefficient the pressure drop across the valve can be significant and is an important parameter to take into account.

Figure 3-5 shows the valve model interface within gCCS. The parameters which can be changed within the model include the flow coefficient which determines the

pressure loss through the valve, the stem position which relates to how far open or closed the valve is and the leakage fraction.

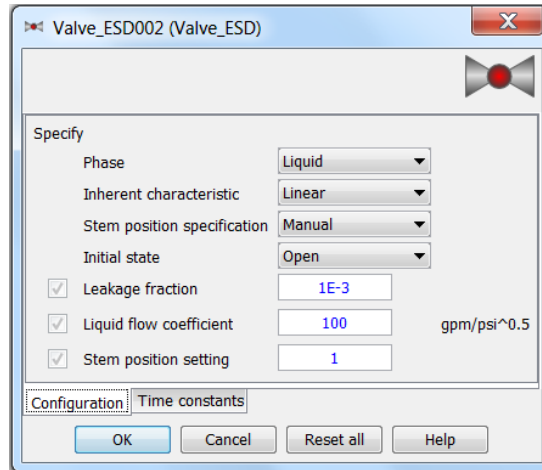


Figure 3-5: ESD Valve Configuration

#### 3.3.4 Distribution Header Model

The distribution header model is used to simulate the distribution of captured CO<sub>2</sub> among several wells. It allows for a single inlet of CO<sub>2</sub> from the pipeline and has connections to allow for several wells to be attached. The model has inputs for the header length, the upstream pipe diameter and the rate of heat input. Figure 3-6 shows the configuration tab for the distribution header.

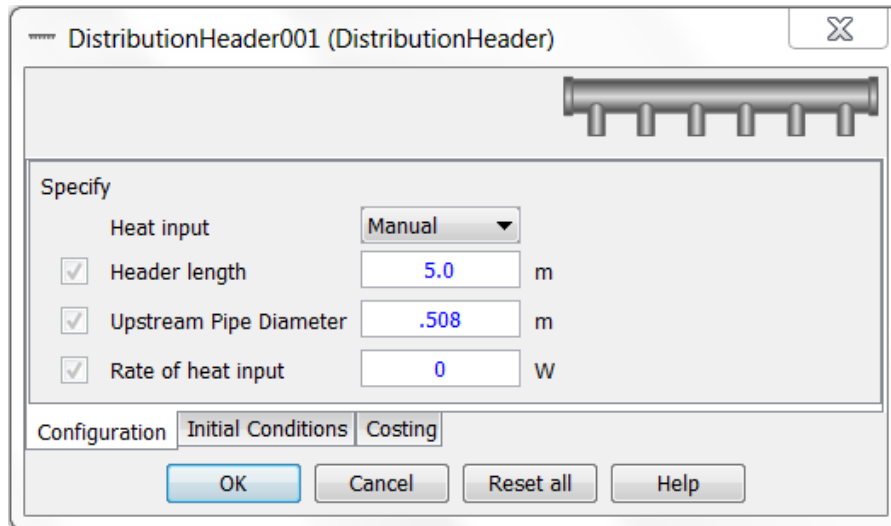


Figure 3-6: Distribution Header Configuration

### 3.3.5 Reservoir

The reservoir model simulates the storage of CO<sub>2</sub> in underground reservoirs and is modelled as a pressure vessel. There are two methods in which the reservoir pressure can be specified, either by specifying the pressure directly in which case the model will maintain a constant reservoir pressure, or the pressure can be determined via an external file which contains data on how the reservoir pressure will change depending on the mass of CO<sub>2</sub> injected into the reservoir.

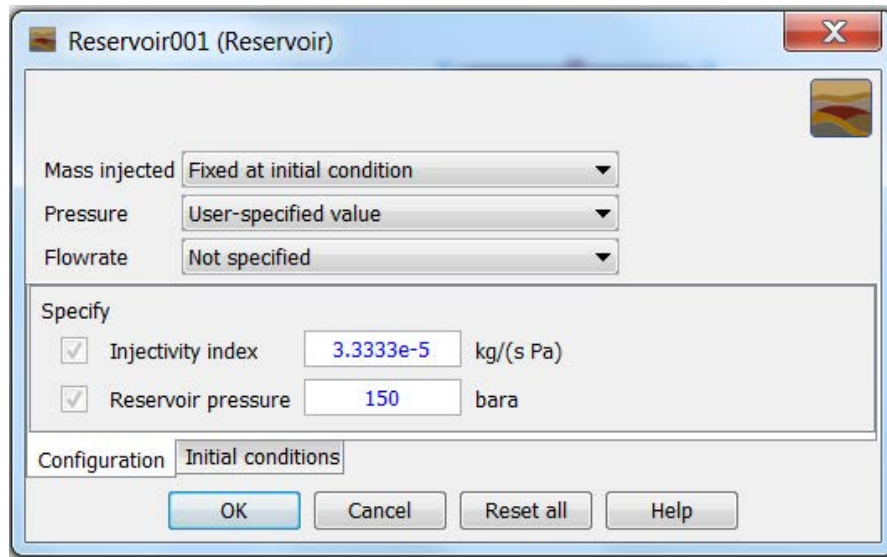


Figure 3-7: Reservoir Configuration

A study has been conducted to compare the different effects of changing the inlet flowrate of a CO<sub>2</sub> pipeline, simulating CO<sub>2</sub> being in both the liquid and supercritical phase. Along with comparing the different phases of CO<sub>2</sub>, the addition of different impurities in the CO<sub>2</sub> stream has been studied. The need for this research comes from the lack of work carried out in this area, most importantly how varying flows into the pipeline system effect the flow within the pipe. This will be of utmost importance for the cases of load following power plants with CCS. The aim is to gain greater knowledge in this area to help in the operation of CO<sub>2</sub> pipelines and storage sites.

The study was carried out using a simulation tool known as gCCS which has been developed by Process Systems Enterprise as a tool to model full chain CCS systems. For the purpose of this study only the transport, injection and storage models have been used. The software is based on gSAFT to predict the thermodynamic properties of the fluids in question. As previously mentioned gSAFT is a predictive tool and is seen as the most appropriate method in simulating CO<sub>2</sub>



pipelines due to the lack of experimental data available which is a requirement for other cubic equations of state such as PengRobinson.

### **3.4 Carbon Dioxide Pipeline Model Development**

The setup of the model can be seen in Figure 3-8. The source of the CO<sub>2</sub> is taken from the compression system which is located at the site of the power plant and the capture plant. There is an Emergency Shut Down (ESD) valve directly before a 52000 m pipeline and another ESD valve located directly after this pipeline. There is then another 52000m pipeline and ESD valve which is followed by a distribution header which is connected to a 1200m well. The vertical well leads to a reservoir where the CO<sub>2</sub> is stored.

The technical specifications for each part of the system can be seen in Tables 3-1 to 3-6. The pipeline setup for the simulations done in both the liquid and supercritical phase were identical to allow for accurate comparison between the results. The initial simulation was carried out using pure carbon dioxide to present a base case in which all others could be compared. It was necessary to repeat the simulations, each with a longer simulation time than the previous until the system reached a steady state. The initial time period tested was 100,000 seconds (27.78 hours) with an increase of 100,000 seconds (27.78 hours) for each subsequent simulation. Steady state in the pipeline was assumed when the outlet flowrate of the pipeline matched that of the inlet flowrate.

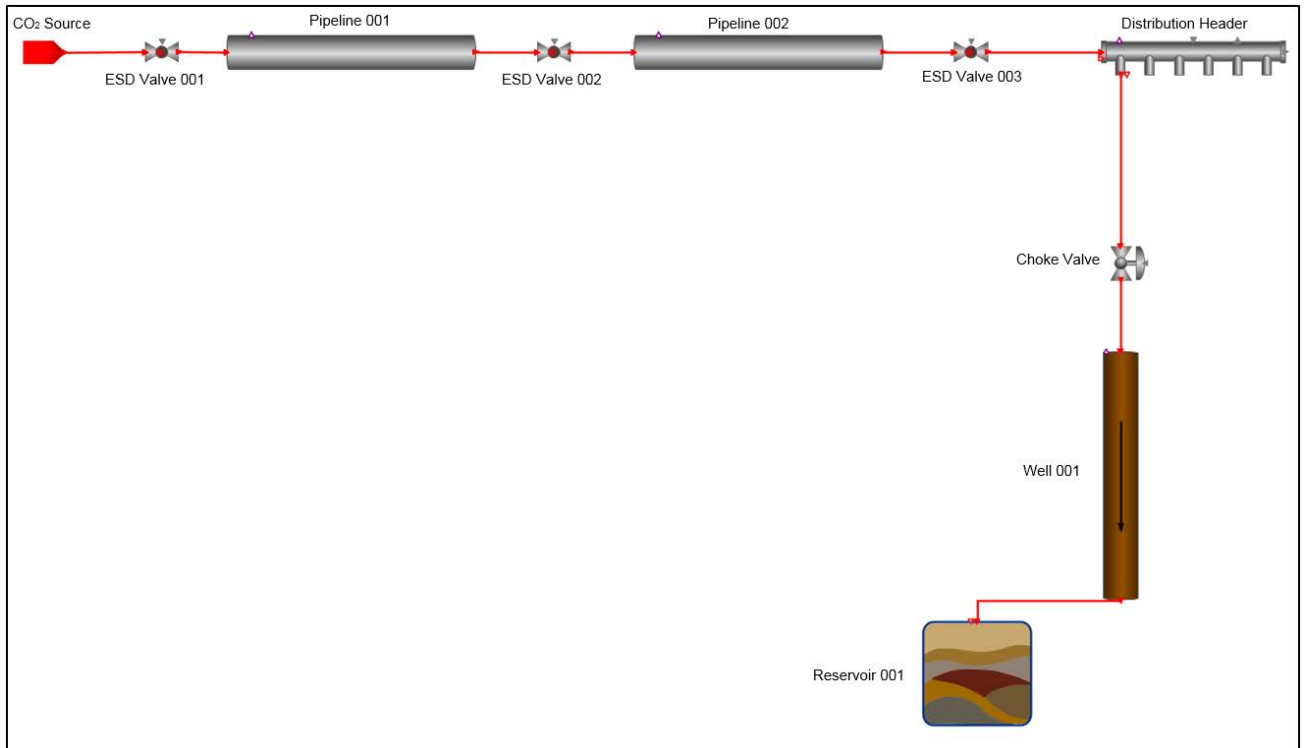


Figure 3-8: Model Pipeline Topology

The model was set to simulate a case in which there is a linear reduction in flowrate at the inlet of the pipeline, with a starting flowrate of  $100 \text{ kg s}^{-1}$  which was then programmed to decrease to  $50 \text{ kg s}^{-1}$  over a period of 12.5 minutes.

Table 3-1: CO<sub>2</sub> Source Parameters

CO <sub>2</sub> Source		
Property	Value	Unit
CO <sub>2</sub> Mass Fraction	1	-
Temperature	293	K
Ramp Rate	4	Kg s <sup>-1</sup> min <sup>-1</sup>

The CO<sub>2</sub> source indicates a single point source of CO<sub>2</sub>. In this case the fluid is pure carbon dioxide.

Table 3-2: ESD Valve Design Parameters

ESD Valves		
Property	Value	Unit
Leakage Fraction	0.001	-
Liquid Flow Coefficient	100	gpm/psi <sup>0.5</sup>
Stem Position Setting	1	-

Table 3-3: Pipeline Section Design

Pipe Sections		
Property	Value	Unit
Material	Carbon Steel	-
Pipe Section Length	52000	m
Elevation Change	0	m
Pipe Internal Diameter	0.6096	m
Pipe Thickness	0.01	m
Pipeline Depth	1	m

Table 3-4: Choke Valve Design

Choke Valve		
Property	Value	Unit
Leakage Fraction	0.001	-
Liquid Flow Coefficient	100	gpm/psi <sup>0.5</sup>
Stem Position	1	-

Table 3-5: Well Design

Well		
Property	Value	Unit
Material	Carbon Steel	
Pipe Section Length	1200	m
Elevation Change	1200	m
Pipe Internal Diameter	0.3	m
Pipe Thickness	0.01	m
Overall Heat Transfer Coefficient	11	W m <sup>-2</sup> K <sup>-1</sup>

Table 3-6: Reservoir Parameters

Reservoir		
Property	Value	Unit
Injectivity Index	$3.3333 \times 10^{-5}$	$\text{Kg s}^{-1} \text{Pa}^{-1}$
Specified Reservoir Pressure	150	bar

The code for the process to produce the change in flowrate can be seen in Appendix A.1. The code describes a process in which the initial setup is allowed to continue for 30 seconds. At this point the inlet flowrate from the CO<sub>2</sub> source is reduced. The change is a ramp down in the mass flowrate at a rate of  $4 \text{ kg s}^{-1} \text{ min}^{-1}$ . This means it will take the system 750 seconds to reach the set point of  $50 \text{ kg s}^{-1}$ . The system is then allowed to continue for 500,000 seconds (139.89 hours). This value has been used as through repeating this test it was found that it takes approximately 500,000 seconds (138,89 hours) for the entire system to completely settle and reach an equilibrium. This simulation time is taken as the base case for this project. A single ramp down was used to show how the system responds when the simplest changes are made to the system. It is also necessary to mention that a ramp down in the flowrate of CO<sub>2</sub> is a consequence from a changing output from a power plant, therefore this case simulates expected conditions for a load following power plant with CCS.

### **3.5 Simulation Output Analysis**

#### **3.5.1 Liquid Phase Transport**

The initial simulation was set up for transporting CO<sub>2</sub> in the liquid phase, with an inlet temperature of 20°C. The areas which are of significance in the transport of CO<sub>2</sub> are the flowrate, pressure, temperature and the density profiles. These variables show how the CO<sub>2</sub> is flowing and whether there is any change of phase along the pipeline.

##### *3.5.1.1 Flowrate*

Figure 3-9 shows how the flowrate changes at the inlet and the outlet of each pipeline over the simulation time period. The inlet flowrate to Pipeline001 is equivalent to the specified flowrate from the CO<sub>2</sub> source and the outlet flowrate of Pipeline001 is equal to the inlet flowrate to Pipeline002. There are three distinct phases that occur that can be seen from Figure 3-9, the first phase which is highlighted in the blue dashed lines, shows that as the inlet flowrate drops to the set point the outlet flowrate from Pipeline001 falls at a slower rate. Figure 3-10 shows a close up of the initial drop in CO<sub>2</sub> flow and shows more clearly the difference in time taken for the inlet and outlet flowrates of each pipeline to reach a steady state. This delayed response can be explained through the physical properties of CO<sub>2</sub> as there is a temperature drop as the flowrate decreases at the outlet of the pipeline yet the temperature at the inlet remains constant. The large difference in temperature means that the density at the inlet is lower than the density at the outlet and hence the flowrates at these two points will be different. The current literature on CO<sub>2</sub> pipelines has not identified this significant time delay when a flowrate

change occurs and is hence a novel finding in how a CO<sub>2</sub> pipeline reacts to changes in the inlet flowrate. This initial response to the change in the flowrate will be referred to as the 'delayed response phase'.

The second phase shown by the red dashed box in Figure 3-9 shows that the outlet flowrate reaches an initial steady state that is approximately 4kg/s higher than the inlet flowrate. This offset lasts for a period of 23,000 seconds (6.39 hours). This will be referred to as the 'offset phase'.

After the offset phase the outlet flowrate declines further from 54 kg s<sup>-1</sup> to 50 kg s<sup>-1</sup>. This same response is shown in Pipeline002 however it takes a further 230,000 seconds (63.89 hours) for the flowrate to fall from 54 kg s<sup>-1</sup> to 50 kg s<sup>-1</sup>. This will be referred to as the 'reduction phase'.

To understand what is occurring within the pipeline, Figure 3-11 shows the flowrate profile along the axial length of Pipeline001. Figure 3-11 shows that a wave like flowrate profile develops within the pipeline, this wave then travels along the pipe length. When the wave reaches the end of the pipeline the outlet flowrate then falls to the set point. The wave then carries on to the second pipe length until it again reaches the outlet of the pipe. The reason behind this phenomena is unknown and there are two possibilities behind such outputs; the wave like profile could be a consequence of the compressibility of the CO<sub>2</sub> in which there is a large density change of the fluid over a small distance of pipe length. However there is also a possibility that this phenomena is a result of the model itself and is not a real consequence of changing the CO<sub>2</sub> flowrate.

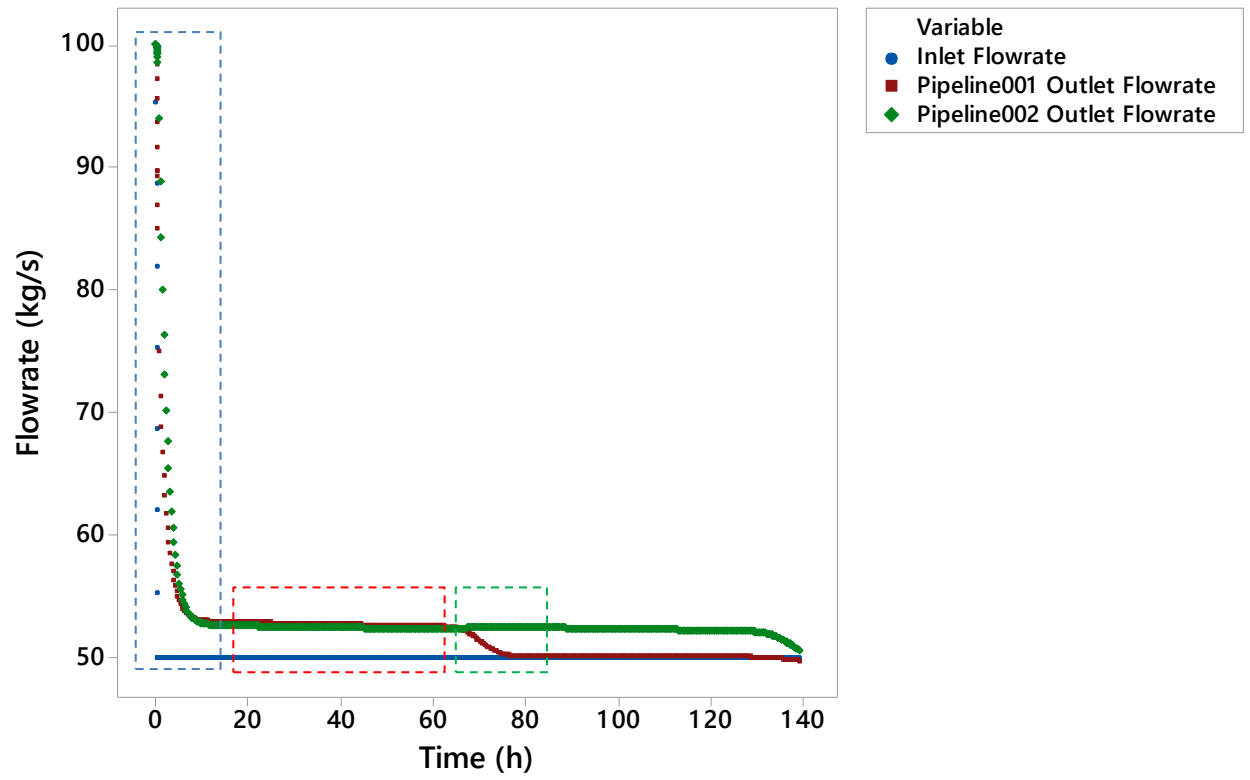


Figure 3-9: Inlet and Outlet Flowrate Profile for Pipeline 1 and 2

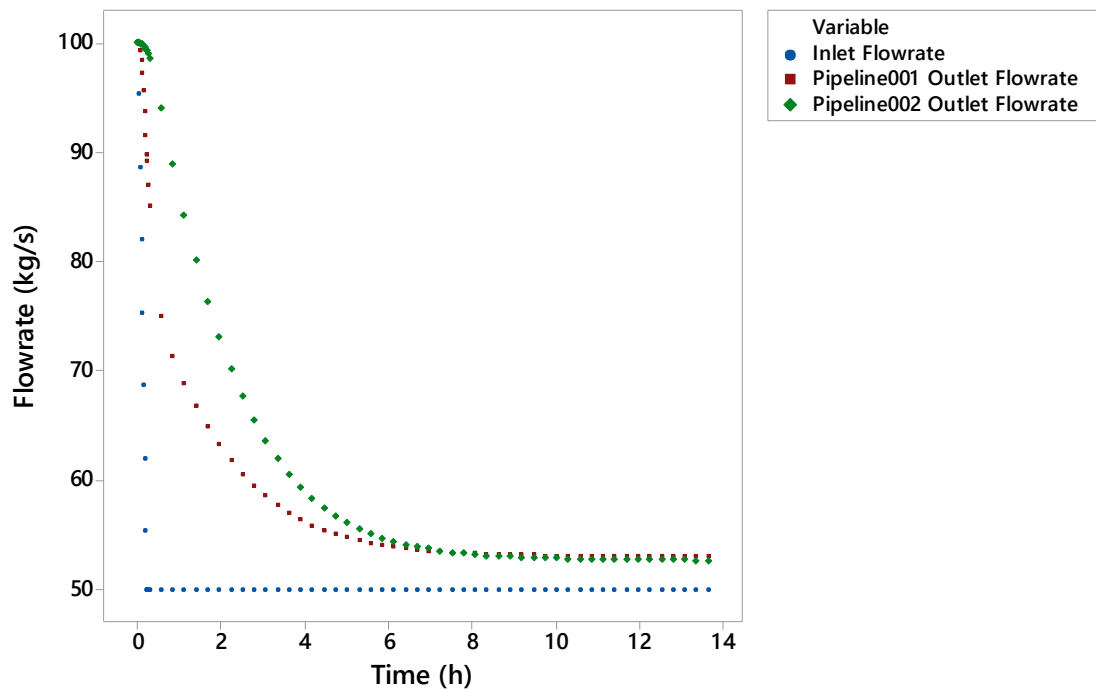


Figure 3-10: Inlet and Outlet Flowrate Profile for Pipeline 1 and 2

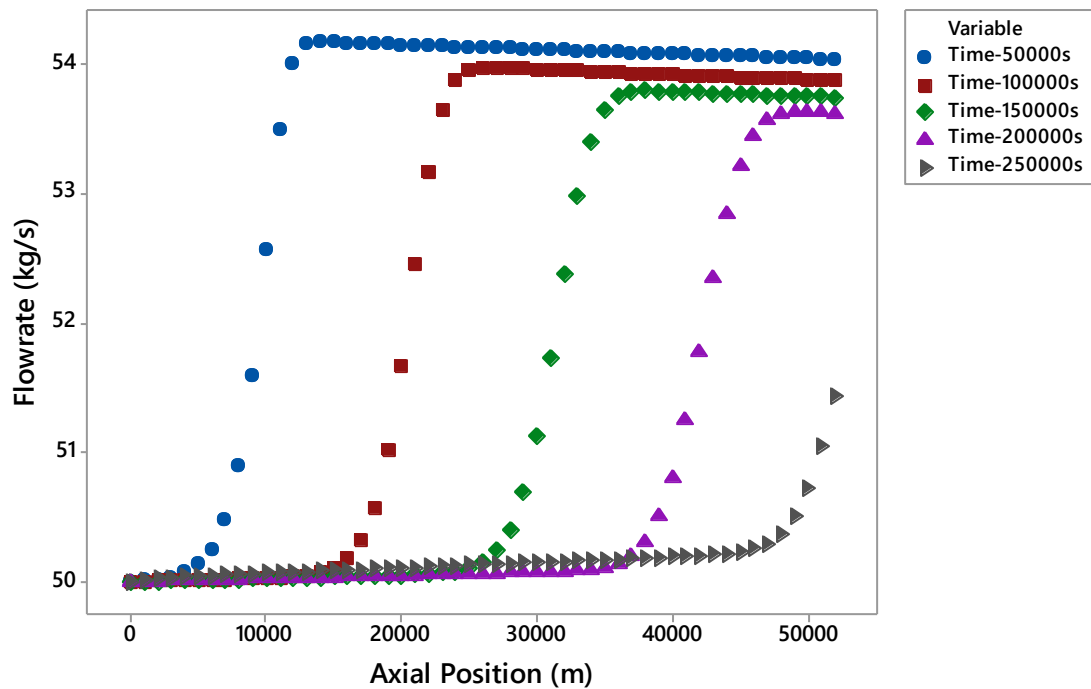


Figure 3-11: Flowrate Profile along Pipeline001



### 3.5.1.2 Pressure

Within the model the inlet pressure of the fluid is determined by the reservoir pressure. At the initial flowrate of 100kg/s the pressure at the inlet to the pipeline is 14187 kPa; this is greater than the critical pressure of CO<sub>2</sub> of 7.39MPa. The pressure at the outlet of pipeline001 is 14121 kPa giving a pressure drop along the length of the pipeline of 66 kPa. Since there is no elevation of the pipeline the static pressure losses amount to zero, therefore the pressure drop can be attributed to the frictional pressure loss alone. Figure 3-12 shows that as the flowrate at the inlet drops both the inlet and the outlet pressures also fall. There is a difference between the response of the flowrate and the response of the pressure when a drop in flowrate occurs. Unlike the outlet flowrate, the outlet pressure drops at a similar rate as the inlet pressure and no offset is observed like that of the flowrate. An important observation from Figure 3-10 is that the pressure of the fluid does not fall below the critical pressure of CO<sub>2</sub>. This indicates that two phase flow doesn't occur within the pipeline.

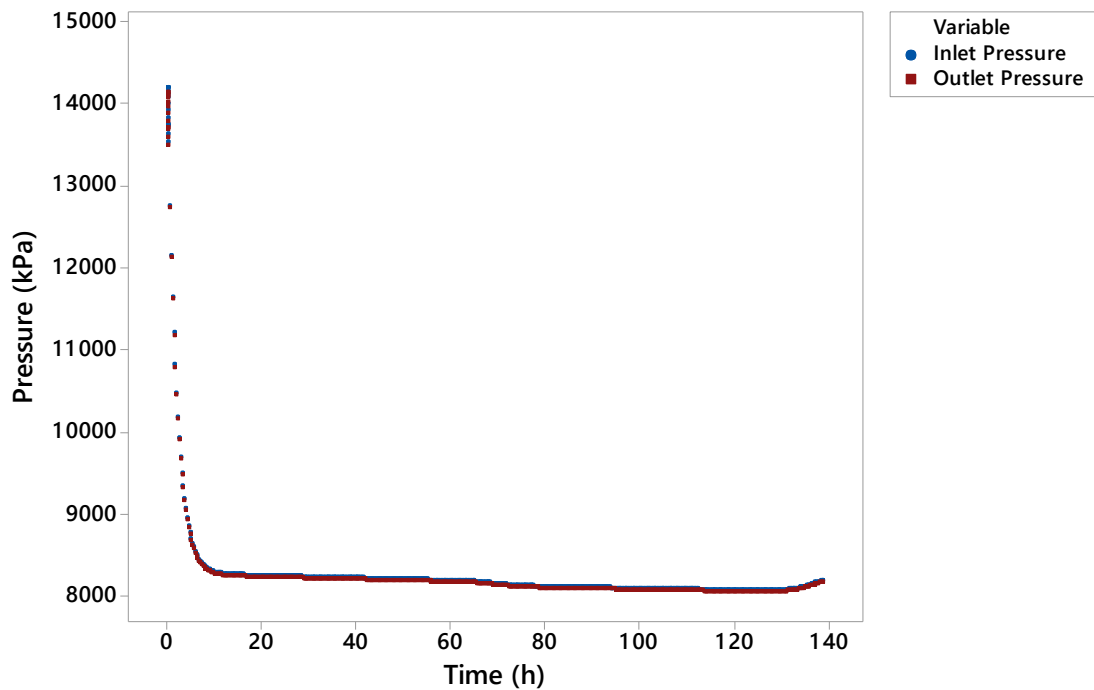


Figure 3-12: Inlet and Outlet Pressure for Pipeline 001

### 3.5.1.3 Temperature

The temperature profiles at the inlet and outlet of Pipeline001 can be seen in Figure 3-13. The pipeline inlet temperature is designed to stay constant and ensures that CO<sub>2</sub> doesn't move between the liquid and the supercritical phase. The temperature along the pipeline can vary through heat losses or gains to and from the surrounding pipeline material. Figure 3-14 shows that the outlet temperature of Pipeline001 falls as the flowrate drops, with a drop in fluid temperature of 6K. When the outlet flowrate initially reaches an equilibrium the rate of change of the temperature decreases, until the point at which the outlet flowrate begins to fall. As the flowrate drops from 50kg/s to 54kg/s the temperature increases, until the point at which the flowrate reaches the set point at which point the temperature settles at approximately 294.8K. The temperature at the outlet of the pipeline does not change intuitively as

there is a decrease and then an increase in the temperature. Heat loss from the fluid over a section  $\Delta x$  is calculated using the following equation [69].

$$q = \frac{4U_o d_o}{d_2} (T_o - T_f)$$

This equation does not explain the pipeline outlet temperature change. It is possible however that there is an unknown interaction occurring within the model that cannot be explained without the detailed code that underpins the software.

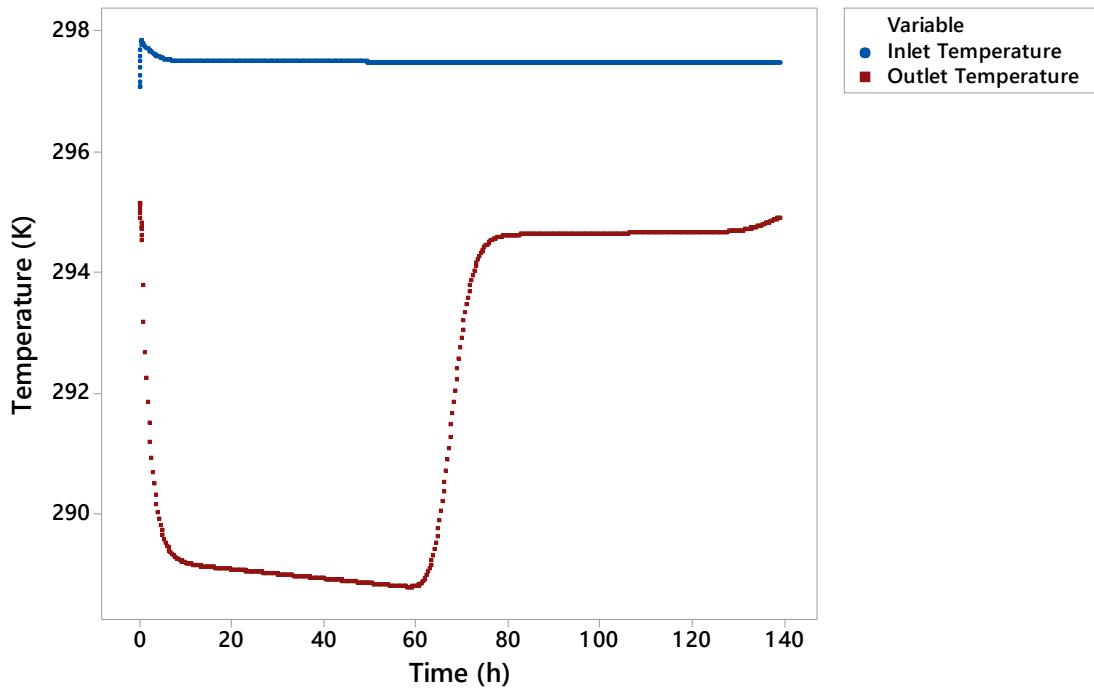


Figure 3-13: Inlet and Outlet Temperature for Pipeline 001

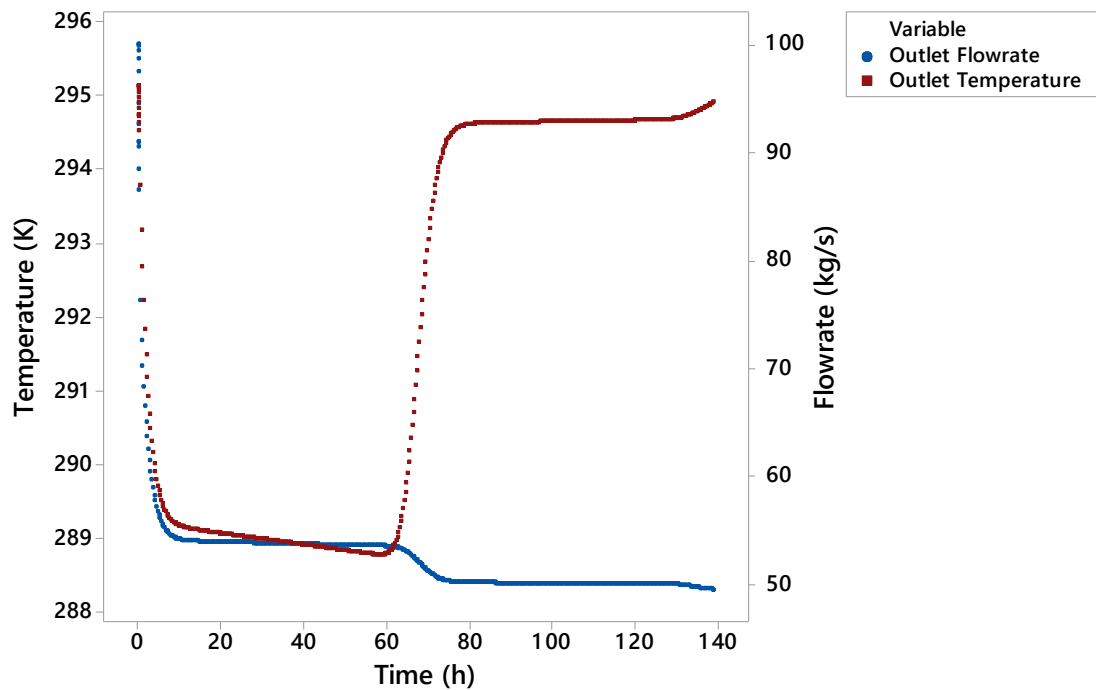


Figure 3-14: Outlet Flowrate and Outlet Temperature for Pipeline 001

### 3.5.2 Supercritical Phase Transport

In comparison to transporting the CO<sub>2</sub> in the liquid phase, the same simulations were repeated however this time the CO<sub>2</sub> at the inlet was modelled to be in the supercritical phase. The one difference here is that the temperature of the CO<sub>2</sub> at the inlet of the pipeline is above the critical temperature of 304.25K (31.1°C). To ensure the CO<sub>2</sub> is in the supercritical phase an inlet temperature of 313K was used.

#### 3.5.2.1 Flowrate

Figure 3-15 shows the flowrate profiles for Pipeline001 inlet, Pipeline001 outlet and Pipeline002 Outlet. Similar to the liquid phase flowrate profile there is delay between the inlet flowrate and the outlet flowrate showing that the model predicts that the delayed response phase also occurs when CO<sub>2</sub> is transported in the supercritical

phase. The extent of the delay between the inlet and the outlet flowrate can be seen in Figure 3-16 again.

As with the simulation with liquid CO<sub>2</sub> the same three distinct phases, 'delayed response phase', 'offset phase' and 'reduction phase' occur and are shown by the blue, red and green areas on Figure 3-16. The delayed response phase can be justified through the same phenomena that was discussed for the liquid phase transport and can also be used to explain this occurrence in the supercritical phase, in that due to the temperature drop at the outlet of the pipeline there is a density increase which through the continuity equation explains why there is a higher flowrate at the outlet of the pipeline. For supercritical CO<sub>2</sub> there is a higher temperature drop compared to that observed for liquid CO<sub>2</sub> and hence there is a larger time delay between the change at the inlet and the outlet reaching a steady state.

The model again predicts that there is an offset phase which occurs between the inlet and the outlet flowrate which lasts for approximately 53 hours. The time in which the offset phase occurs is shorter than the offset phase for the liquid phase model. This is due to the higher velocity observed when in the supercritical phase which in turn is due to the decrease in the density from the liquid to the supercritical phase.

Figure 3-16 shows the first 14 hours of the simulation, this illustrates the extent of the delay as the flowrate within the pipeline drops between the inlet of pipeline001 and the outlet of pipeline001 and pipeline002.

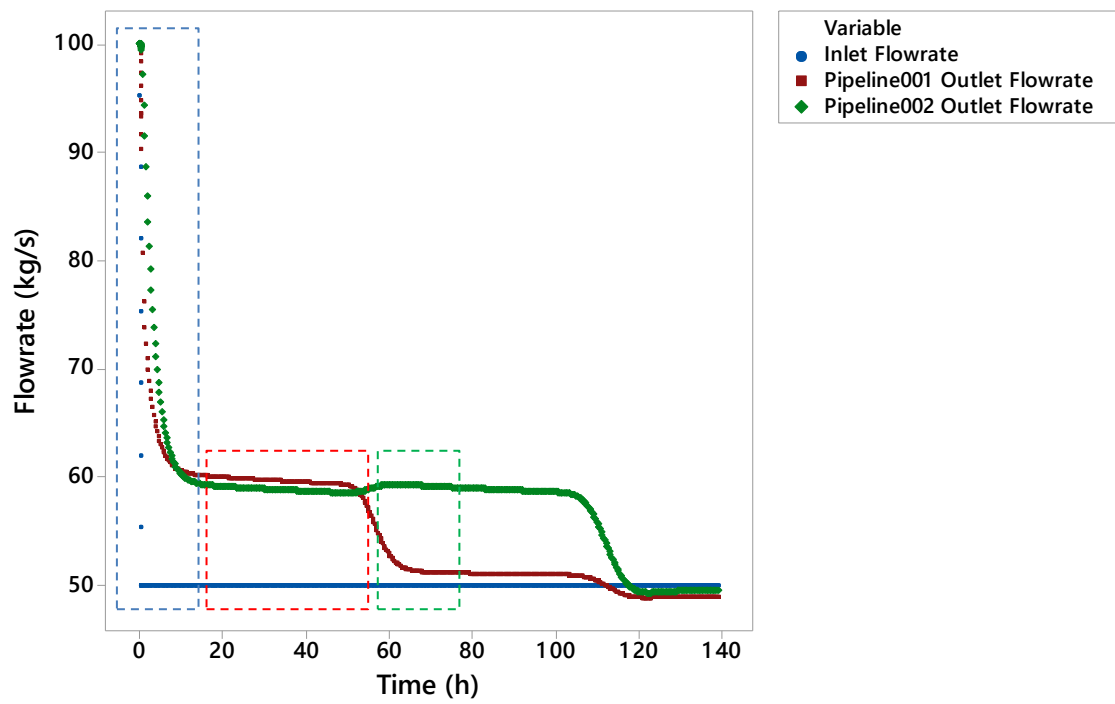


Figure 3-15: Inlet and Outlet Flowrate for Pipeline 001 and 002

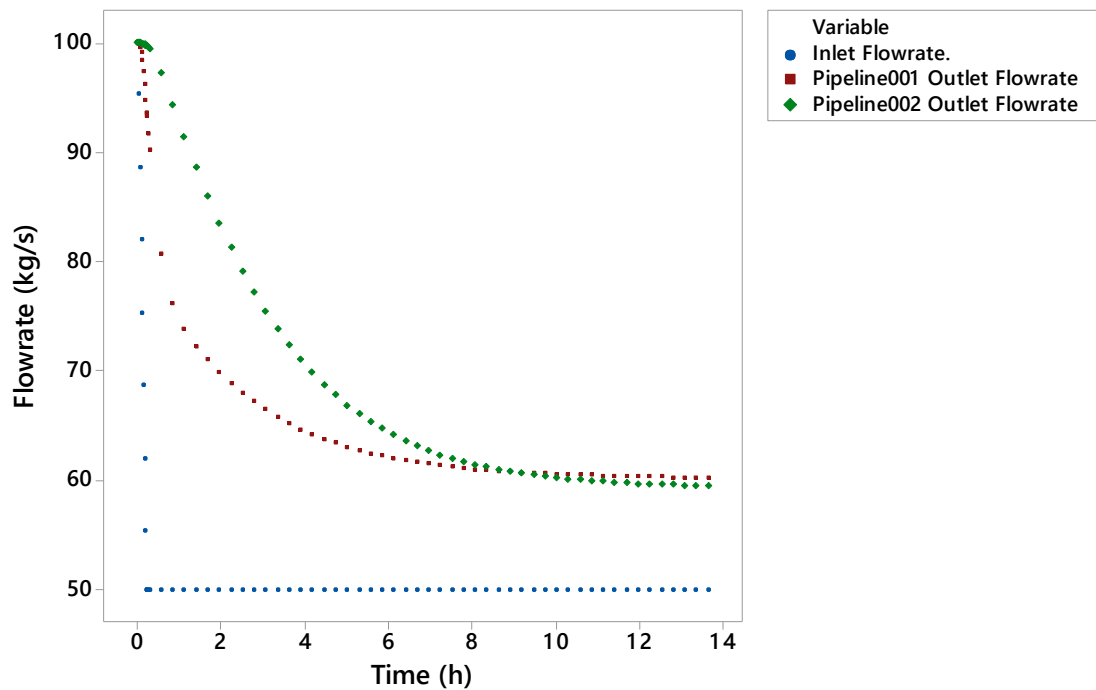


Figure 3-16: Inlet and Outlet Flowrate for Pipeline 001 and 002

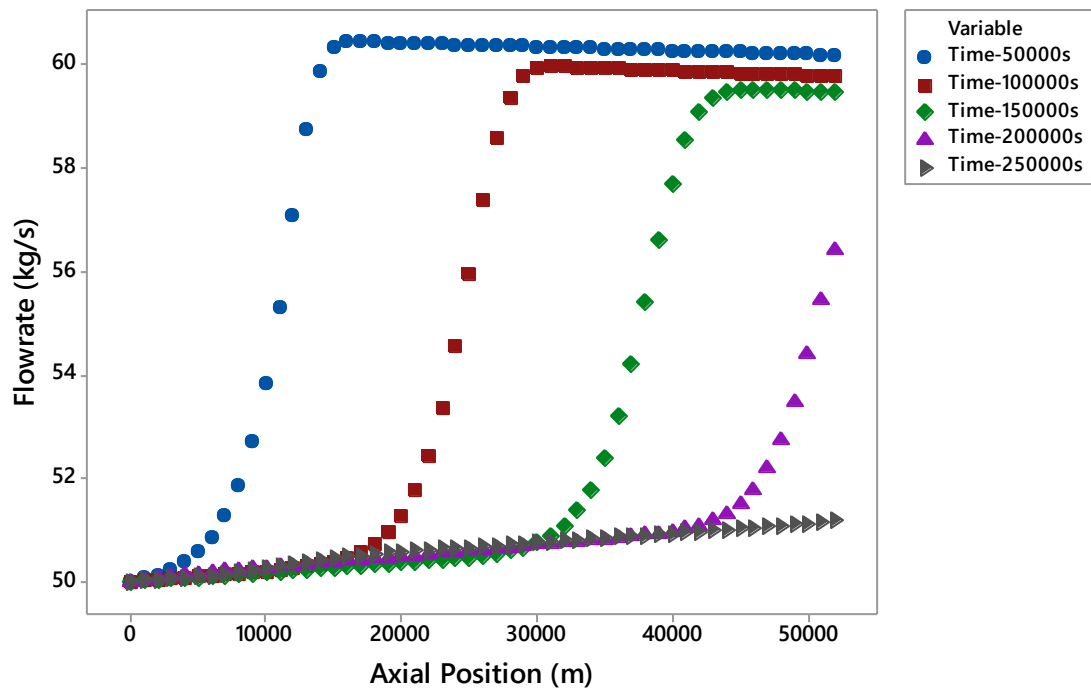


Figure 3-17: Flowrate Profile along Pipeline001

### 3.5.2.2 Pressure

Figure 3-18 shows how the pressure changes as the flowrate at the inlet of the pipeline drops. The required initial inlet flowrate is calculated at 15600 kPa. As the flowrate decreases, the pressure at both the inlet and the outlet of the pipeline also decreases until it reaches approximately 10000 kPa. The pressure initially falls at a rate of 990 kPa/h<sup>-1</sup> for approximately 7 hours, at which point the rate of change of the pressure, at both the inlet and the outlet of the pipeline slows and the pressure remains between 9400 and 9800 kPa. A significant observation from Figure 3-18 is that the pressure does not fall below the critical pressure, indicating that two phase flow doesn't occur within the pipeline as a result of the inlet flowrate falling by 50%.

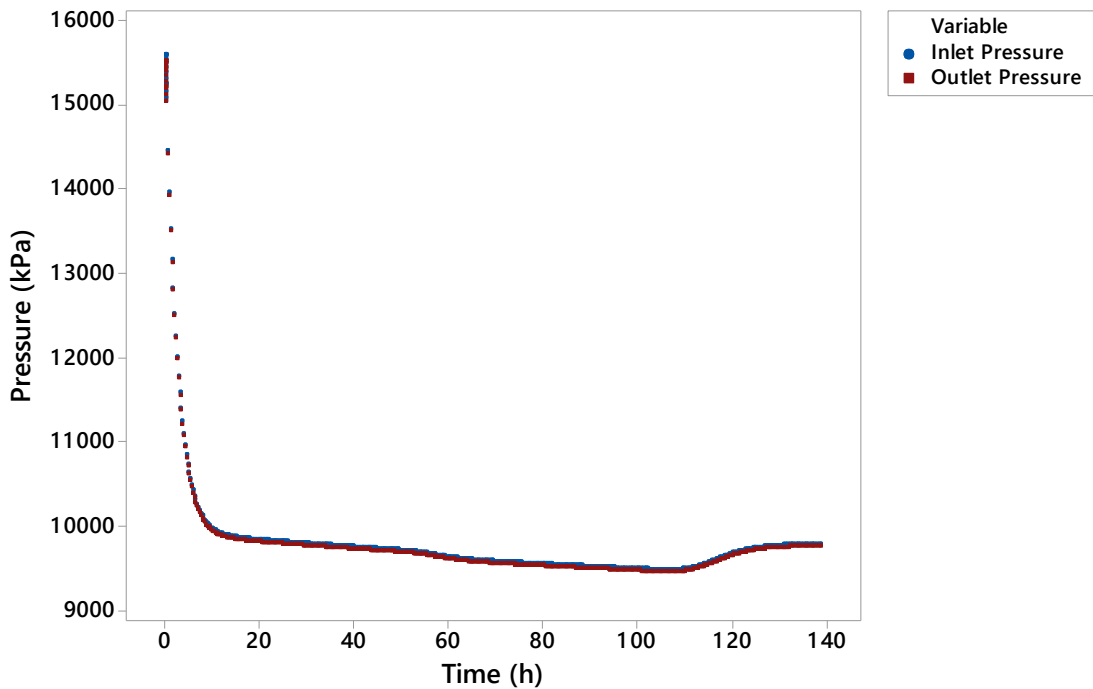


Figure 3-18: Inlet and Outlet Pressure for Pipeline 001



### 3.5.2.3 Temperature

Figure 3-19 shows the inlet and outlet temperature profiles for Pipeline001. To ensure that the CO<sub>2</sub> remains in the supercritical phase the temperature was specified in the CO<sub>2</sub> source at 313K and was maintained at this temperature throughout the simulation period.

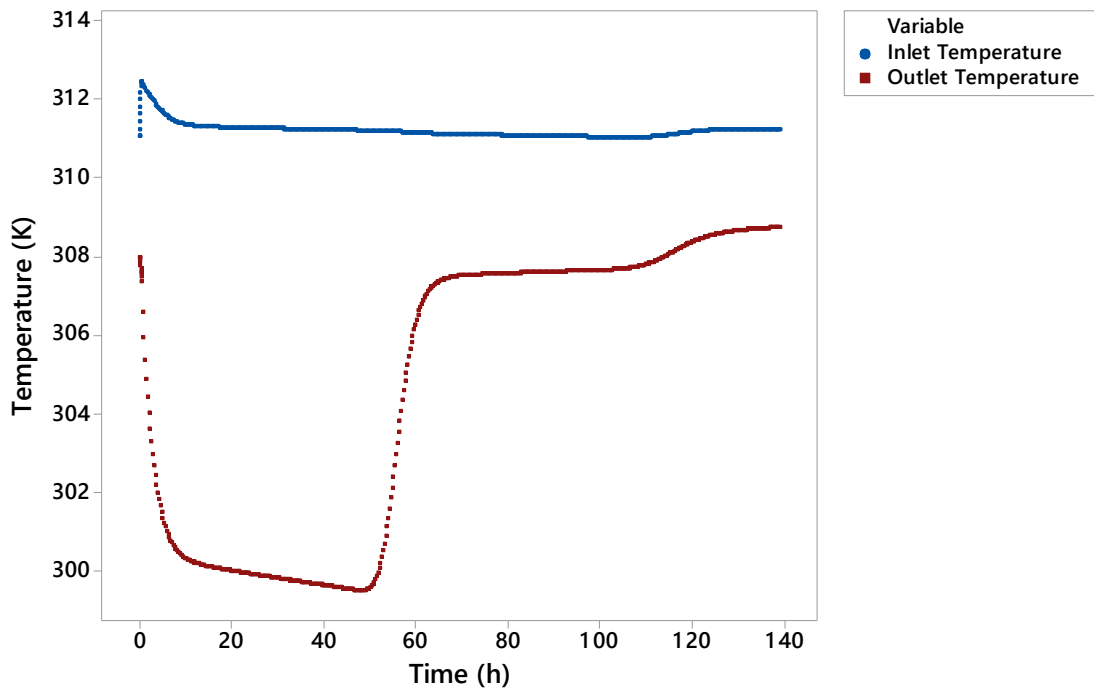


Figure 3-19: Inlet and Outlet Temperature for Pipeline 001

Figure 3-19 shows that while the temperature at the inlet remains above the critical temperature the temperature at the outlet of the pipeline drops below 304.25K as the flowrate falls. The model is therefore predicting that the CO<sub>2</sub> will transition from the supercritical phase, into the liquid phase. The model however didn't indicate that there was two phase flow within the system at any point during the simulation. To explain this, it can be reasoned that the supercritical phase is an intermediary phase between the gas phase and the liquid phase as it has a density similar to a liquid

but a viscosity more similar to a gas and therefore the transition between the two phases is more subtle and the changes in the physical properties are less extreme than between the gas phase and the liquid phase.

The temperature losses between the inlet and the outlet of the pipeline can be explained by the heat losses between the pipe wall and the surrounding material which had a specified temperature of 278 K.

As shown with the liquid phase CO<sub>2</sub> simulation, there is a correlation between the temperature and the flowrate which can again be explained by the effect of temperature on the fluid density, however as with the liquid CO<sub>2</sub> simulation the change in temperature at the outlet of the pipeline cannot be explained with the heat loss equations.

### 3.5.3 Carbon Dioxide Phase Evaluation

The aim of this study was to compare and contrast the response of liquid and supercritical phase CO<sub>2</sub> to reducing the flowrate to the inlet of a pipeline. The areas in which the two phases are to be compared are flowrate, pressure and temperature.

#### 3.5.3.1 Flowrate

Figure 3-20 shows the inlet and outlet pipeline flowrate for both the supercritical and liquid phase simulations. There are two observable differences between the response in the outlet flowrate from a drop at the inlet flowrate. Both phases show an offset between the inlet flowrate and the outlet flowrate however the difference between the two is that in the size of the offset. The liquid phase simulation has shown an offset of approximately 4kg/s whereas the supercritical phase simulation

shows a much greater offset of approximately 10kg/s. It has already been reasoned that the offset is caused by the temperature drop causing a change in the density and hence affecting the flowrate. Figure 3-23 shows a greater temperature drop when the CO<sub>2</sub> was transported in the supercritical phase when compared to the temperature drop in the liquid phase. The reason behind this is due to the greater temperature difference between the fluid in the supercritical phase and the surrounding material, therefore there is a greater driving force for heat loss which results in a larger temperature drop along the pipeline.

The second difference the model shows between transporting CO<sub>2</sub> in the supercritical phase and the liquid phase is the time it takes for the offset at the outlet of the pipeline to decrease. Figure 3-21 shows that the flowrate 'wave' in the supercritical phase travels at a greater velocity along the pipe than the 'wave' shown in the liquid phase simulation, this results in the outlet flowrate reaching the set point faster when transporting supercritical CO<sub>2</sub> compared to liquid CO<sub>2</sub>.

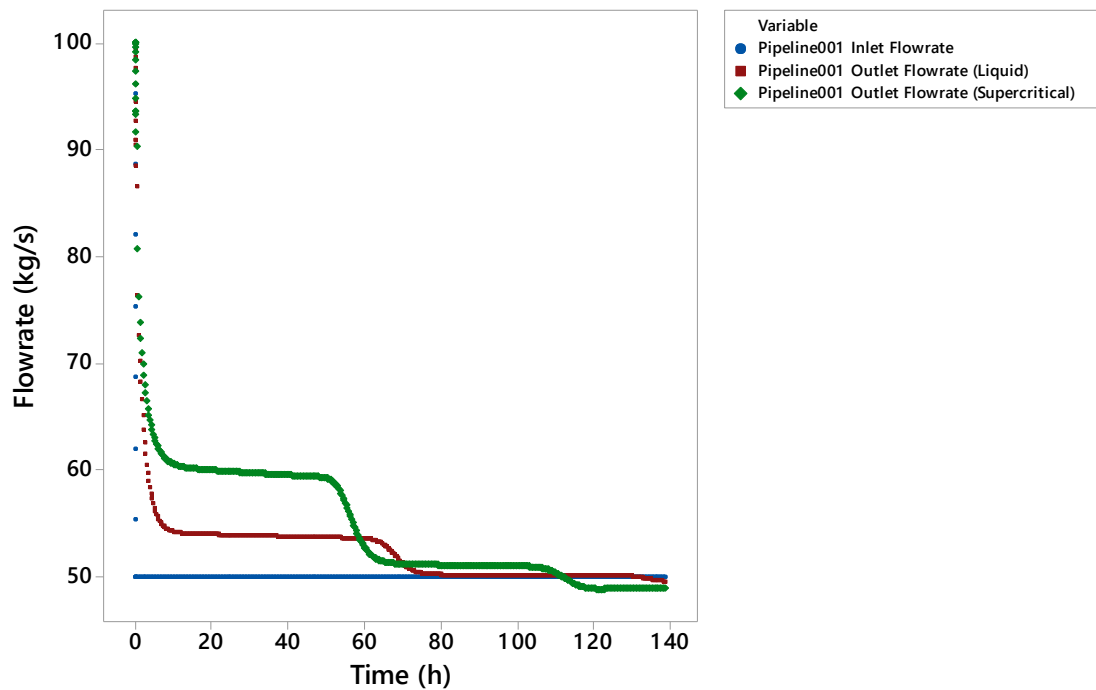


Figure 3-20: Inlet and Outlet Flowrate for Liquid and Supercritical CO2

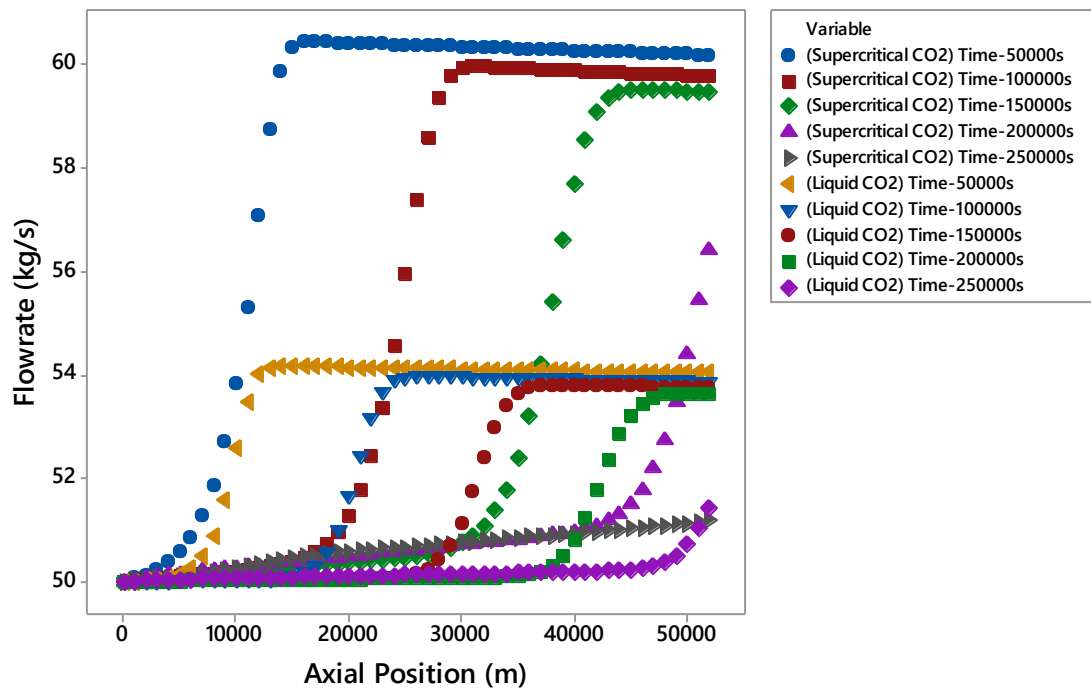


Figure 3-21: Flowrate profile along Pipeline001 for Supercritical and Liquid CO2

### 3.5.3.2 Pressure

The pipeline inlet and outlet pressures can be seen in Figure 3-22 for both supercritical phase and liquid phase CO<sub>2</sub> models. The model shows a higher inlet pressure requirement for CO<sub>2</sub> in the supercritical phase than in the liquid phase. The reason behind this is due to the greater pressure drop along the pipeline when transporting in the supercritical phase compared to the liquid phase, which is due to supercritical CO<sub>2</sub> having physical properties between that of a liquid and a gas. This can be further explained with the Darcy-Weisbach equation which shows that the pressure drop along a pipeline is a function of the fluid density and the flow velocity squared. As the density of the liquid CO<sub>2</sub> is higher than that of supercritical CO<sub>2</sub> this will increase the pressure drop, however the flow velocity of the supercritical phase CO<sub>2</sub> will be higher than that of the liquid phase when the mass flowrates of both are the same, which is the case in this scenario. As the flow velocity in the Darcy-Weisbach equation is squared, this will have a greater impact on the pressure drop than the fluid density and is therefore the reason that a higher pressure is necessary for supercritical phase CO<sub>2</sub> compared to when it is in the liquid phase.

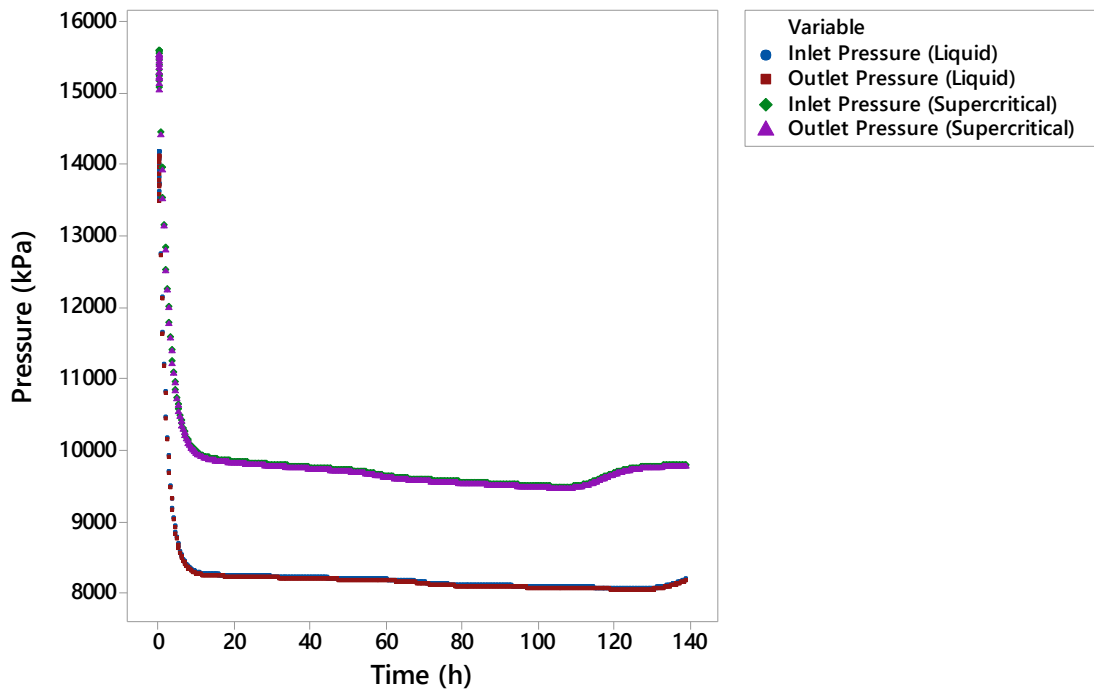


Figure 3-22: Inlet and Outlet Pressure for Liquid and Supercritical CO<sub>2</sub>

### 3.5.3.3 Temperature

Figure 3-23 shows the temperature profiles at the inlet and outlet of pipeline001 for both the liquid and supercritical phase CO<sub>2</sub>. The temperature at the inlet of the supercritical phase is 13K higher than that of the liquid phase CO<sub>2</sub>. This is because both these values were predefined in the model to ensure that the fluid entered the pipeline in the desired phase.

From observing the temperature difference between the inlet and the outlet of the pipeline it can be seen that there is a greater temperature drop along the length of the pipeline when transporting in the supercritical phase, where at time 0 there is a temperature drop of 4K whereas in the liquid phase, there is a smaller temperature drop of 1.96K. The reason behind this observation is that there is a greater temperature difference between the supercritical phase CO<sub>2</sub> and the surrounding

material of the pipeline; this therefore provides a greater driving force for heat loss from the fluid which consequently causes a larger temperature drop.

Comparing the temperature change over time at the outlet of the pipeline, for the liquid and the supercritical phase CO<sub>2</sub>, it is observed that there is a greater temperature drop in the supercritical phase CO<sub>2</sub> when the flowrate is reduced but the temperature rises again after a shorter period of time when compared to the liquid phase CO<sub>2</sub>. This difference is comparable to the differences observed in the flowrate where there is a larger offset but lasts for a shorter duration.

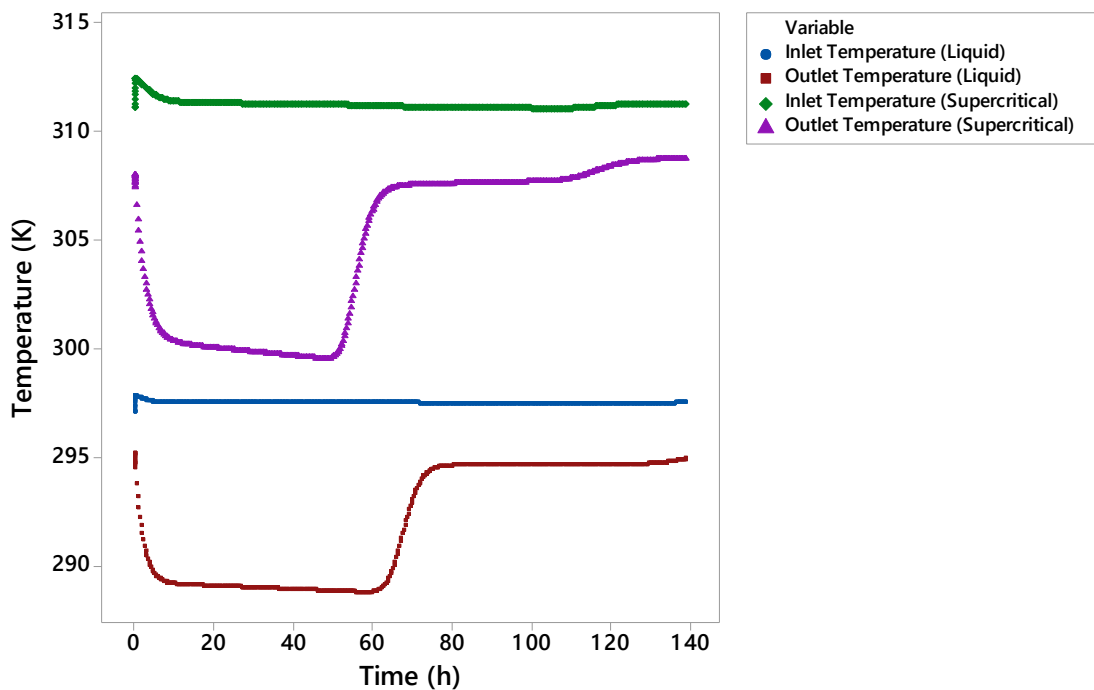


Figure 3-23: Inlet and Outlet Temperature for Liquid and Supercritical CO<sub>2</sub>

### 3.6 Conclusion

The simulation of a pipeline transporting CO<sub>2</sub> in the liquid and supercritical phases has given results which show how the flowrate, pressure and temperature of the CO<sub>2</sub> change when there is a drop at the inlet of the pipeline. The outputs from the model show that the

flowrate at the outlet of the pipeline in both the liquid and supercritical phase falls at a rate slower than the inlet and an offset in the flowrate occurs between the inlet and the outlet. The duration of the offset is determined by the velocity of the fluid, this explains why the offset occurs for a shorter duration when transporting in the supercritical phase when compared to the liquid phase as the same inlet mass flowrate was prescribed for both phases which results in the velocity of the fluid being greater for the supercritical phase CO<sub>2</sub>. The results from the modelling also mean that the hypothesis can be accepted as the model indicates that the gCCS model will show that the rate of change in the outlet flowrate of a CO<sub>2</sub> pipeline when the inlet flowrate is reduced, will be greater when the CO<sub>2</sub> is transported in the subcooled liquid phase compared to the supercritical phase.

The simulation outputs show that the pressure of the CO<sub>2</sub> transported in the supercritical phase will be required to be 12 bar higher at the pipeline inlet than when transported in the liquid phase, this has been explained with the use of the Darcy-Weisbach equation. This result can be justified by the requirement of the reservoir to maintain a constant pressure of 150bar. This higher pressure at the inlet makes up for the lower pressure increase as the fluid flows through the well.

The results from the simulations show that there is a temperature drop along the pipeline for both liquid and supercritical phase CO<sub>2</sub>. The reason behind this temperature drop is due to the temperature of the surrounding soil being lower than the fluid temperature. There is a greater temperature drop of the fluid along the pipeline when the CO<sub>2</sub> is transported in the supercritical phase. This is due to the higher inlet temperature of the supercritical CO<sub>2</sub> which means there is a greater



temperature difference between the fluid and the surrounding soil and hence a greater driving force for heat loss and a greater temperature change.

There are some outputs from the simulations that cannot be explained such as the pipeline outlet temperature change, however it can be theorised that this is occurring due to unknown interactions within the code that underpins the software. However given that there is limited access to this code, a precise understanding of why the model behaves in this way cannot be developed.

## **Chapter 4 – Effects of Impurities and Multiple Sources of CO<sub>2</sub> on Pipeline Flow**

## 4.1 Introduction

Chapter 3 covered a CO<sub>2</sub> transport scenario in which pure carbon dioxide was transported via a single pipeline from a single CO<sub>2</sub> source. This allowed for a base case scenario to be developed in which other scenarios can be compared. In this chapter, two scenarios will be investigated that will build on the work presented in Chapter 3.

In a real CCS process there is likely to be impurities in the CO<sub>2</sub> which are known to effect the physical properties of the fluid. The impurities within the CO<sub>2</sub> vary depending on the capture process used. It is therefore important to understand how these impurities effect the flow of CO<sub>2</sub> within the pipeline. It has been argued in the literature review that the gCCS software is the most appropriate software as it has the capability to model impurities within CO<sub>2</sub> with greater accuracy than other commercial software packages as it uses statistical associating fluid theory to determine the equations of state, which are believed to be more accurate than cubic equations of state in the absence of experimental data. It is for this reason that gCCS was the software of choice to model CO<sub>2</sub> pipelines.

In the development of carbon capture and storage, it has been found that the building of clusters of CO<sub>2</sub> sources which share transportation infrastructure is the most economic way to perpetuate the expansion of the technology. The concept behind this is that multiple sources of CO<sub>2</sub> whether from IGCC plants or CCGT's will connect via a branch pipeline to a trunk pipeline that will transport the CO<sub>2</sub> to the site for sequestration. As there are different sources of CO<sub>2</sub> it is expected that each will operate differently from each other. For the research presented here, the flow

of CO<sub>2</sub> from an IGCC and a CCGT are modelled. The reason behind modelling these two different plants is that IGCC plants are expected to operate as base load, given the inflexibility of this technology and hence the CO<sub>2</sub> flowrate will remain relatively consistent. CCGT's are operated as peaking plants, so the flow of CO<sub>2</sub> to the pipeline is expected to be variable. This chapter will investigate the effects of a consistent flow of CO<sub>2</sub> into a pipeline and a variable flow.

## **4.2 Hypothesis**

For this chapter two hypothesis will be investigated. The first will cover the effects of impurities on the flow of CO<sub>2</sub> in the pipeline and will try to prove or disprove the following;

'The gCCS modelling tool will demonstrate that impurities within the carbon dioxide transported for CCS will cause a different response in the fluid dynamics to changing the inlet flowrate compared to when transporting pure CO<sub>2</sub>'

The second part of this chapter will aim to prove or disprove the following hypothesis;

'The gCCS modelling tool will show that varying the flowrate of one of two sources of CO<sub>2</sub> will have a different effect on the fluid dynamics of the CO<sub>2</sub> within the trunk pipeline, compared to when there is only a single source of CO<sub>2</sub>'

## **4.3 CO<sub>2</sub> with Impurities Case Model Development**

The model that has been developed to test the effects of impurities on the flow of CO<sub>2</sub> within a pipeline is the same as the model in Chapter 3 where the base case scenario of pure CO<sub>2</sub> in a single pipeline was analysed. The only difference between the scenarios is the composition of the CO<sub>2</sub> entering the pipeline. Keeping all other

parameters the same allows for a direct comparison between transporting pure CO<sub>2</sub> and CO<sub>2</sub> with impurities. The topology for this scenario is the same as that in Figure 3-8.

#### 4.3.1 Impurities

The impurities to be investigated are those which are likely to be found within the captured CO<sub>2</sub>. The three CCS capture technologies contain different impurities. Post combustion capture contains nitrogen as the main impurity, this is due to the combustion of the natural gas in air in CCGT power plants. Pre-combustion carbon capture contains hydrogen as the main impurity which is due to the gasification process which produces hydrogen as the product. After the capture process not all the hydrogen is separated from the CO<sub>2</sub> and remains in small quantities. Oxyfuel combustion contains oxygen as the impurity due to the combustion of the fuel with pure oxygen instead of air. These three components are therefore the ones of interest to understand the effects of impurities on the flow of CO<sub>2</sub>. While it has been mentioned in Chapter 2 that there are other impurities within the CO<sub>2</sub> these are in significantly low quantities and have therefore not been included in the analysis in this research.

To develop the scenario it is also important to know what proportion of the fluid entering the pipeline is the impurity. This has been covered in the literature and is summarised in Table 4-1. However to allow for a direct comparison between each impurity the same percentage was used for each in the simulation. A value of 0.2 mol/mol was used as the input into the model for each case as this was the lowest concentration of any of the impurities and therefore indicates whether the smallest concentration of any of the impurities would have any effect on the system.

Table 4-1: Common Impurities Found in Captured CO<sub>2</sub>

Capture Technology	Main Impurity	% vol/vol
Post-combustion capture	Nitrogen	0.2
Pre-combustion capture	Hydrogen	1.5
Oxyfuel combustion	Oxygen	3.2

The simulation carried out for this scenario is the same as that of the base case developed in chapter 3, in which the flowrate into the pipeline begins at a steady state of 100 kg s<sup>-1</sup>. The flowrate then falls to 50 kg s<sup>-1</sup> at a rate of 4 kg s<sup>-1</sup> min<sup>-1</sup>. The code used to produce this simulation is shown in Appendix A.1.

## 4.4 Results

### 4.4.1 Nitrogen Case

The results for the nitrogen impurities case are shown in Figure 4-1 to 4-4. Figure 4-1 shows the flowrate change at the inlet and outlet of pipeline 001. As with the base case there are three distinct phases in the outlet flowrate of the pipeline which result from the change in the inlet flowrate. The three phases are the 'delayed response phase', the 'offset phase' and the 'reduction phase'. This indicates that the presence of nitrogen as an impurity does not affect the shape of the response at the outlet of the pipeline.

Figure 4-4 shows the results from the nitrogen impurity scenario along with the base case scenario. Observing Figure 4-4 shows that the presence of nitrogen in the CO<sub>2</sub>

does impact on the fluid dynamics. The presence of nitrogen in the CO<sub>2</sub> is shown to cause an increase in the offset from the base case. The increase in the offset between the base case and the nitrogen impurity case is approximately 1 kg/s.

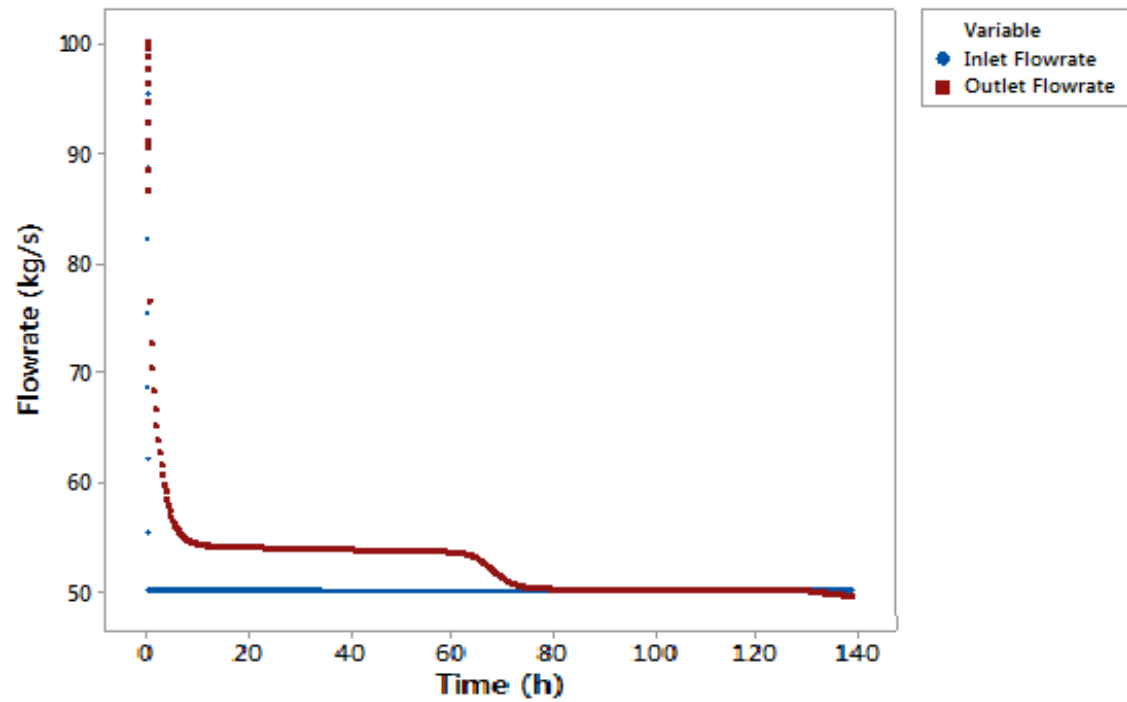


Figure 4-1: Pipeline Inlet and Outlet Flowrate (CO<sub>2</sub> + N<sub>2</sub>)

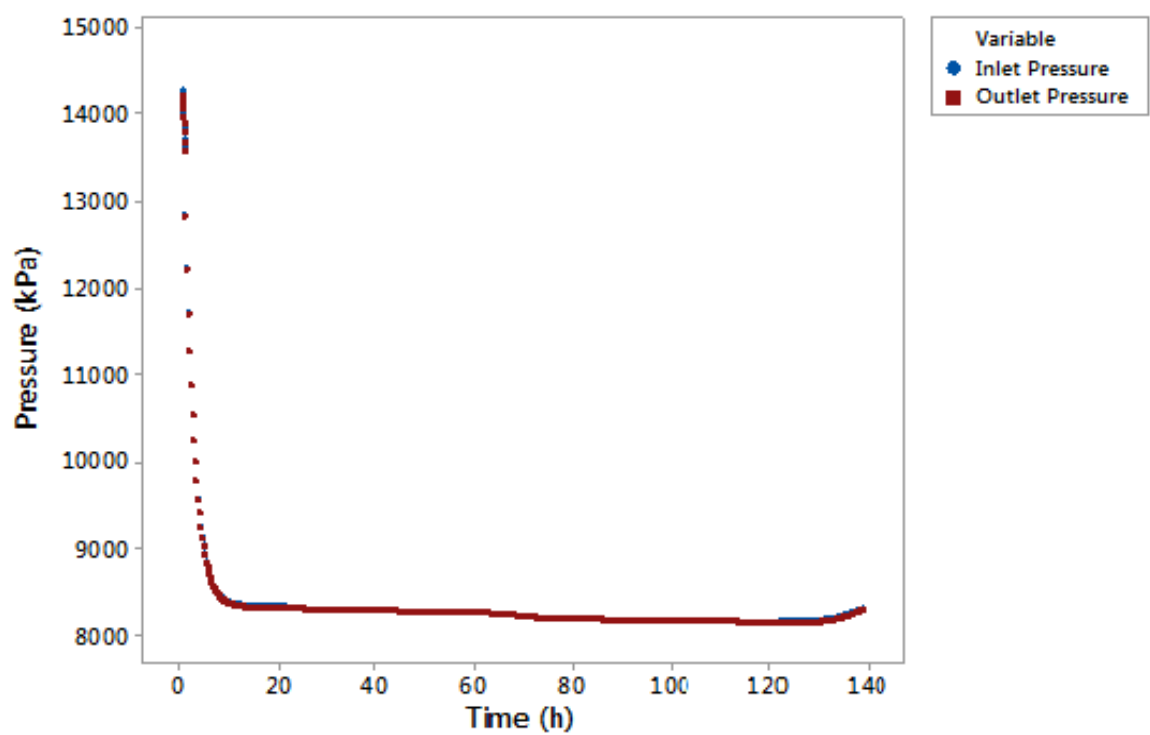


Figure 4-2: Pipeline Inlet and Outlet Pressure ( $\text{CO}_2 + \text{N}_2$ )



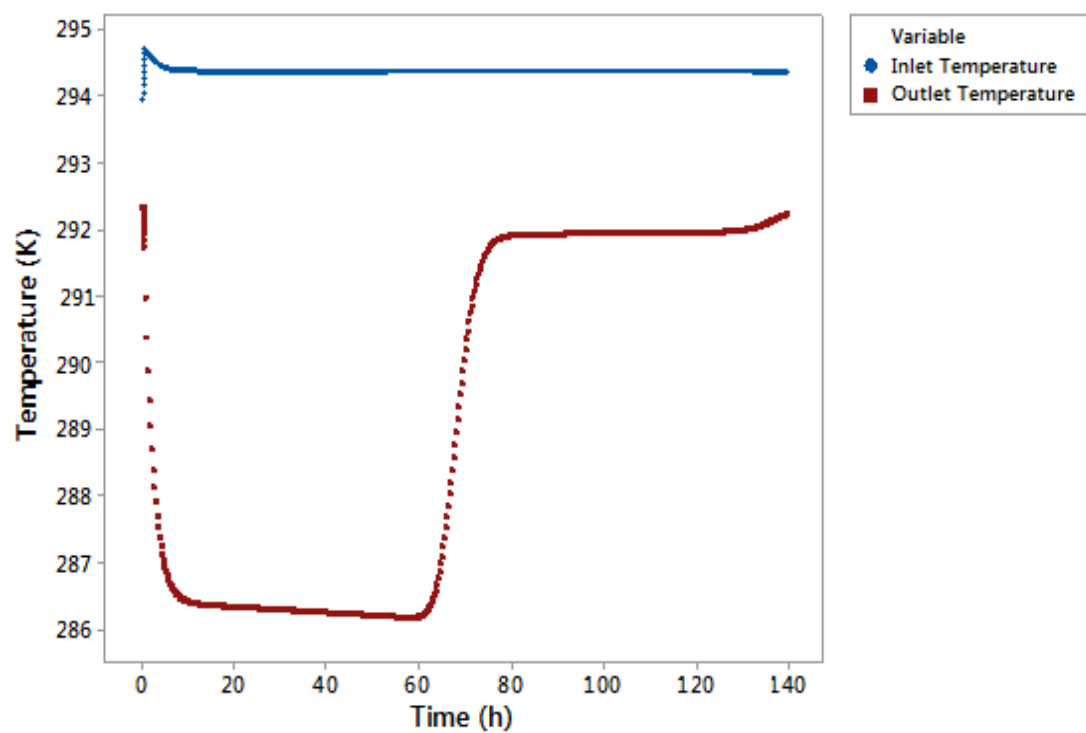


Figure 4-3: Pipeline Inlet and Outlet Temperature (CO<sub>2</sub> + N<sub>2</sub>)

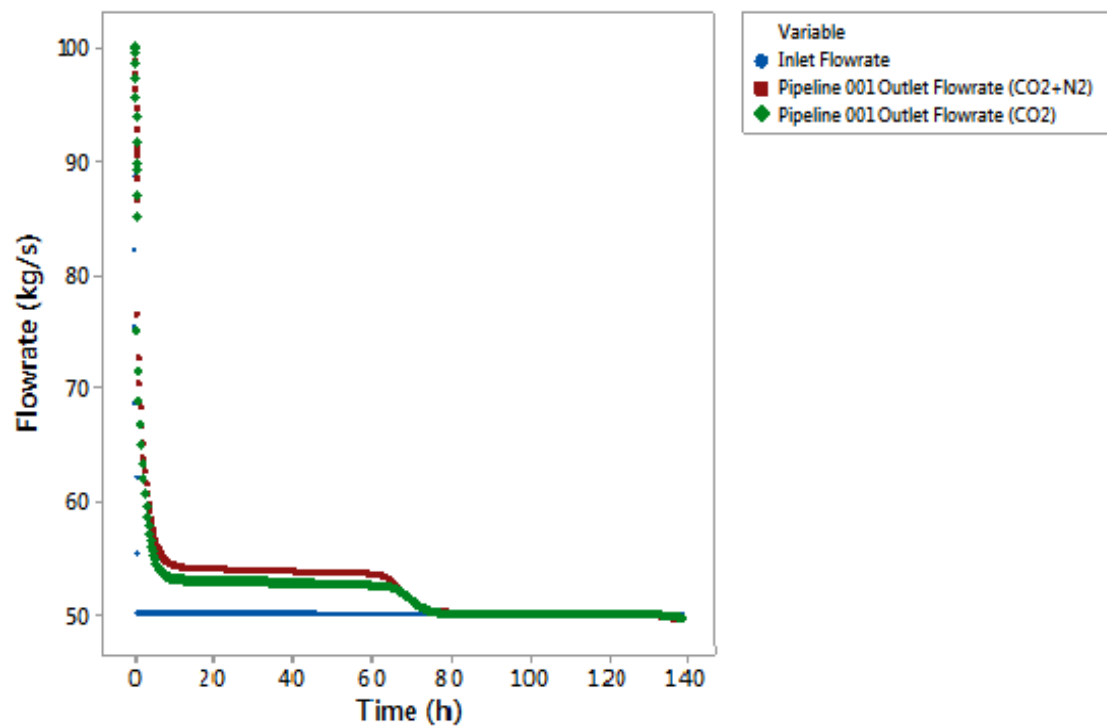


Figure 4-4: Pipeline Inlet and Outlet Flowrate (Pure CO<sub>2</sub> & CO<sub>2</sub> + N<sub>2</sub>)

#### 4.4.2 Hydrogen Case

Figures 4-5 to 4-8 show the flowrate results for the H<sub>2</sub> and CO<sub>2</sub> scenario. Figure 4-5 shows that the three phases as seen in the base case are also observed when there is hydrogen as an impurity. Figure 4-8 Shows that the addition of hydrogen in the CO<sub>2</sub> does impact the response at the outlet of the pipeline when compared to the base case of pure CO<sub>2</sub>. In the same manner that the addition of nitrogen caused an increase in the offset during the 'offset phase' the addition of hydrogen also caused this same increase in the offset. However the addition of hydrogen caused a greater impact than the nitrogen with an increase in the offset of approximately 2kg/s.

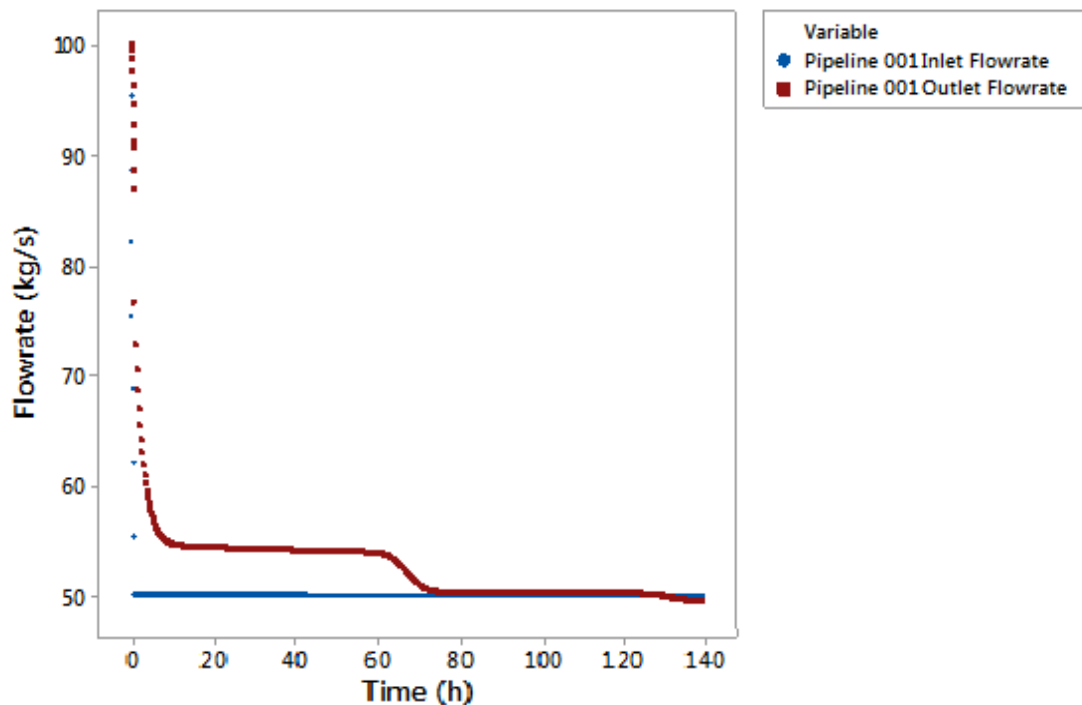


Figure 4-5: Pipeline Inlet and Outlet Flowrate (CO<sub>2</sub> + H<sub>2</sub>)

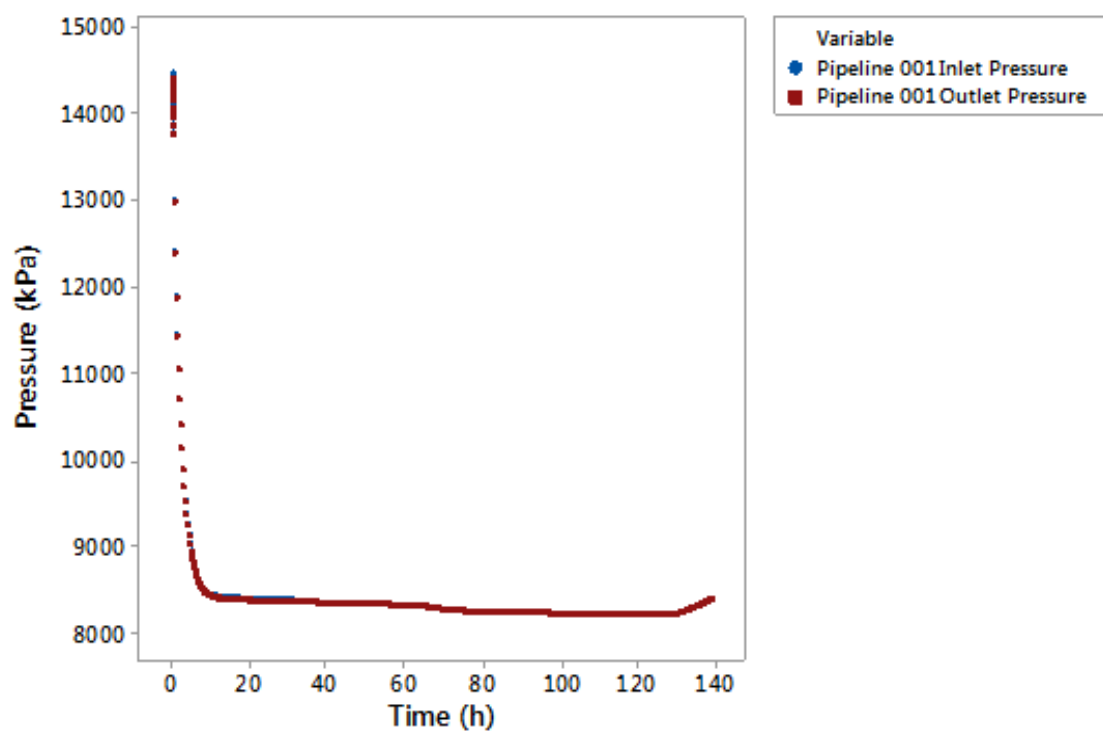


Figure 4-6: Pipeline Inlet and Outlet Pressure ( $\text{CO}_2 + \text{H}_2$ )

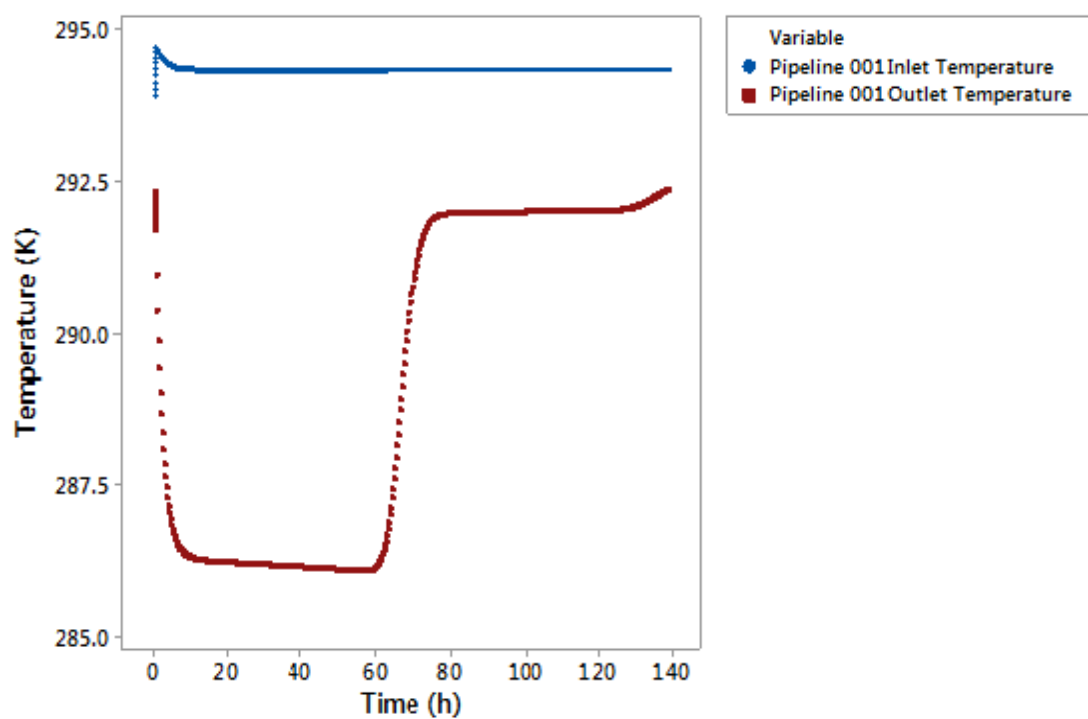


Figure 4-7: Pipeline Inlet and Outlet Temperature ( $\text{CO}_2 + \text{H}_2$ )

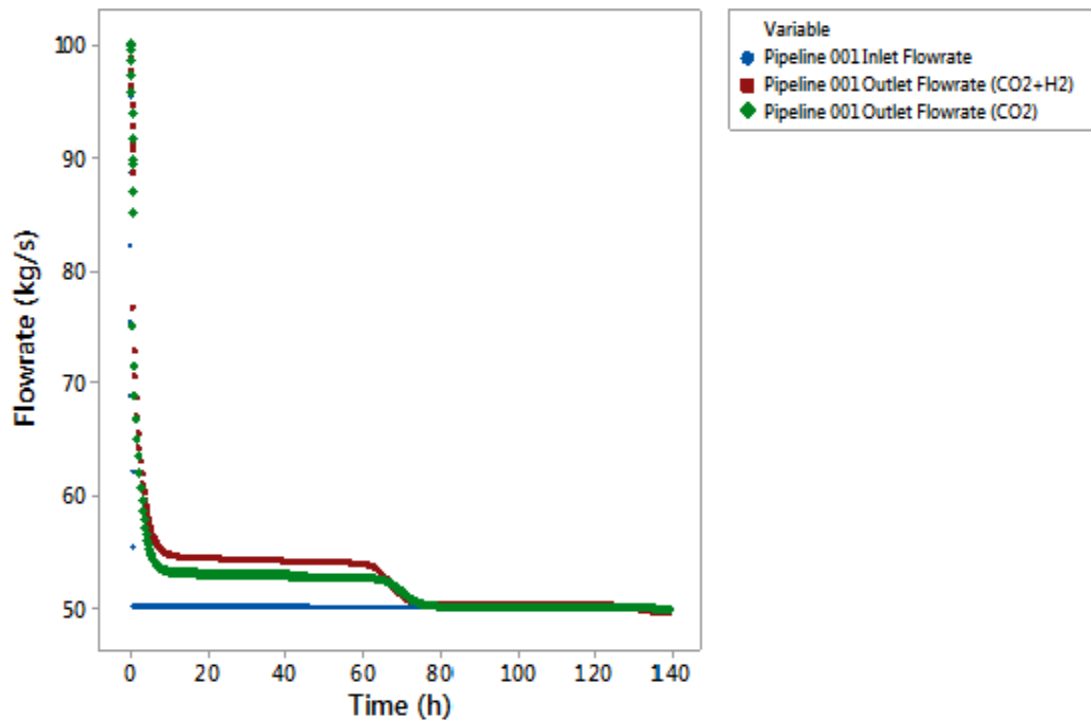


Figure 4-8: Pipeline Inlet and Outlet Flowrate (Pure CO<sub>2</sub> & CO<sub>2</sub> + H<sub>2</sub>)

#### 4.4.3 Oxygen Case

Figures 4-9 to 4-12 show the results from the carbon dioxide and oxygen simulation. As with the nitrogen and the hydrogen simulations the response in the flowrate, temperature and pressure at the outlet of the pipeline follows the same profile as that of the base case simulation. The difference in the offset phase between the pure CO<sub>2</sub> and the oxygen impurity is again observed. In the case for the presence of oxygen as in impurity, there is an increase in the offset at the outlet of the flowrate of approximately 1 kg/s which is similar to that of the nitrogen impurity case.

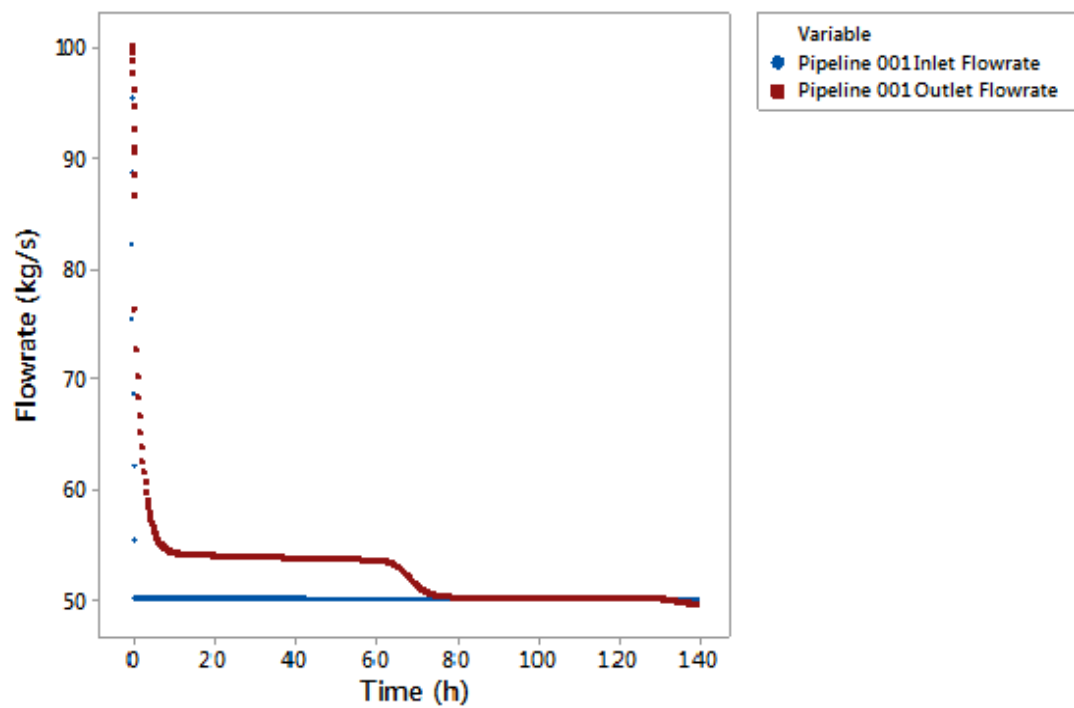


Figure 4-9: Pipeline Inlet and Outlet Flowrate ( $\text{CO}_2 + \text{O}_2$ )

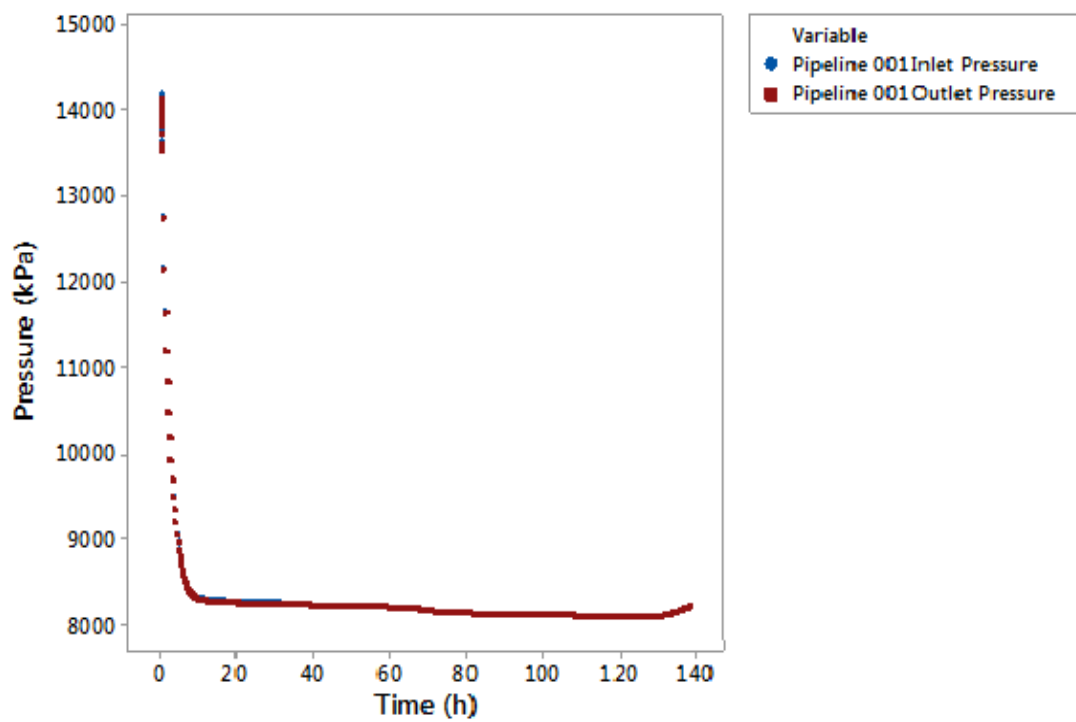


Figure 4-10: Pipeline Inlet and Outlet Pressure ( $\text{CO}_2 + \text{O}_2$ )

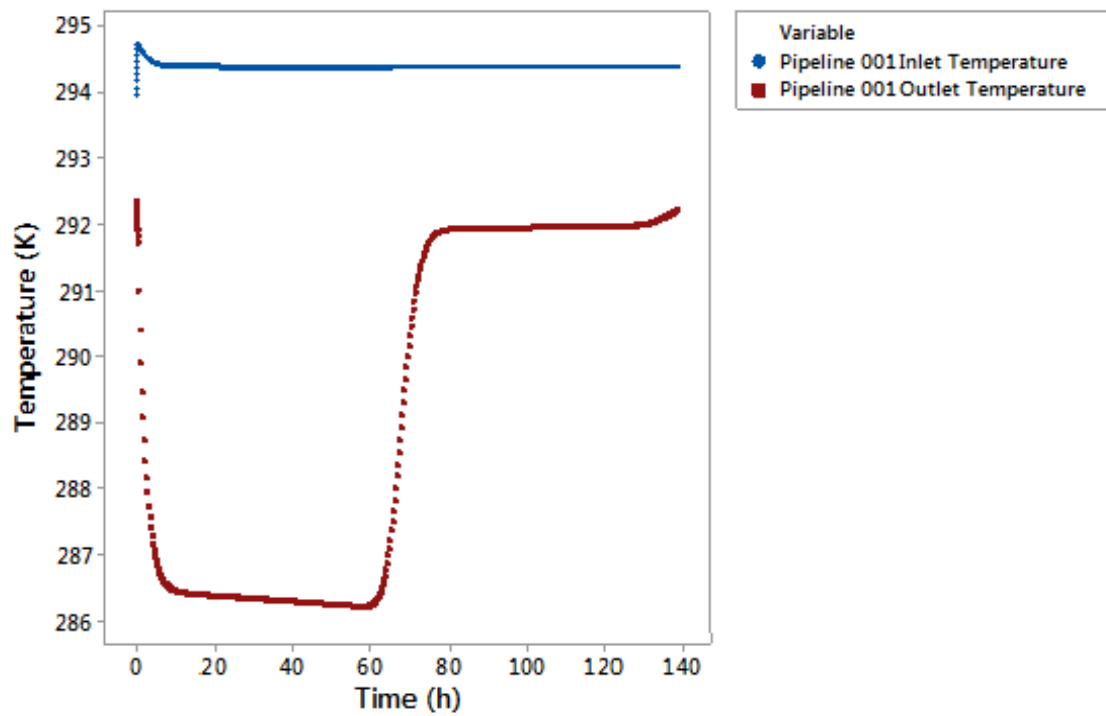


Figure 4-11: Pipeline Inlet and Outlet Temperature ( $\text{CO}_2 + \text{O}_2$ )

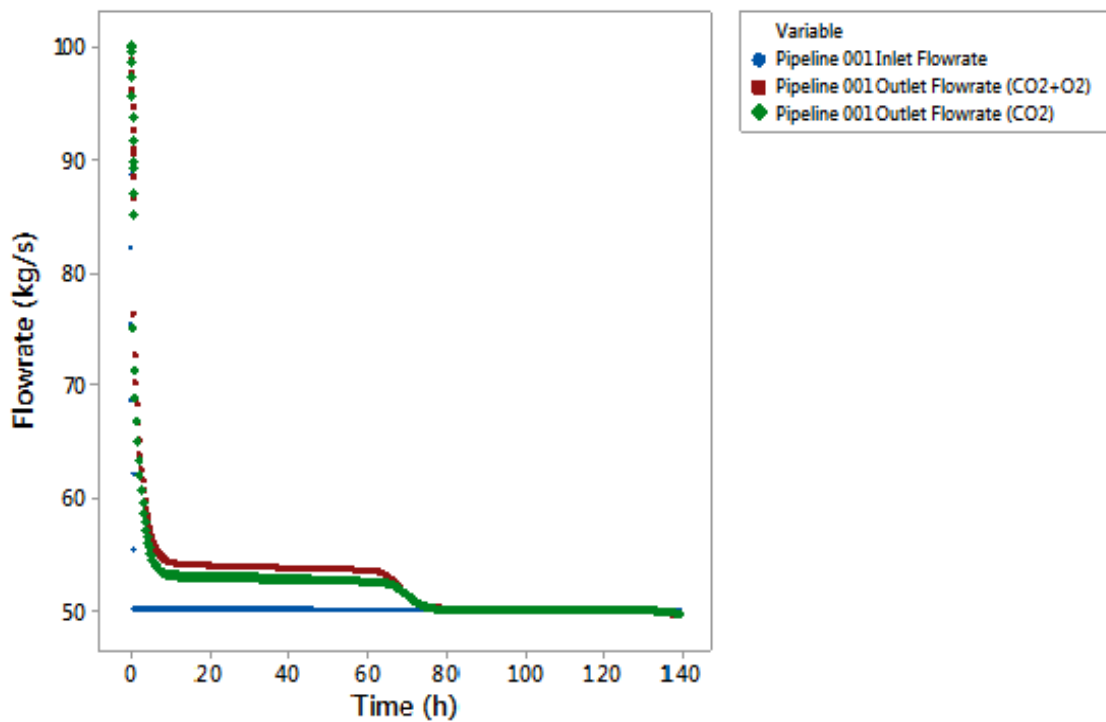


Figure 4-12: Pipeline Inlet and Outlet Flowrate (Pure  $\text{CO}_2$  &  $\text{CO}_2 + \text{O}_2$ )

## 4.5 Analysis

The three scenarios that have been developed and modelled show the impact of impurities in the CO<sub>2</sub> on the flow dynamics when the inlet flowrate to the pipeline is reduced. In all three cases there is the same three phases as observed in the base case scenario. The difference between the base case and the impurities case is the difference in the 'offset phase'. The modelling of the three scenarios shows that the addition of nitrogen, hydrogen or oxygen cause an increase in the offset between the inlet flowrate and the outlet flowrate. This effect can be explained through the impact of impurities on the physical properties of the fluid entering the pipeline. As nitrogen, hydrogen and oxygen all have different molecular weights to carbon dioxide they will affect the total density of the fluid and hence affect the flowrate.

There is also a difference between each of the impurities, with oxygen having the smallest impact on the offset and hydrogen having the greatest impact on the offset. This again can be explained through the difference between each of the impurities compared to carbon dioxide, as oxygen has the closest molecular mass to carbon dioxide and hydrogen has the biggest difference in molecular mass to carbon dioxide. This theory is supported by how both nitrogen and oxygen have the same approximate impact on the offset and both have the closest molecular mass out of the three impurities, with nitrogen having a molecular mass of 28 g mol<sup>-1</sup> and oxygen having a molecular mass of 32 g mol<sup>-1</sup>. This therefore explains why the results from the hydrogen impurity scenario would deviate the most from the base case with pure carbon dioxide. This therefore indicates that the three carbon capture technologies; pre-combustion, post-combustion and oxyfuel combustion will all

have different flow dynamics during transportation, due to the presence of the specific impurities present in the CO<sub>2</sub>. It is expected that the greater the amount of an impurity in the CO<sub>2</sub>, the greater the effects of the presence of the impurity will be.

The results from the simulations show that the original hypothesis was correct, as the model shows that the presence of impurities that are likely to be found within captured CO<sub>2</sub> do impact on the flowrate at the outlet of the pipeline.

## **4.6 Multiple Sources of CO<sub>2</sub> Model Development**

### **4.6.1 Pipeline Dimensions**

To develop the model it was first necessary to understand how a pipeline receiving CO<sub>2</sub> from multiple sources would be designed. To avoid over complicating the model, the simplest scenario of two CO<sub>2</sub> sources was chosen as the modelling case. A previous study looking at CO<sub>2</sub> flow from multiple sources modelled the system with two parallel pipelines from the two sources which then mix the flows downstream and enter a larger diameter single pipeline which then transports the CO<sub>2</sub> to a reservoir to be sequestered. A similar approach was taken here to develop the pipeline model. As the two parallel pipelines from the CO<sub>2</sub> sources are transporting a smaller amount of fluid than the main trunk line further downstream, the pipeline diameter of these two lines is smaller which gives greater economic benefit than having oversized pipelines for the branch lines. Table 4-2 shows the length and internal diameter of the pipelines shown on Figure 4-13. The well dimensions used in this model are the same as those used for the two previous scenarios, with the reservoir also having the same inputs.



Table 4-2: Pipeline Dimensions

Pipeline segment	Internal Diameter (m)	Length (m)
Pipeline 001	0.3048	2000
Pipeline 002	0.3048	2000
Pipeline 003	0.6096	52000
Pipeline 004	0.6096	52000

#### 4.6.2 Pipeline Flows

The temperature and pressure of the pipelines was set up the same as the base case pipeline model in chapter 3. The flowrate of the fluid however was set so that the initial total flowrate in the trunk pipeline was the same as the flowrate within the pipeline in in chapter 3. The flowrate of the branch pipelines was split equally so that each CO<sub>2</sub> source has an outlet flowrate of 50 kg s<sup>-1</sup>. The simulation was set up so that the flowrate from Source 001 was reduced from 50 kg s<sup>-1</sup> to 25 kg s<sup>-1</sup> while the flowrate from Source 002 was kept constant throughout the simulation, this therefore gives a total flowrate in Pipeline 003 of 75 kg s<sup>-1</sup>. This approach was taken to simulate a base load power plant with CCS and a load following power plant with CCS which both feed CO<sub>2</sub> into the same trunk pipeline.

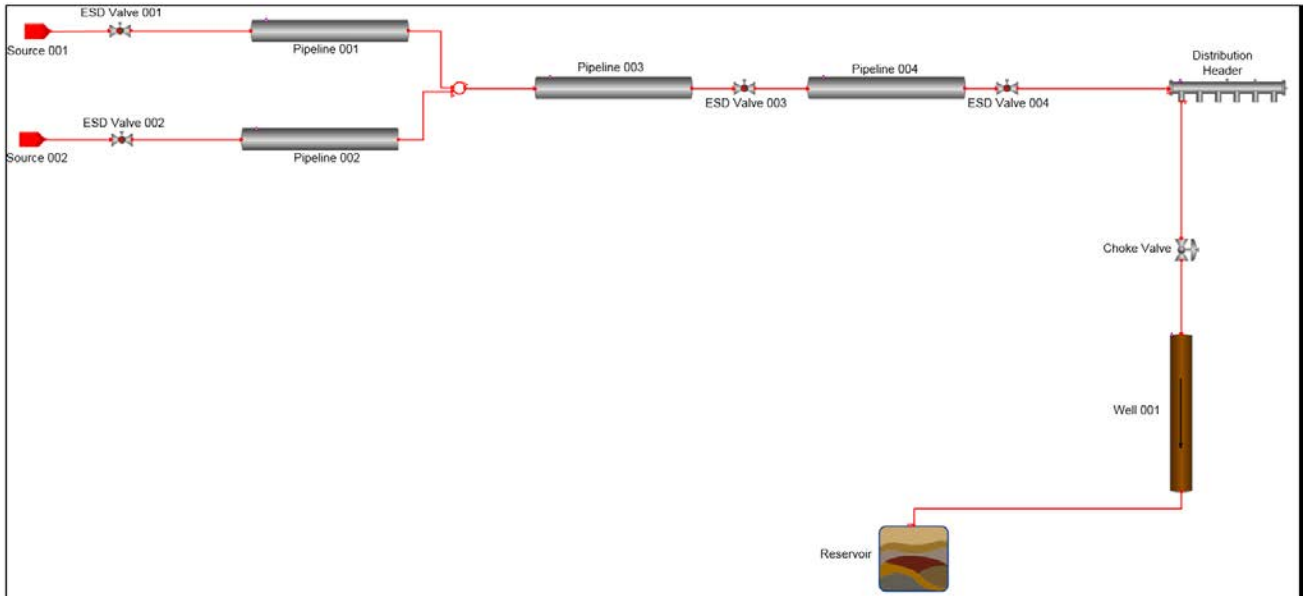


Figure 4-13: Pipeline Topology with Multiple Sources of CO<sub>2</sub>

## 4.7 Results

The results from the simulation are focussed on the input and output variables of Pipeline 001, Pipeline 002 and Pipeline 003. The flowrate, temperature and pressure are the areas of interest and where the analysis of the simulation is focussed.

### 4.7.1 Flowrate analysis

Figure 4-14 shows the flowrate profiles at the inlets and outlets of the two branch pipelines, Pipeline 001 and 002 and then the main trunk Pipeline 003. The results show that the flowrate at the outlet of Pipeline 001 falls at the same rate as the inlet flowrate is reduced and reaches the output within minutes of the step change occurring and does not show an 'offset phase' as seen when the flowrate is reduced in the previous scenarios. The reason behind this is likely due to the pipe length of Pipeline 001, which is 50 km less than the pipeline in the single CO<sub>2</sub> source scenarios. Therefore the flowrate at the outlet of the pipeline can reach the set point

in a period of time before the ‘offset phase’ develops. The flowrate at the outlet of Pipeline 002 stays constant throughout the simulation. This demonstrates that the change in flowrate in Pipeline 001 does not cause any back flow within Pipeline 002. The flowrate profile at the outlet of Pipeline 003 follows that of the base case simulation, where there are three distinct phases; the ‘delayed response phase’, the ‘offset phase’ and the ‘reduction phase’.

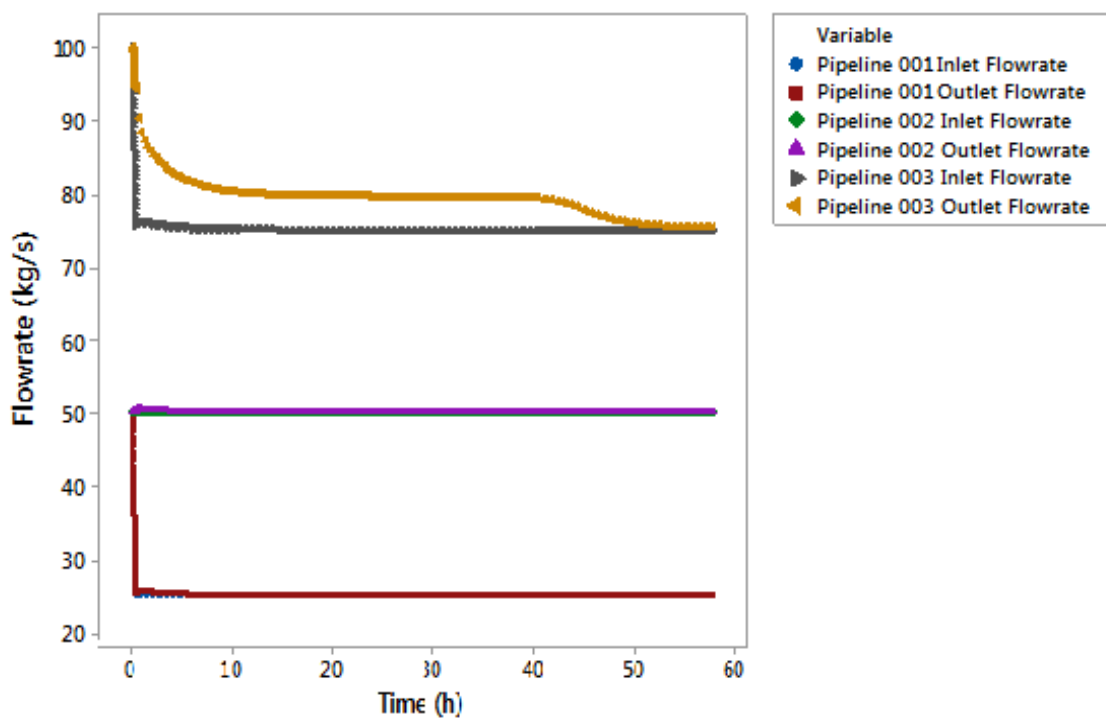


Figure 4-14: Inlet and Outlet Flowrate for Pipeline 001, Pipeline 002 and Pipeline 003

#### 4.7.2 Pressure Analysis

Figure 4-15 shows the pressure profile at the inlets of Pipeline 001, Pipeline 002 and Pipeline 003 and the outlet pressure of Pipeline 003. This results of the simulation show that a change in the flowrate in Pipeline 001 means that there is a requirement for the pressure at the inlet of Pipeline 002 to decrease at the same rate as the pressure in Pipeline 001. The reason that this response is observed is due to the way the model has been developed with the inlet pressures being

determined by the well pressure. This also ensures that there is no back pressure in Pipeline 001.

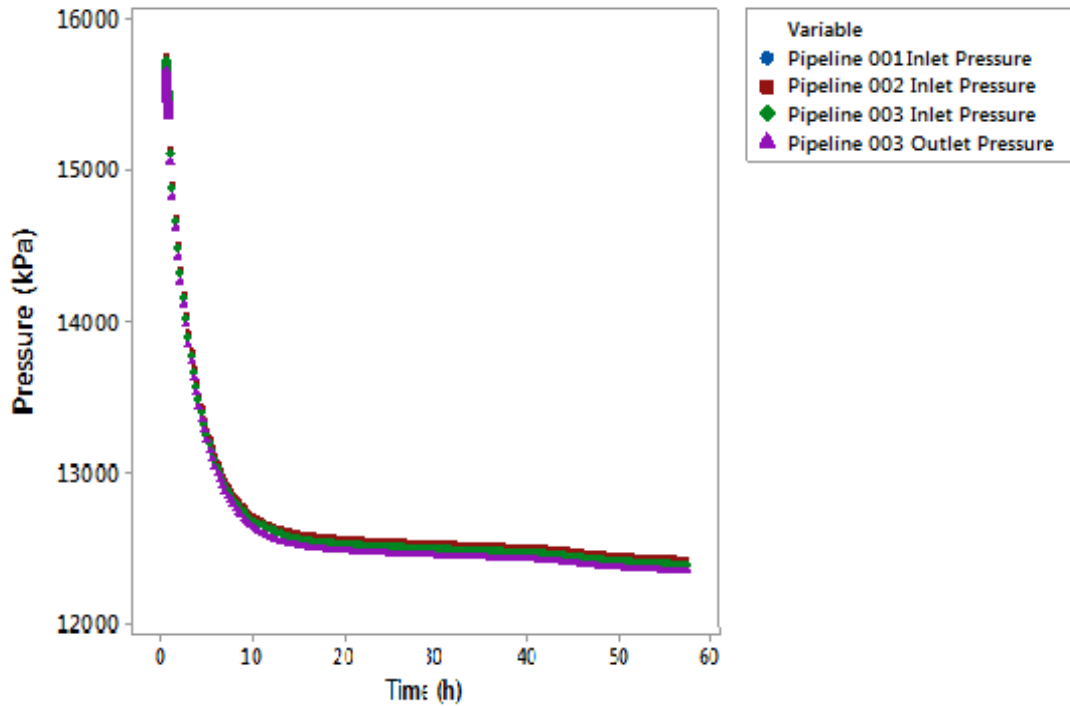


Figure 4-15: Inlet and Outlet Pressure for Pipeline 001, Pipeline 002 and Pipeline 003

#### 4.7.3 Temperature Analysis

Figure 4-16 shows the temperature profile at the inlet and outlet of Pipeline 001, Pipeline 002 and Pipeline 003. The results from the simulation show that the CO<sub>2</sub> at the outlet of Pipeline 001 increases by 1.5K when the flowrate is reduced.

However this is on contrast to the temperature of the CO<sub>2</sub> at the outlet of Pipeline 003 which follows the same profile as the base case developed in chapter 3. The difference in the response in temperature between the outlet of Pipeline 001 and Pipeline 003 can be linked to the differences in the flowrate profile at the outlets of each pipeline. While Pipeline 003 shows an offset phase between the inlet and the outlet, Pipeline 001 does not show such a response.

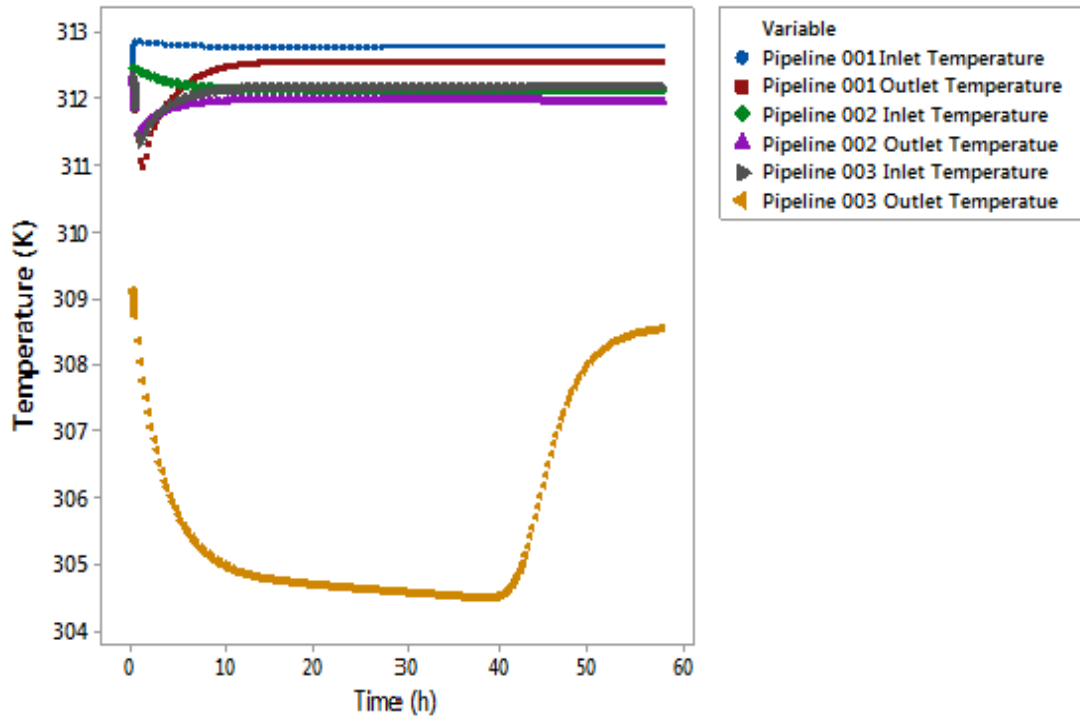


Figure 4-16: Inlet and Outlet Temperature for Pipeline 001, Pipeline 002 and Pipeline 003

## 4.8 Conclusion

The results from the impurities study have proven the original hypothesis correct as the model has shown that the presence of any of the impurities; nitrogen, hydrogen and oxygen, in the carbon dioxide case a different response in the outlet flowrate than when only pure carbon dioxide is transported. The modelling of the impurities scenarios has shown that the presence of any of the three impurities causes an increase in the difference between the inlet and the outlet of the flowrate during the 'offset phase', it is understood that the reason for this effect is due to the impact of the impurities on the physical properties of CO<sub>2</sub>, as the impurities tested within this study have been found to decrease the density of the CO<sub>2</sub> [70] and from the comparison in chapter 3 between liquid and supercritical phase CO<sub>2</sub> a lower density fluid will have a greater offset. The modelling has also shown that hydrogen as an

impurity in carbon dioxide causes a larger difference between the inlet and the outlet of the flowrate than either the oxygen or nitrogen. It is believed that this is due to the difference in the molecular weights, with  $H_2$  having a smaller molecular mass than  $N_2$  and  $O_2$  and therefore having a greater impact on the density of  $CO_2$ . This is also supported by the fact that oxygen which has the closer molecular mass to carbon dioxide than nitrogen, has a smaller impact on the flowrate.

The results from the multiple sources of  $CO_2$  modelling have proven the original hypothesis incorrect, as two sources of  $CO_2$  entering the pipeline did not cause a different response in the flowrate from the base case, of the main trunk line when there is a reduction in the flowrate of one of the sources. This is because the inlet flowrate to Pipeline 003 has the same profile as the set flowrate change to the inlet of Pipeline 001. The results also show that the offset did not occur in Pipeline 001, this will be due to one or a combination of three factors; the pipeline diameter, the pipeline length or the pipeline initial flowrate as these are the three factors in which there is a difference between Pipeline 001 and Pipeline 003. The affects of varying these factors has not been investigated and is therefore an area in which further research can be carried out. The modelling also showed that the temperature effects observed in Pipeline 003 were not observed at the outlet of Pipeline 001. It is understood that the reason for the difference in temperature profiles is due to the difference in the flowrate profile at the outlets of Pipeline 001 and Pipeline 003. The results from the simulation also reveal that under these conditions there is no reverse flow in any of the pipelines and that varying the flowrate from one source does not effect the flowrate in another branch pipeline.

## **Chapter 5 – Modelling of Shell QUEST CO<sub>2</sub> Pipeline**

## **5.1 Introduction**

### **5.1.1 Overview**

The research that has been presented in previous chapters has modelled and simulated pipeline systems which are theoretical, the values that have been used in these models have been based on assumptions. The outputs from the models in the previous chapters have not been able to be validated as there is extremely limited public data on the operation of CO<sub>2</sub> pipelines. The majority of CO<sub>2</sub> pipelines are owned by large organizations who have not published their data. Models which have not previously been validated against real pipeline data are able to predict trends as a response to changes in input variables, but are not able to accurately simulate CO<sub>2</sub> flows. Therefore, in order to be of use for predictive capability, the models require validation using pipeline CO<sub>2</sub> flow data.

During the last year of the PhD an 8 month placement with Shell Canada was organised to facilitate the collection of data from real operating CO<sub>2</sub> pipelines at their recently commenced CCS project in Alberta. Given that it was not feasible to set up a pipeline experiment to produce experimental data for the model, it was necessary to model an existing operational CO<sub>2</sub> pipeline which could be validated against real operational data.

The Shell Quest project is an operating carbon capture and storage facility which captures CO<sub>2</sub> from a hydrogen production facility. Once captured the CO<sub>2</sub> is compressed and then transported via a 65km pipeline to 3 different wellheads where the CO<sub>2</sub> is then sent approximately 2km underground where it is stored in the reservoir.



The aim of the work described within this chapter is to model the Quest pipeline using the gCCS software that has been applied for the simulations reported in earlier chapters. The parameters within the model that were tuned to match that of the Quest pipeline. The model was then set to simulate several different operating situations including start-up, shut-down and flowrate ramps. The output from the model was then compared to real data from the Quest pipeline. This is the first time that the outputs from a CO<sub>2</sub> pipeline model have been compared to real data. This gives a greater indication of the accuracy of the outputs, from the work carried out in previous chapters. This also indicates the accuracy of the SAFT equations of state as well as the gCCS software in general.

#### 5.1.2 The QUEST Carbon Capture Facility

The Shell Quest project is a CCS facility which takes approximately one third of the CO<sub>2</sub> emissions from a hydrogen production facility based in Fort Saskatchewan, Canada. This equates to 1.2 million tons per annum. The hydrogen is produced via steam methane reforming and produces a mixture containing hydrogen, carbon dioxide, carbon monoxide and water. The hydrogen is separated using pressure swing adsorption and produces a stream of approximately 99% purity which is used in upgrading of the oil sands. The rest of the gasses are then sent to the CCS facility for separation and compression. The capture process uses an advanced amine solvent to separate the CO<sub>2</sub> from the flue gasses and uses traditional absorption and stripping units to produce a high purity CO<sub>2</sub> stream. The CO<sub>2</sub> is then compressed and dehydrated in an eight-stage compressor until the CO<sub>2</sub> is in the supercritical phase and at the conditions appropriate for transport along the pipeline. Once compressed to the desired pressure and temperature the high purity CO<sub>2</sub>

stream is transported via pipeline to three different wells where it is then pumped 2km underground into a saline aquifer. Even though the three wells are located at different locations, they each pump the CO<sub>2</sub> into the same aquifer. This CCS project is set to sequester approximately 1.2MT of CO<sub>2</sub> per year. The project began operating in September 2015.

The Quest CCS project is one of the first of its kind and is one of the first to use saline aquifers for the storage of the CO<sub>2</sub> instead of the more popular method of using oil wells with enhanced oil recovery. The cost of Quest including pre-FID, capital and 10 years OPEX was approximately CND \$1.4 billion. The capital ratio was; 80% capture, 10% transport and 10% wells. Approximately CND\$120 million was provided by the Canadian federal government and CND\$745 million was given by the Albertan provincial government [71]. Since most of the costs have been provided by government some of the information regarding Quest has become publicly available. It should be noted however that the publicly available information would not allow for complete modelling of the QUEST pipeline and hence closer relationships with Shell were necessary.

## **5.2 Methodology**

To carry out the research, the first step was to obtain all the relevant information required to produce the model. Some of the design data such as pipeline size, well depths and topography are publicly available and can be found in documents on the Canadian government website. However to model the pipeline accurately it was necessary to obtain data directly from the operators working on the Quest site, as the way in which the system is operated effects how the model needs to be developed. Once the model was formulated, it then underwent testing. The testing

compares the outputs from the model to real data available from the pipeline; this data was provided through a system only accessible through Shell.

### 5.2.1 Pipeline Details

#### 5.2.1.1 *Process Unit*

The first step in producing a model for the Quest pipeline was to connect models of the process units together in gCCS. The input of the model is the source of the CO<sub>2</sub>, as systems upstream of the pipeline were not considered as part of the model in this case. The Quest pipeline includes a 65km pipeline, 6 line-break valves, 3 well heads, 3 × 2km wells each with a choke valve and a single reservoir. Within gCCS there is no specific model for a line-break valve therefore the emergency shutdown (ESD) valve model was used as a substitute. As the three wells are located several kilometres from each other, lateral pipelines that offshoot from the main pipeline were also incorporated into the model. Even though the wells are at different locations the reservoir is considered to homogeneous, it is for this reason only a single reservoir unit was used in the model.

#### 5.2.1.2 *Topography*

Knowledge of the pipeline topography is necessary for an accurate representation of the Quest pipeline. The topography shows how the pipeline elevation changes along its length. Previous models have simulated straight pipelines with no changes in elevation. The changes in elevation are incorporated to simulate the actual features of the pipeline more realistically than the simple straight pipe models are able to. Figure 5-1 [72] shows the topography of the main 65km pipeline along with the location of the 6 line block valves. As can be seen in Figure 5-1 there are elevation changes between each of the valves. Table 5-1 gives more detailed

information regarding the elevation changes between each valve as well as the length and volume of each pipeline segment. The elevation changes vary greatly, with the maximum change of 16.96m in elevation being between LBV#4 and LBV#5. The changes in elevation can be modelled within gCCS to produce an accurate representation of the pipeline.

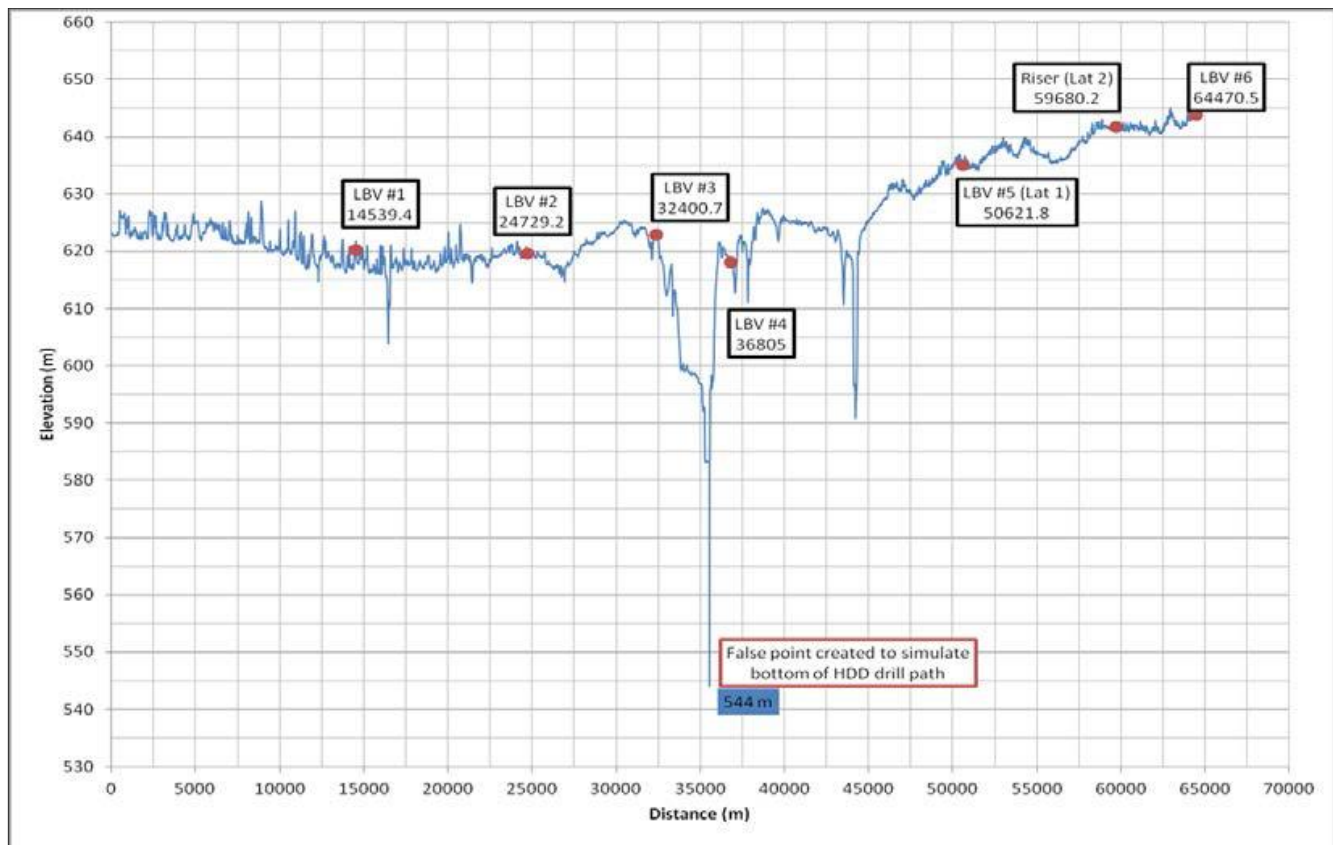


Figure 5-1: QUEST pipeline topography

Table 5-1: QUEST pipeline details

	Length [m]	Elev Change [m]	ID [mm]	Volume [m3]
Scotford-LBV#1	14539	-2.88	299.7	1,026
LBV#1-LBV#2	10190	-0.65	299.7	719
LBV#2-LBV#3	7672	3.28	299.7	541
LBV#3-LBV#4	4404	-4.73	299.7	311
LBV#4-LBV#5	13817	16.96	299.7	975
LBV#5-WS#2	9058	6.65	299.7	639
WS#2-LBV#6	4790	2.11	299.7	338
Lateral 1	1590	0.37	146.3	27
Lateral 2	1962	-0.49	146.3	33
Lateral 3	4727	-3.25	146.3	79
Total	72749			4,687

#### 5.2.1.3 Main and Branch Pipeline Dimensions

Table 5-2 shows the dimensions for both the main pipeline and the lateral pipelines that branch off towards the wells.

*Table 5-2: QUEST pipeline dimensions*

	Main Trunk Line	Well Branches
Diameter-OD [mm]	323.9	168.3
Diameter-IN [mm]	299.7	146.3
Wall Thickness [mm]	12.1	11
Minimum Burial depth [m]	1.5	1.5
Average above ground length at LBV or well pads	20	25

#### 5.2.1.4 Fluid composition

Table 5-3: QUEST fluid composition

Component	Normal Operation Mole%	Upset Condition Mole%
CO <sub>2</sub>	99.2	95
CO	0.02	0.15
N <sub>2</sub>	0	0.01
H <sub>2</sub>	0.68	4.27
Methane	0.09	0.57
Water	<52ppm	52ppm

#### 5.2.1.5 Pipeline Operating Conditions

Table 5-4 shows the operating conditions of the pipeline for both winter and summer conditions. It is necessary to model the conditions for the seasons separately. Due to the geographic location of the pipeline; temperatures can vary from an average low of -19.5°C in January to an average high of 23.4°C in July [73]. The difference in atmospheric temperatures means that the CO<sub>2</sub> temperature can change between the seasons and hence cause different dynamics within the system. Table 5-4 also gives information regarding full operation and turn down which will allow for accurate outputs when simulating the transition from one operating state to another.

Table 5-4: Quest pipeline operating conditions

	Winter Conditions	Summer Conditions
Pipeline Inlet Temperatures [°C]	43	49
Operating Pressure [barg]		
Normal Min	80	80
Normal Max	110	110
Maximum Design	140	140
Flowrate	Rated Capacity	Turndown
Flow into Pipeline [kg/hr]	152207	45662
3 Wells Operating [kg/hr/well]	50736	N/A
2 Wells Operating [kg/hr/well]	76104	N/A
1 Wells Operating [kg/hr/well]	120497	45662
Ambient Temperature	-40	35
Ground Temperature at pipeline burial depth [°C]	0	11
Heat Transfer Coefficient [BTU h <sup>-1</sup> ft <sup>2</sup> °F <sup>-1</sup> ]		
Minimum	0.35	0.35
Maximum	1	1



#### 5.2.1.6 Reservoir Operating Conditions

As previously stated, the reservoir, as well as the pipeline, was modelled as part of the simulations. Within gCCS little information is required for the reservoir model due to its relative simplicity. The data in Table 5-5 shows the information that has been used for the modelling work carried out by Shell prior to start-up of the Quest project. As this is not actual data from the reservoir the injectivity values are given as a range. Within this study low, high and middle values were used in three different simulations. The middle value was taken as the average of the high and low values.

*Table 5-5: Reservoir Operating Conditions*

Reservoir Characteristics	
Reservoir Temperature [deg C]	60
Reservoir Pressure [bar]	200
Max allowable bottomhole pressure	280
Reservoir Injectivity [m <sup>3</sup> /d/Mpa]	
Low	300
High	3,000

#### 5.2.2 Pipeline Operation

The way the pipeline conditions are controlled has a significant effect on how the model was developed. There are three main parameters within the Quest pipeline that are controlled; the inlet pipeline temperature, the pressure before wellhead 1 and the flowrate before wellhead 2. The temperature at the inlet of the pipeline is

controlled to stay at approximately 316K, at this temperature the CO<sub>2</sub> is in the supercritical phase. The pressure before wellhead 1 is maintained at a pressure above the critical pressure to avoid the CO<sub>2</sub> entering the gas phase within the pipeline; the pressure is set to remain at approximately 8700kPa. The flowrate at the second well has been set at 70,000 kg/h, any variability in mass flowrate at the inlet is absorbed into the flowrate going to the first well. The variables are maintained using PID control schemes. The model was produced with control schemes similar to that observed on the Quest pipeline, the PI control schemes are shown in Figure 5-7.

### 5.2.3 Simulation details

With the model set up as stated, simulations were developed for different process operations: ramp-up, ramp-down and changes in inlet temperatures. These simulations have been set with input conditions to match those recorded in the pipeline to allow comparison of the outputs with the real data. The limitation of the modes of the simulations is due to the lack of data available from the Quest pipeline for certain operations. While start-up procedure can be simulated and verified using historical plant data there hasn't to date been any need for shut down of the pipeline. While the shut-down of the pipeline can still be simulated, there is no data available for verification.

#### 5.2.3.1 Pipeline Data

The data from the Quest pipeline have been collected through a program known as PI ProcessBook. This software allows access to all networked electronic measurement devices on the plant including the pipeline and contains all historical

data. PI Process Book allows all data to be transferred into Excel, where it can be manipulated and plotted. There are some limitations to the data in that the measurement devices are located at specific places along the pipeline. It is therefore not possible to obtain data along the full length of the pipeline. Flow and temperature measurements are recorded from the pipeline inlet and at points before each reservoir. Pressure measurements are recorded at the inlet and on either side of each valve.

After collecting the data set, the next step was to determine how the simulation would be run. To do this all historical flowrate data of the pipeline was plotted. The simulations have been designed to simulate the effects of flowrate ramp-up, ramp-down, steady state and start-up. By looking at the historical flowrate data, certain time periods were chosen in which the simulated inlet flowrate can match that of the pipeline. Figure 5-3 shows the inlet flowrate data for the dates between the 8th October 2015 and the 30<sup>th</sup> November 2015. As can be seen, the flowrate is variable and has several options to simulate the desired operation. To simulate steady state mode, only a single point is needed to compare the outputs of the model to that of the Quest pipeline. When simulating the dynamics of the flowrate, dynamic data over a period of time is required from the Quest pipeline. To simulate a ramp down and a ramp up in the CO<sub>2</sub> flow there are three possible times which could be simulated as shown in Figure 5-3. Figures 5-4 to 5-6 show the time-periods and the changes in inlet flowrate; which have been simulated to compare the model's ability to produce accurate results.

The time periods that are shown in Figures 5-4 to 5-6 show both an initial ramp down followed by a period of steady state operation and then a ramp-up. The three

time-periods give similar changes in flowrate with approximately 20% reduction in flow.

#### 5.2.4 Data Analysis

Before running the model it was necessary to analyse the data that is obtained from the pipeline to gain an understanding of how the flowrate varies. There is a limit to how much information can be obtained about the pipeline from the measurement devices, as they are confined to certain locations. The flowrate measurement devices are limited to the inlet of the pipeline and the inlet to the well, the same is for the temperature sensors. Pressure sensors are located at the inlet of the pipeline, on either side of each of the line break valves and at the entry to the well. However the temperature readings were recorded from the line block valves using an infra-red gun as the valves are above ground so approximate temperature readings can be made.

#### 5.2.5 Measurement Devices

##### 5.2.5.1 Flowrate measurement device

The measurement devices that are used to measure the mass flowrate are Coriolis meters. A Coriolis meter measures the mass flow directly; it works on the principle of changes in the vibration of the flow meter as the mass flow increases and decrease. The Coriolis meters also measure density, along with the mass flowrate a volumetric flowrate is calculated through the following relationship;

$$v = \frac{m}{\rho}$$

*Equation 5-1: Density Equation*

Two types of Coriolis meters are used. The one measuring the inlet mass flow has an accuracy of  $\pm 0.05\%$  of the reading. The ones measuring the mass flow at the entry to the well have an accuracy of  $\pm 0.10\%$  of the operating range. As the mass flow is measured at both wells there are two measurement devices, therefore doubling the possible error. The operating range for these devices is 0 – 120,000 kg/h. Coriolis meters are known for having high degrees of accuracy and it can be seen in Figure 5-4 to 5-6 that the errors are generally insignificant when it comes to analysing the mass flow data.

#### *5.2.5.2 Temperature measurement device*

The temperature sensors used at the inlet and outlet of the pipeline are resistance temperature detectors (RTD) also known as resistance thermometers. RTD's are made from metallic conducting materials, platinum, copper or nickel. Platinum 100 $\Omega$  RTD's are used as the temperature sensors at both the inlet and outlets of the pipeline. These have a normal operating range between 70 and 870K with an accuracy of  $\pm 0.4\text{K}$ . The temperature of the CO<sub>2</sub> at the pipeline inlet is kept constant at approximately 316K. The temperature of the CO<sub>2</sub> decreases along the length of the pipeline however at no point during operation has it decreased below the lower operating range of the sensor. The RTD works by utilizing the increasing electrical resistance with temperature in metals.

#### *5.2.5.3 Pressure measurement device*

The pressures at the inlet and along the length of the pipeline are measured using sensors that work using the piezoresistive effect. The piezoresistive effect is the change in electrical resistivity of a metal when mechanical strain is applied. Figure 5-2 [74] shows how the specific pressure sensor used on the Quest pipeline works.

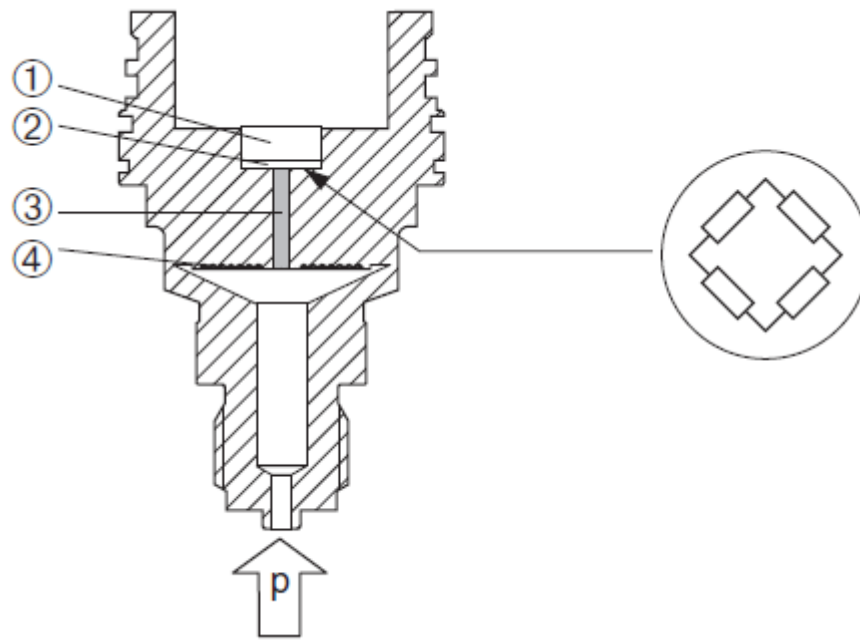


Figure 5-2: Pressure sensor

1. *Silicon measuring element, substrate*
2. *Wheatstone bridge*
3. *Channel with fill fluid*
4. *Metal process isolating diaphragm*

This sensor works by the operating pressure deflecting the process isolating diaphragm and the fill fluid transfers the pressure to a resistance bridge (semiconductor technology). The pressure dependent change in the bridge output voltage is measured and evaluated [74]. The pressure sensor has an accuracy of  $\pm 0.075\%$ .

#### 5.2.6 Simulation Periods

Figure 5-3 shows the inlet mass flowrate and the combined mass flowrate entering each of the two wells for the 8<sup>th</sup> October to the 30<sup>th</sup> November 2015. The errors associated with each of the devices shown by the error bars in black. These indicate that the errors associated with the measurement devices are significantly small. One of the main observations from Figure 5-3 is that the inlet flow doesn't always directly match the total outlet flow at a given time. It can also be seen that there is a point where the flowrate becomes negative, this was due to an unplanned shutdown of the pipeline which impacted on the measurement device.

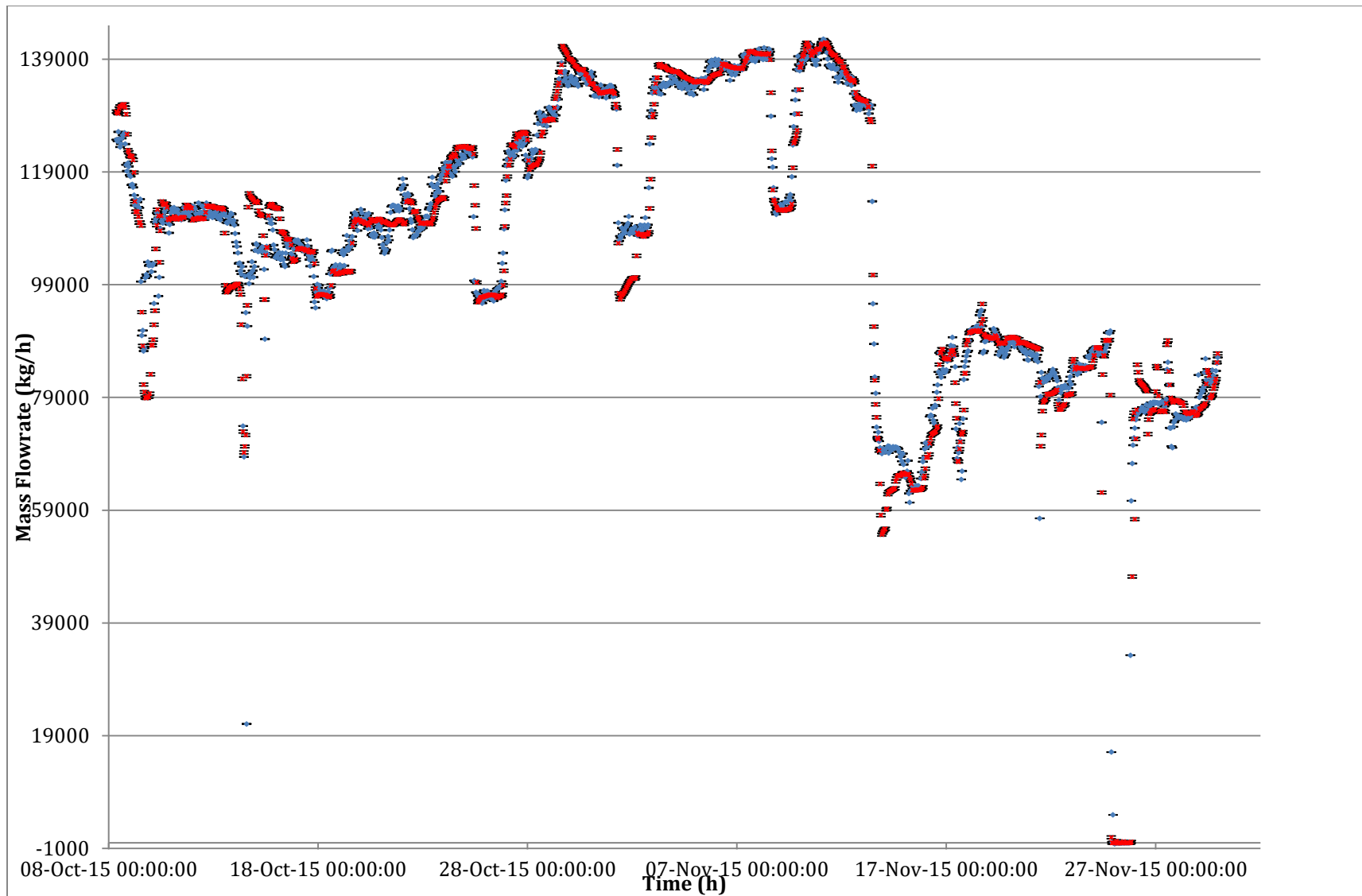
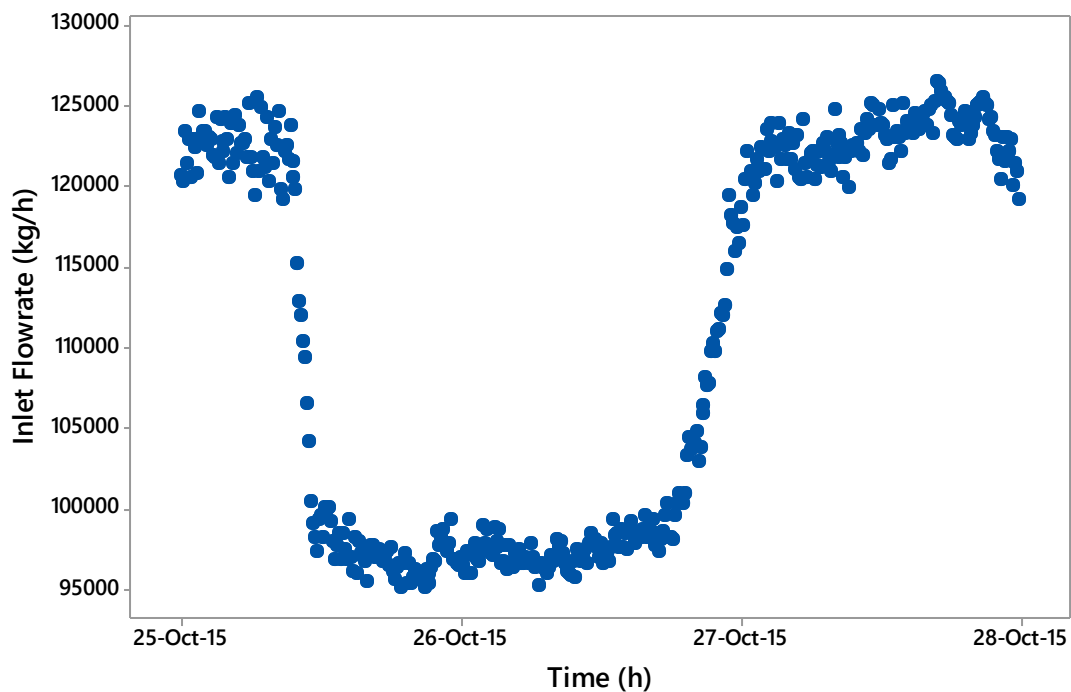


Figure 5-3: Inlet and Outlet mass flowrate of the Quest pipeline between 07/10/15 and 28/11/15



Figures 5-4 to 5-6 show the data from the quest pipeline that is to be simulated within the model. As can be seen the mass flowrate contains a significant amount of small changes, for reasons of practicality these small changes were not simulated. The purpose of the simulations is to understand the effects of significant changes in the system. As shown in Figure 5-4 the initial flowrate lies between 120000kg/h and 125000kg/h. Within the model an initial flowrate of 34.6kg/s (124,560 kg/h) was used.



*Figure 5-4: QUEST pipeline inlet mass flowrate data from 25/10/15 to 28/10/15*

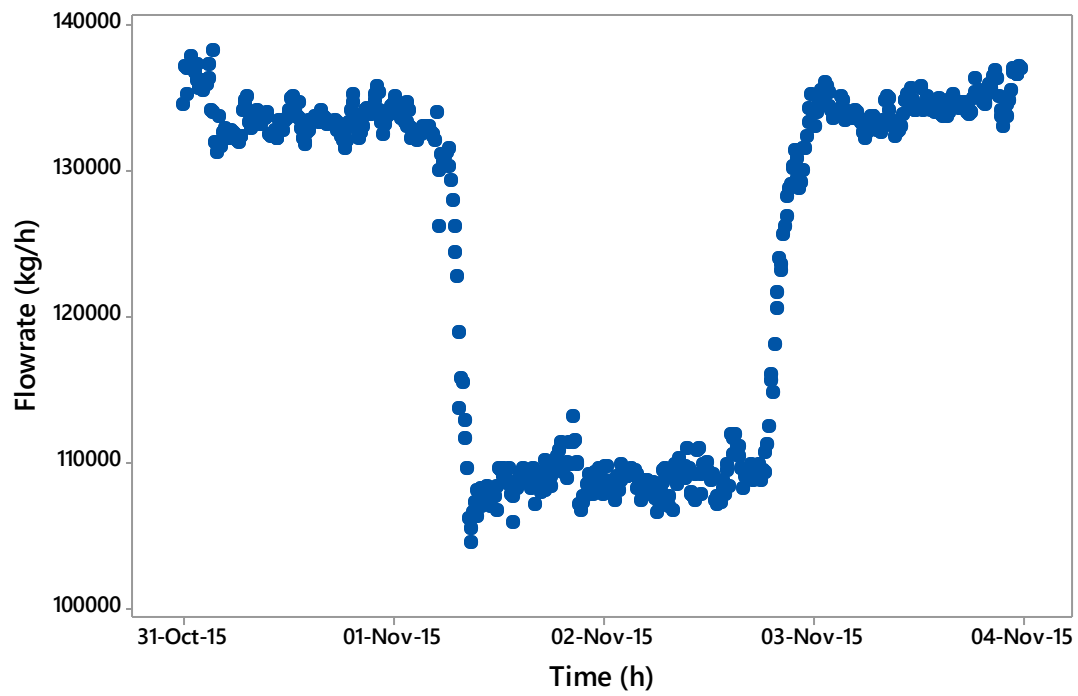


Figure 5-5: QUEST pipeline inlet mass flowrate data from 31/10/15 to 04/11/15

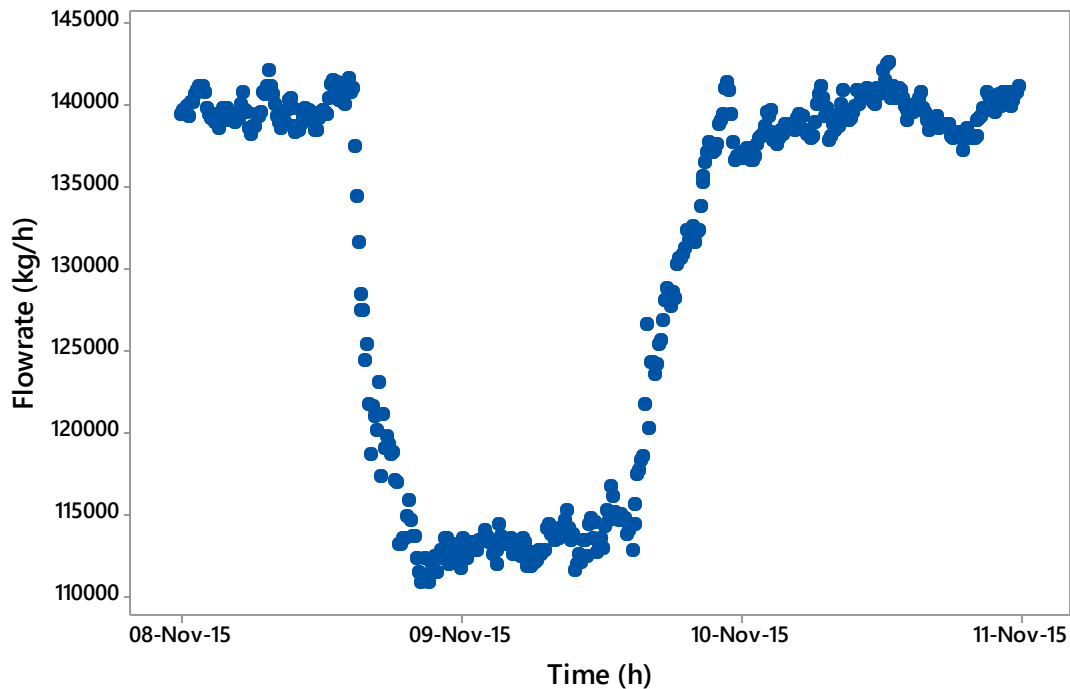


Figure 5-6: QUEST pipeline inlet mass flowrate data from 08/11/15 to 11/10/15

### 5.3 Initial Model Development

#### 5.3.1 Topology

Using the Quest design and operating information a pipeline model was produced which is schematically shown in Figure 5-7. The pipe dimensions are the same as those reported in Table 5-1, all parameters shown within Table 5-2 and Table 5-3 are also included within the model. The ground temperature at burial depth is taken as the winter conditions of 273K. This was chosen as the time-periods in which the simulations replicated are closer to the winter season and therefore the ground temperature is expected to be colder. However it should be noted that this may not be the actual ground temperature at pipeline burial depth but is an assumption that is made based on the flow assurance report developed by Shell [72]. It is reasonable to assume that the ground

temperatures used in the flow assurance report have the greatest reliability amongst the literature on ground temperatures, as it is specific to the area where the QUEST pipeline is buried. Actual ground temperatures could not be obtained as there is no available equipment to measure the ground temperature at burial depth. Other parameters such as pipe wall roughness, valve leakage fraction and liquid flow coefficient were not obtainable, therefore the default values within gCCS were utilized.

### 5.3.2 Control Schemes

#### *5.3.2.1 Pressure Control*

The pressure to the well is controlled to maintain a constant pressure of 87,000kPa. This is to ensure that the pressure within the pipeline does not fall below the critical pressure of CO<sub>2</sub> and therefore does not enter the gaseous phase. To control the pressure a PI feed forward controller was modelled, which is the same type of control used at the Quest site.

#### *5.3.2.2 Flow Control*

The flowrate to the second well is controlled to maintain a constant flowrate of 70,000kg/h. The reason for controlling the flowrate to the second well was to allow the testing of the pipe flow and the effects on the reservoir. To control the flowrate a feed forward PI controller is used.

### 5.3.3 Schedule

The model was simulated to observe the effects of changing the inlet flowrate on parameters within the pipeline, including flowrate, temperature, pressure and density. The schedules (Appendix C.1 – Appendix C.2) were written to imitate the changes in flowrate shown in Figures 5-4 to 5-6. To allow for the entire system to settle, the end of

the schedule was written to give 200,000 seconds (55.55 hours) for equilibrium to be reached.

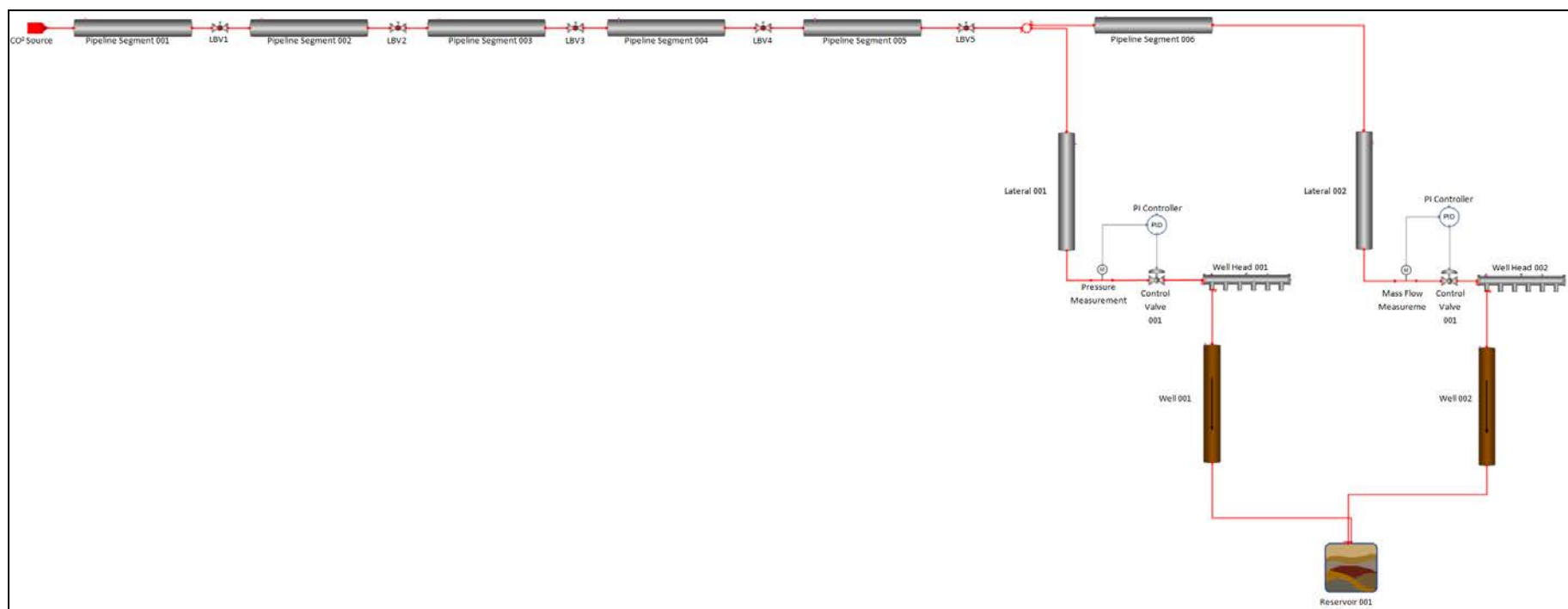


Figure 5-7: Initial pipeline model

#### 5.3.4 Initial Model Analysis

The model was set up to directly represent the Quest CO<sub>2</sub> pipeline, as closely as the software would allow. This included control schemes that maintained the flowrate and the pressure within the pipeline at desired set points. There were two problems that occurred with this set up of the model; the first was related to the pressure controller in that there is an over specification with the reservoir pressure and the pressure controller. As the pressure is being specified in two parts of this system the simulation would not allow this to be completed and produced an error when simulating. The control scheme for the pressure control was removed and the simulation initialized again. The second problem that occurred was related to the flow controller. The simulation was able to complete, however when observing the response from the control valve used to maintain the mass flowrate, the stem position remained constant and the flowrate through the valve varied as the pipeline inlet flowrate changed. It has been understood that the reason for this behaviour of the flow controller is due to flow constraints caused by the split of the CO<sub>2</sub> flow between lateral 001 and lateral 002.

#### 5.3.5 Secondary Model Development

To model the pipeline in a way that is representative of how the pipeline is operating, a new set up was developed in which the well and reservoir were not incorporated into model. The outlets of the two lateral pipelines were replaced with CO<sub>2</sub> sink models. The sink connected to lateral 1 specifies a pressure of 87MPa while the sink connected to lateral 2 specifies a flowrate of 69,840 kg/h. Developing the system in this way means that the set points for the pipeline outlets can be maintained even when there are changes

in the system, therefore operating similar to the action of a controller. The topology for the model can be seen in Figure 5-8.

Using the same schedule as used previously, the simulations were repeated. With the new model the system was able to operate in accordance with the Quest pipeline, whereby the outlet flowrate and pressure specifications are the controlled variables



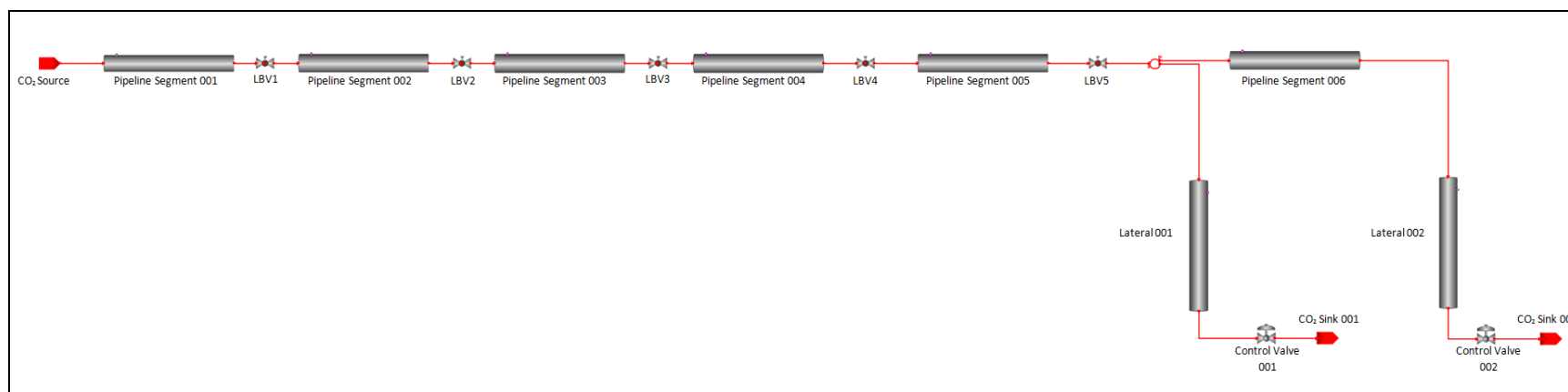


*Figure 5-8: Simplified QUEST pipeline model*

## 5.4 Comparison Between Model and QUEST Data

### 5.4.1 Flowrate

The three different scenarios have been modelled and the three primary parameters have been compared with that of the Quest pipeline. Figures 5-9 to 5-11 show the comparison between the model data and the Quest data for all three scenarios. The flowrate is taken from three points on the pipeline, at the inlet and the two outlets where the flow would enter the well-head. From Figures 5-9 to 5-11 it can be seen that the inlet flowrate profile from the model almost perfectly matches that of the Quest pipeline in all three cases. The inlet flowrate was one of the two controlled variables, the second being the outlet to Lateral002 which also show a close match between the model and Quest. The dependent variable when observing the flowrate change is at the outlet to Lateral001. Figure 5-9 shows that the model gives a flowrate profile for the outlet of Lateral001 close to that of Quest however it can be observed that the reaction time of the model is quicker than that of the actual pipeline whereby the flowrate in the model drops at a faster rate. Figure 5-10 shows that the initial drop in flowrate to Lateral001 is modelled tightly with the Quest data however as the model settles at an approximate flowrate of 37000kg/h the Quest data shows a further decrease and settles at approximately 28000kg/h. The flowrate then increases and settles at the model value of 37000kg/h.

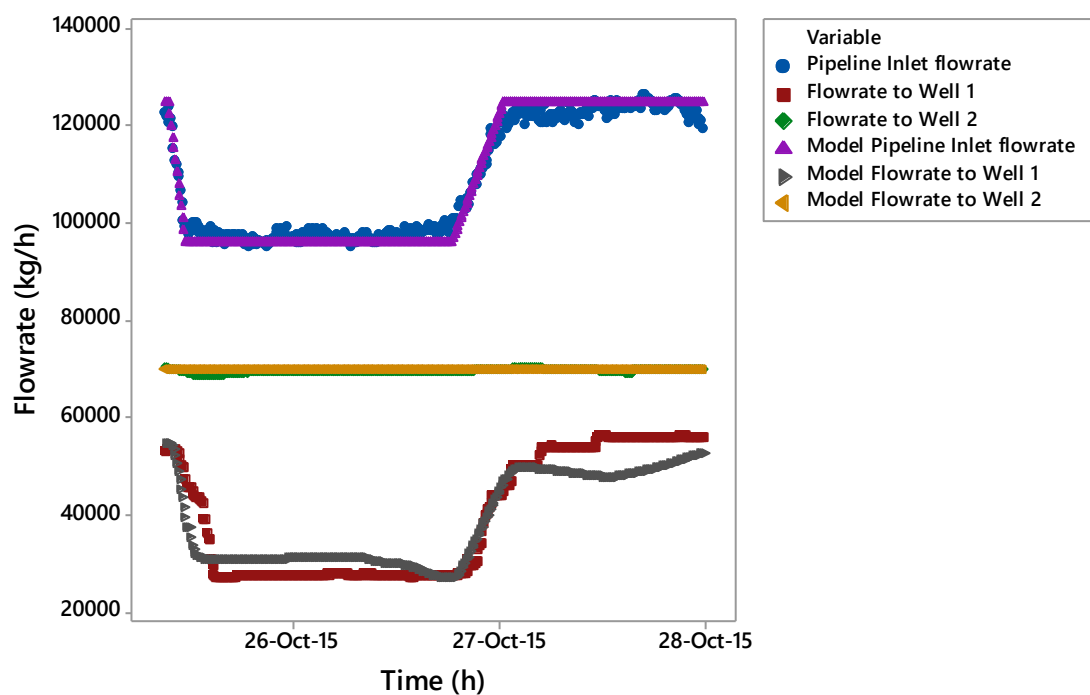


Figure 5-9: Model and QUEST pipeline inlet and outlet flowrates 24/10/15 – 28/10/15

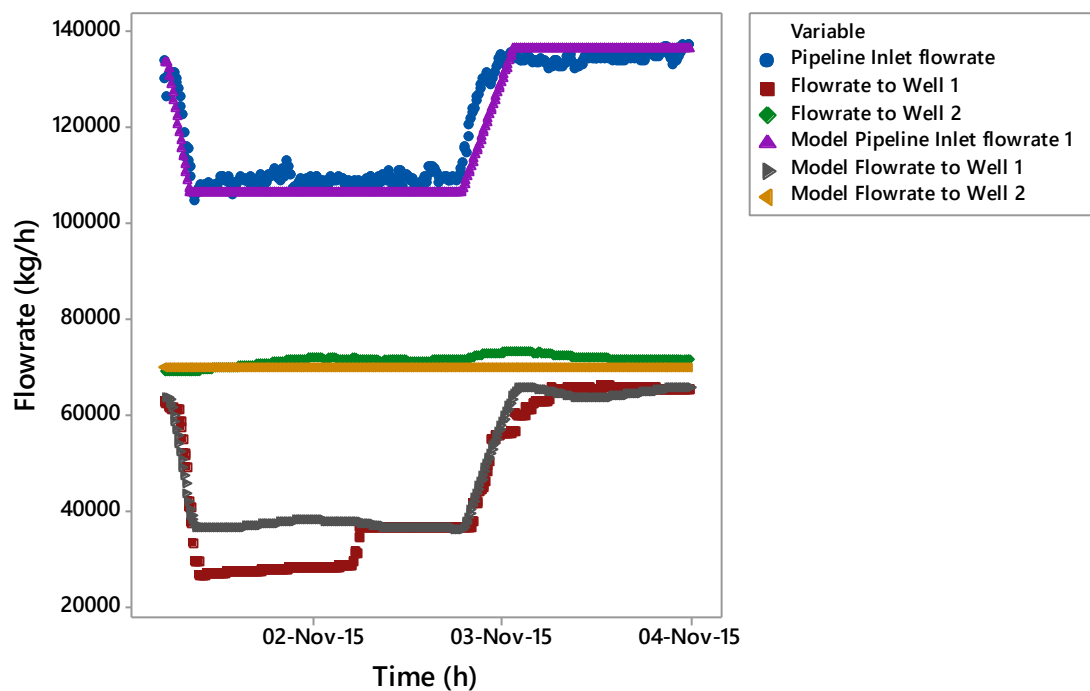


Figure 5-10: Model and QUEST pipeline inlet and outlet flowrates 31/10/15 – 04/11/15

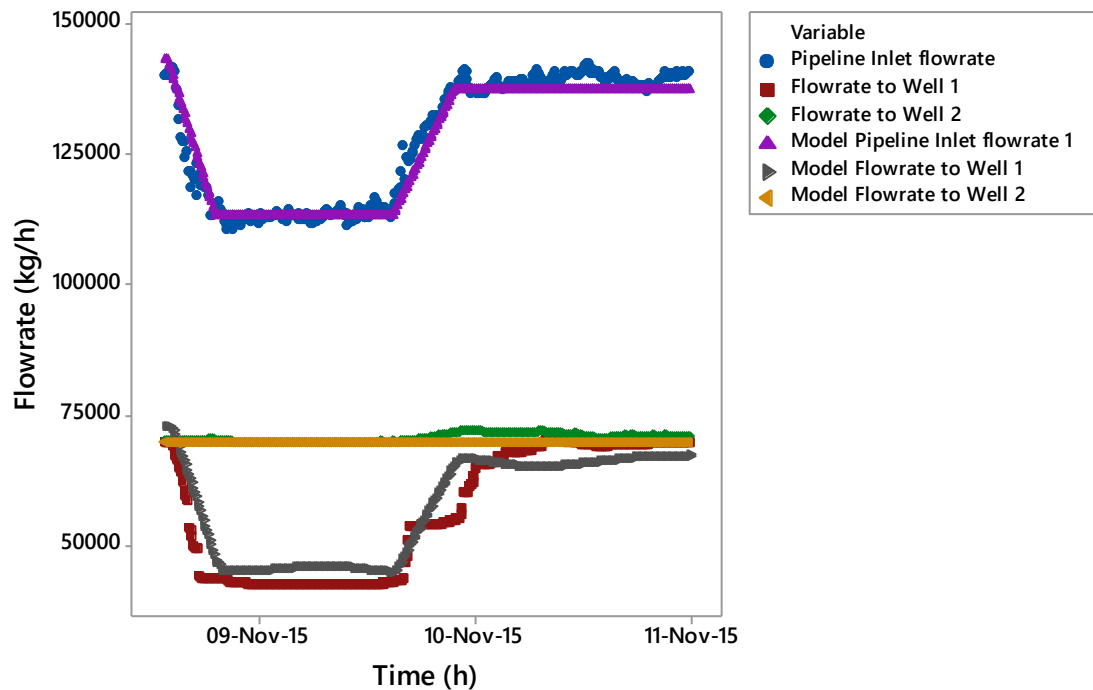


Figure 5-11: Model and QUEST pipeline inlet and outlet flowrates 08/11/15 – 11/11/15

To compare the inlet flowrate change with the outlet flowrate dynamics, the outlet flowrates to both wells were summed for both the model and the Quest data. Figures 5-12 to 5-14 give a greater indication on how the outlet flowrate responds to a change at the inlet. An analysis of this shows that there is a time delay between in the decrease in flowrate from the inlet to the outlet. There is also a difference in the gradient whereby the inlet flowrate drops at a faster rate than the outlet flowrate. Taking a point at which the inlet flowrate has reached 98186 kg/hr at time (25-Oct-2015 11:30:00) the outlet flowrate reaches a flowrate of 98299kg/hr at time (25-Oct-2015 14:30:00). This is a difference of 3 hours for the flowrate to propagate through the pipeline.

The model shows a shorter time for the flowrate to initially propagate through the system compared to the outlet flowrate of the Quest pipeline however an offset between the model

and the real value is observed between times (25-Oct-15 14:50:00) and (26-Oct-15 20:00:00) at which point the Quest outlet flowrate has reached and settled at the inlet flowrate.

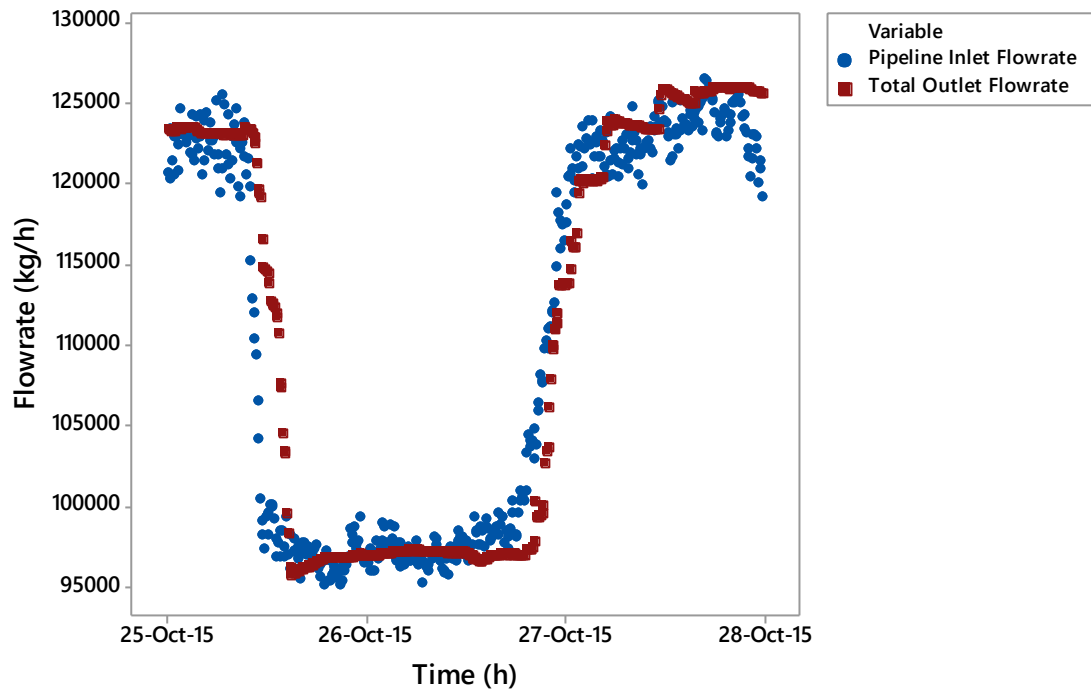


Figure 5-12: Quest pipeline inlet and outlet flowrate 24/10/15 - 28/10/15

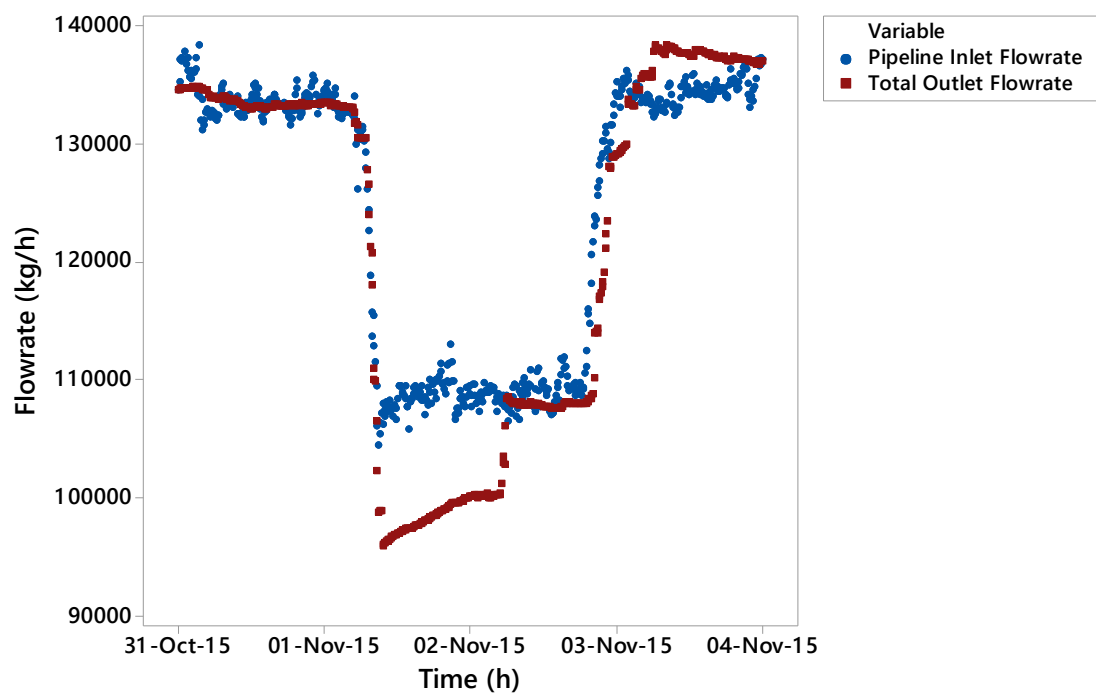


Figure 5-13: Quest pipeline inlet and outlet flowrate 31/10/15 - 04/11/15

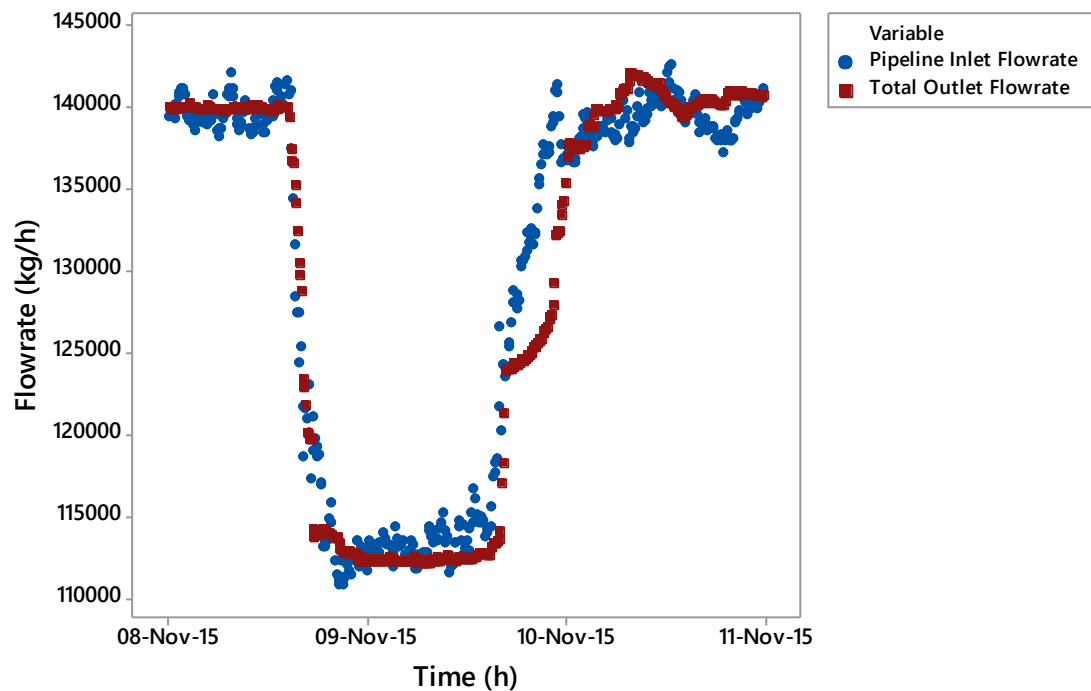


Figure 5-14: Quest pipeline inlet and outlet flowrate 08/11/15 - 11/11/15

#### 5.4.2 Pressure

Along the Quest pipeline there are pressure sensors located at the inlet to the pipeline, on either side of each LBV valve and at the well sites. The only pressure specification that was implemented was the pressure to well head 1 which was set at 87,000kPa. All other values of pressure were calculated by gCCS. Figure 5-15 to 5-17 shows the Quest pipeline pressures and the model determined pressures. For ease of observation only, the pressures downstream of each of the valves are shown. An initial observation shows that the model predicted pressures upstream have greater agreement with that of the Quest pipeline when compared with that of the pressures downstream. Figure 5-16, 5-19 and 5-22 show the first 10 data points of figures 5-15, 5-18 and 5-21 respectively. These charts show the pressures at the pipeline inlet, upstream of LBV2 and upstream of LBV5 and provide clearer images for more detailed comparison of how the pressure changes along the pipeline. From observing how the pressures change over time, the initial pressure drop gives a tight relationship between the model and the observed data. When the pressure has reached the minimum the model and the observed data start to deviate with the model giving a constant slight decline while the pressure at Quest shows a staggered increase. The largest difference between the model and the data is at the point when the pressure starts to increase, these can be seen in more detail in Figures 5-17, 5-20 and 5-23. The third significant observation from Figure 5-15, where the observed pressure has increased to a maximum and slowly starts to decrease while the predicted pressure shows a steady increase.

The lower accuracy of the model the further downstream of the pipeline is caused by the model calculating larger pressure drops compared to the observed data. This can be explained through the differences of the pressure drop through the valves, as any differences will accumulate and cause greater deviations the further along the pipeline. The discrepancy

between the model and the Quest data over the time period may be caused by actions taken by the pipeline operator trying to increase the pressure of the fluid.

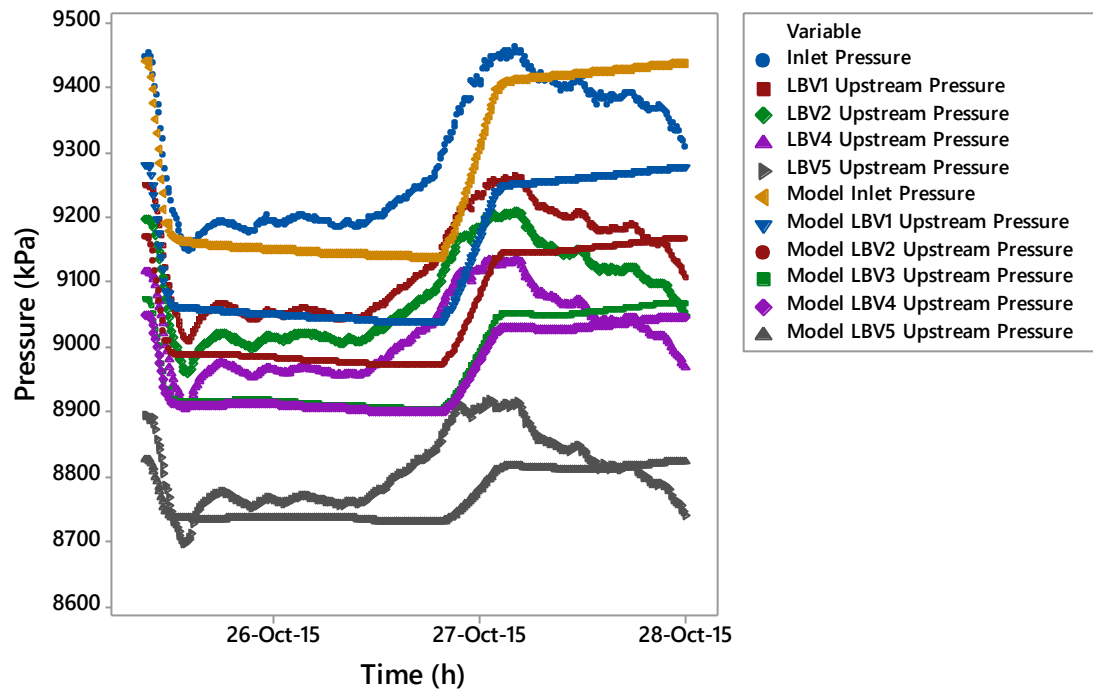


Figure 5-15: Model and QUEST pipeline pressures 24/10/15 – 28/10/15



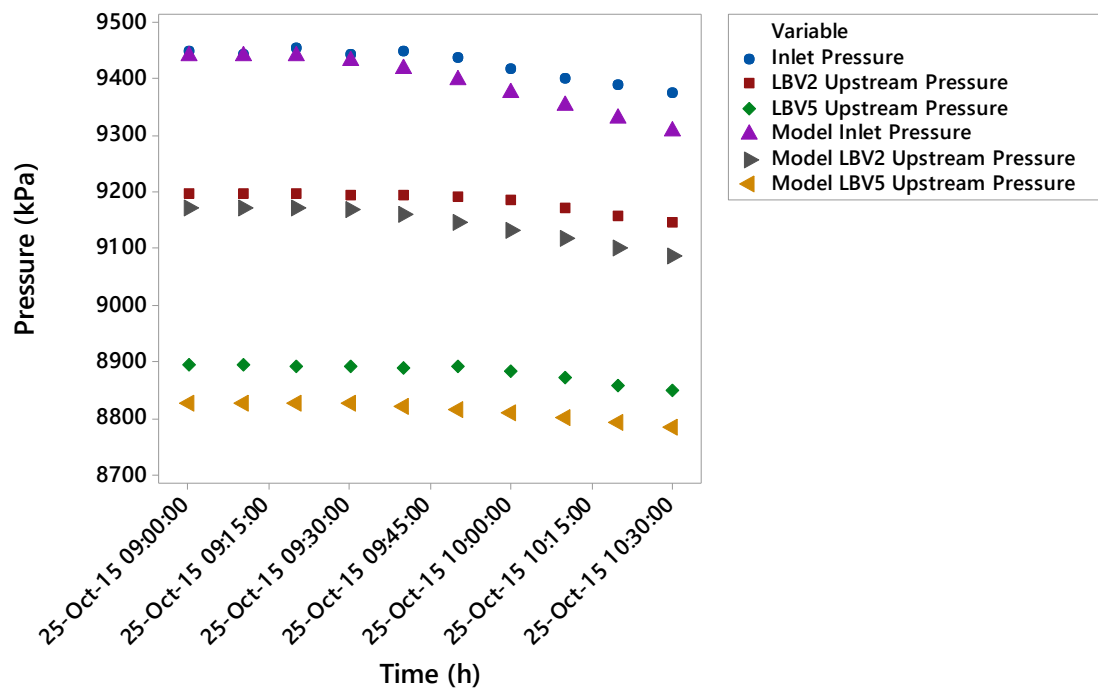


Figure 5-16: Model and QUEST pipeline pressures 25/10/15 09:00 - 25/10/15 10:30

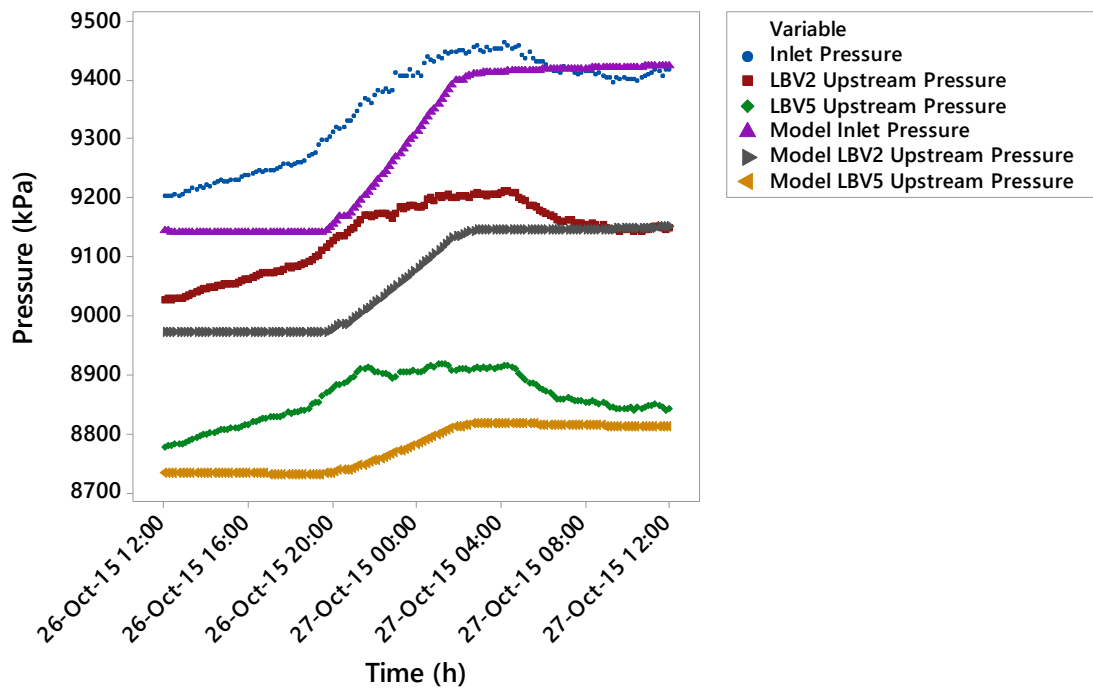


Figure 5-17: Model and QUEST pipeline pressures 26/10/15 12:00 - 27/10/15 12:00

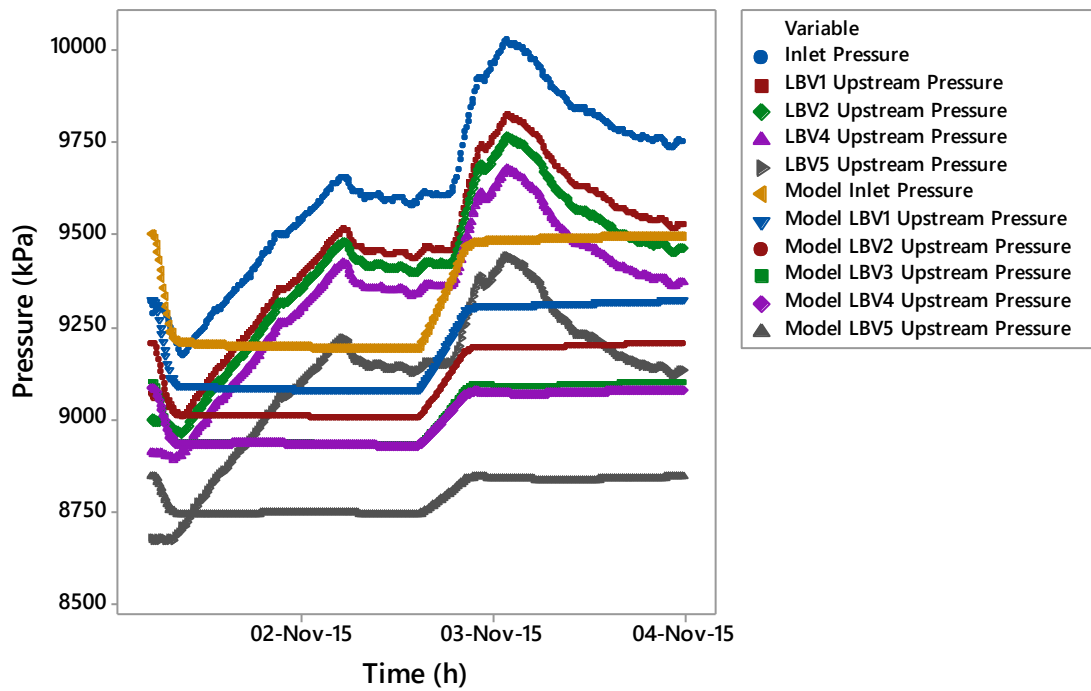


Figure 5-18: Model and QUEST pipeline pressures 31/10/15 – 04/11/15

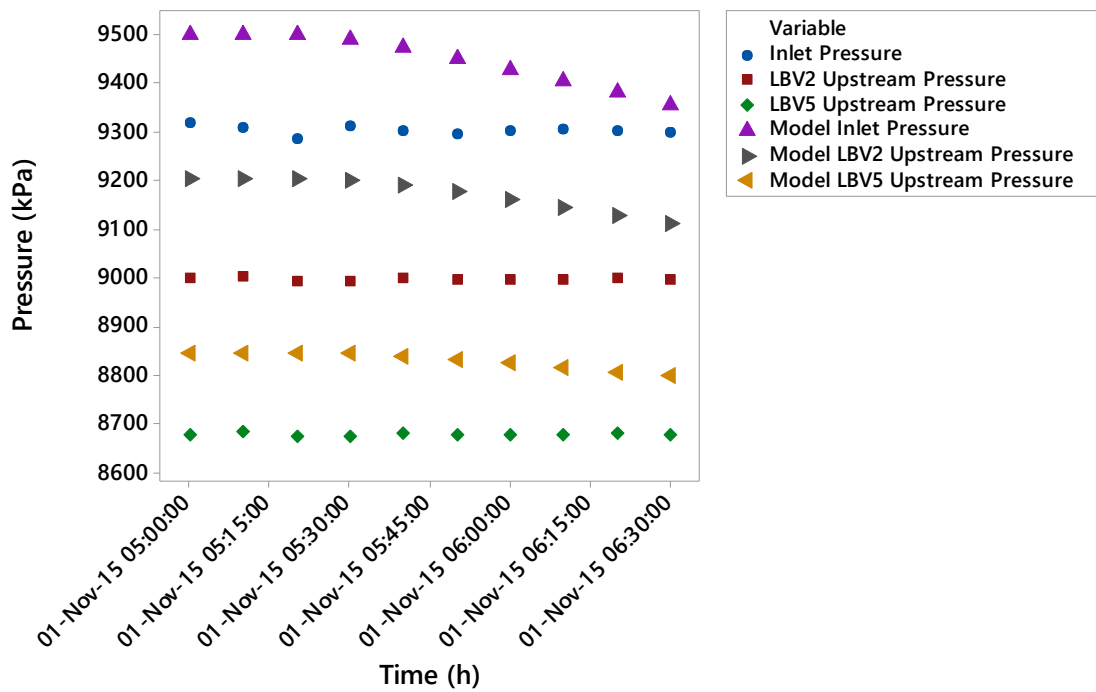


Figure 5-19: Model and QUEST pipeline pressures 01/11/15 05:00 – 01/11/15 06:30

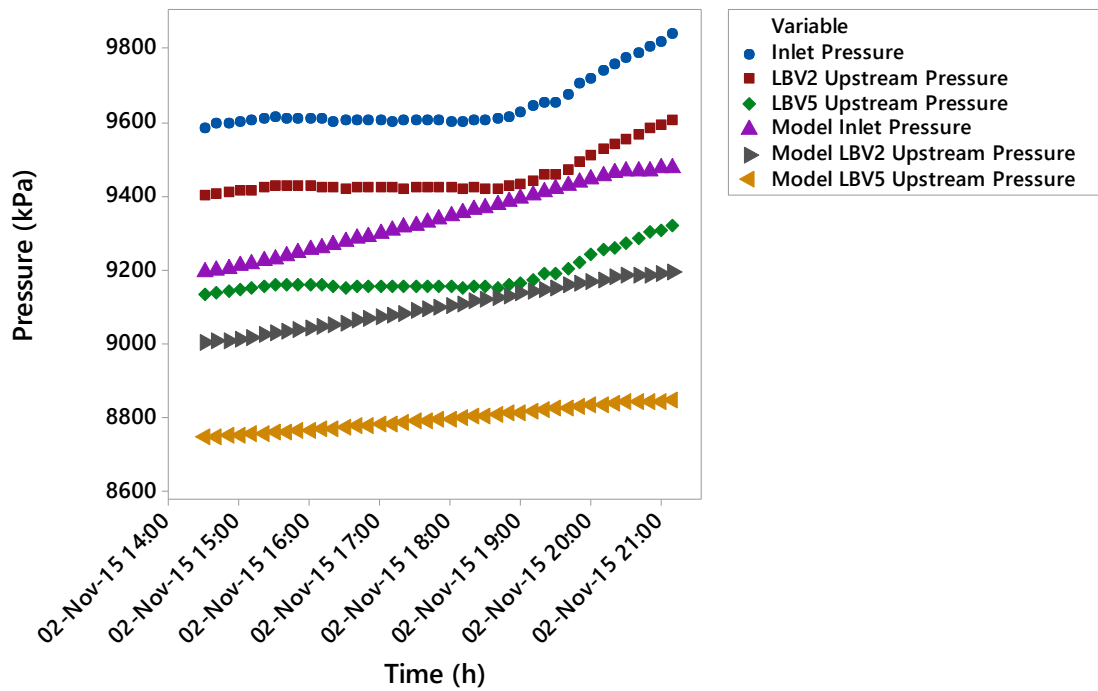


Figure 5-20: Model and QUEST pipeline pressures 02/10/15 14:00 – 02/11/15 21:00

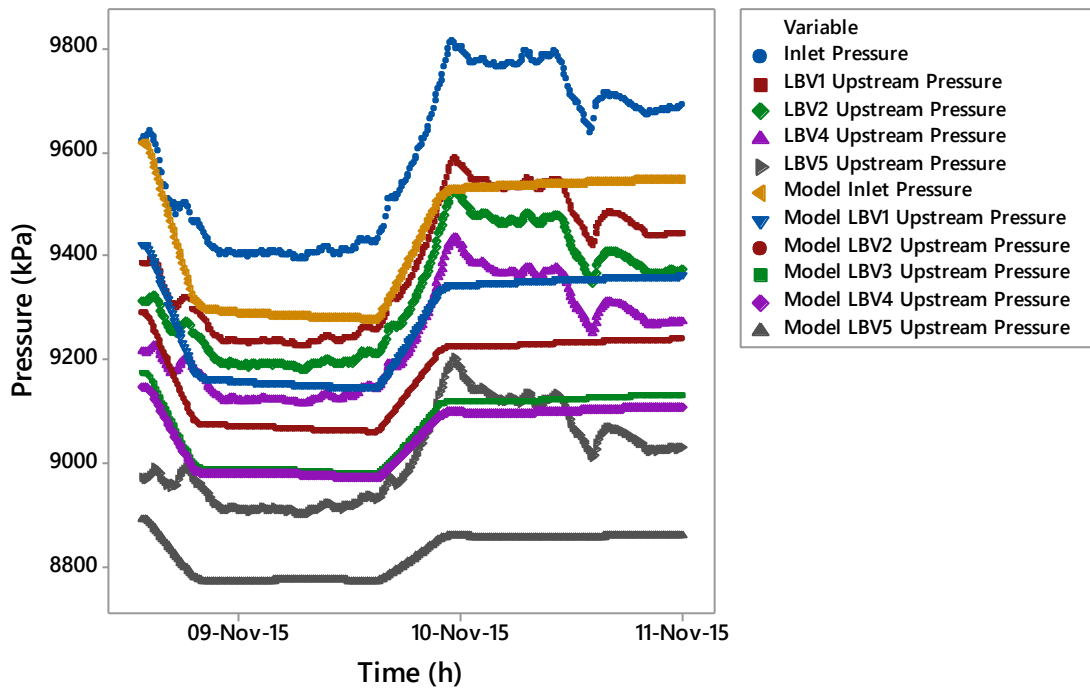


Figure 5-21: Model and QUEST pipeline pressures 08/11/15 – 11/11/15

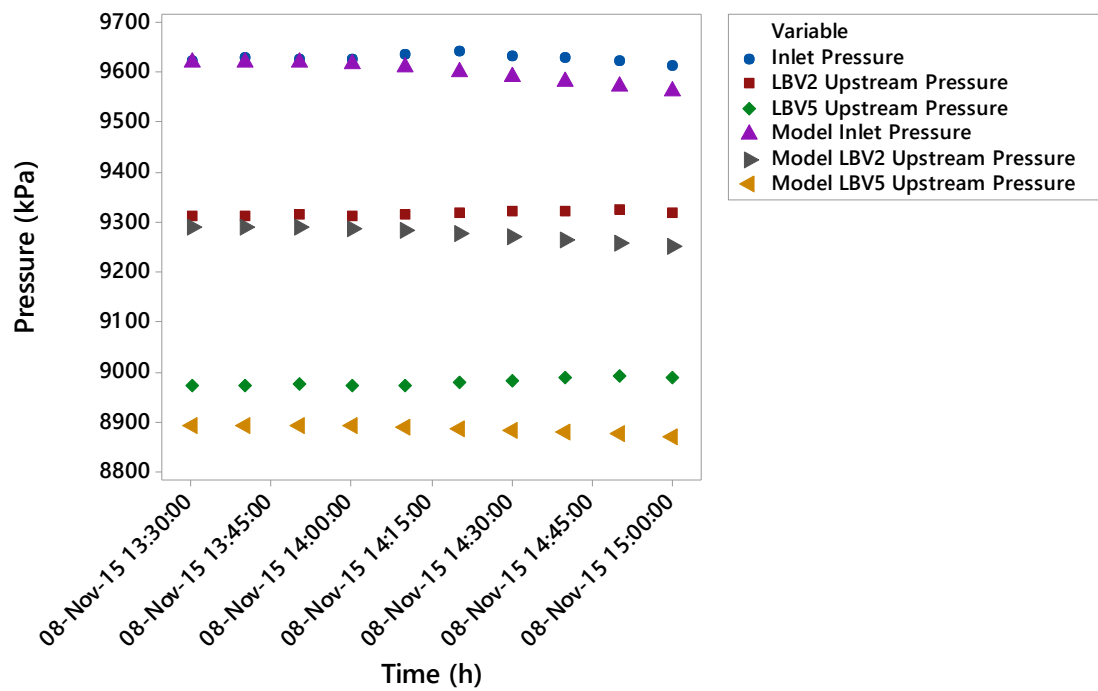


Figure 5-22: Model and QUEST pipeline pressures 08/11/15 13:30 – 08/11/15 15:00

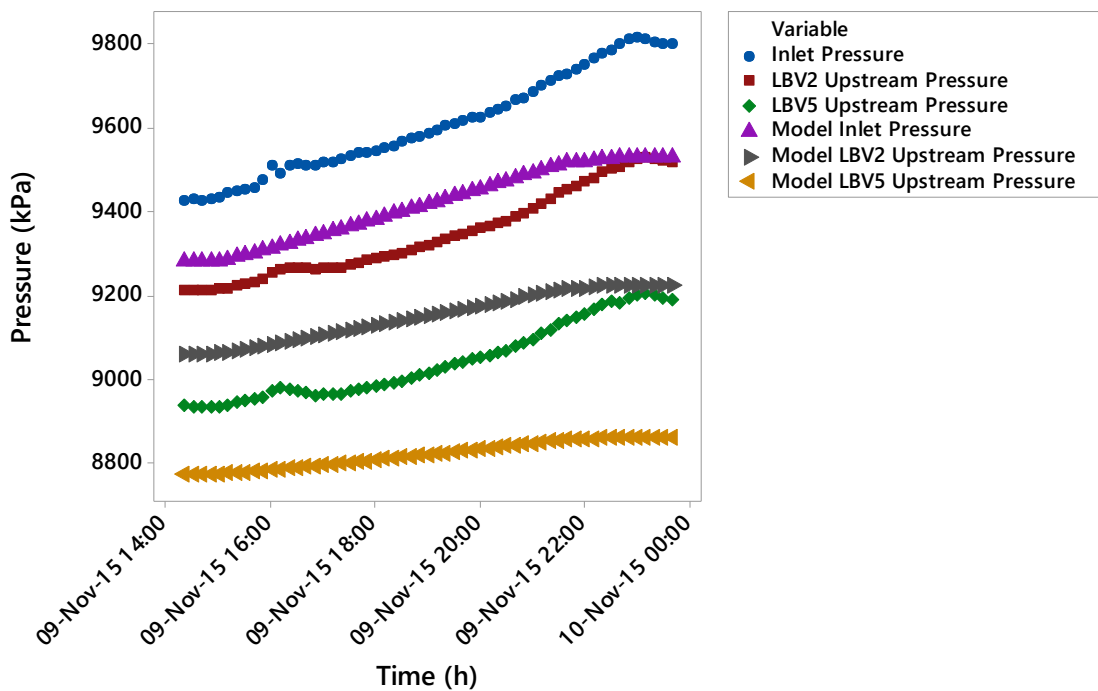


Figure 5-23: Model and QUEST pipeline pressures 09/11/15 14:00 – 10/11/15 00:00

### 5.4.3 Temperature

Along the pipeline there is either a rise or a fall in temperature of the fluid depending on the temperature difference between the fluid and the surrounding material. Since the temperature at the pipeline inlet is greater than the ambient temperature of the surrounding soil, the temperature of the fluid would decrease over the pipeline length. Figures 5-18 to 5-20 shows the model and the Quest temperatures at the inlet to the pipeline and before each well. The inlet temperature remains constant throughout the time period and is one of the variables that is decided by the user, hence a high degree of accuracy between the model and the observed data. When comparing the temperatures from before the wells it is clear that the model and the Quest data have a high degree of disparity. Figures 5-18 to 5-20 show that the model predicts a smaller temperature drop along the pipeline to the recorded value, with the model predicting values of the temperature at the outlet of the pipeline greater than 25°C and the data from the QUEST pipeline showing temperatures lower than 20°C. Since the model calculates the surrounding soil temperature based on the ambient temperature, pipeline depth and soil type it is a reasonable assumption that the reason behind the discrepancy is the difference in the temperature gradient along the soil depth. This determines the temperature of the soil surrounding the pipeline and hence the driving force for heat loss along the pipeline. This is likely to be one of the most difficult parameters to determine as the soil thermal properties can vary significantly. Previous studies have shown that there are several factors that affect the thermal properties of the soil. These include the composition, the volume, soil density, porosity and water migration. The main components of soil can be seen in Table 5-6[75] along with their thermal conductivities.

Table 5-6: Soil Material & Thermal Conductivities

Material	Thermal Conductivity ( $\text{W m}^{-1} \text{K}^{-1}$ )
Quartz	8.4
Soil Minerals*	2.9
Soil Organic Matter*	0.25
Water	0.6
Air	0.026

\*Approximate Average Values

From Table 5-6 it becomes apparent that the composition of the soil can have significant impacts on the total thermal conductivity of the soil, with the thermal conductivity of the individual components ranging from  $0.026 \text{ W m}^{-1}\text{K}^{-1}$  to  $8.4 \text{ W m}^{-1}\text{K}^{-1}$ . The model however has pre-determined values for the thermal conductivity related to each soil type which cannot be changed. This is one of the limitations of the modelling software and is an improvement that would allow the model to have greater accuracy in determining the temperature losses along the pipeline.

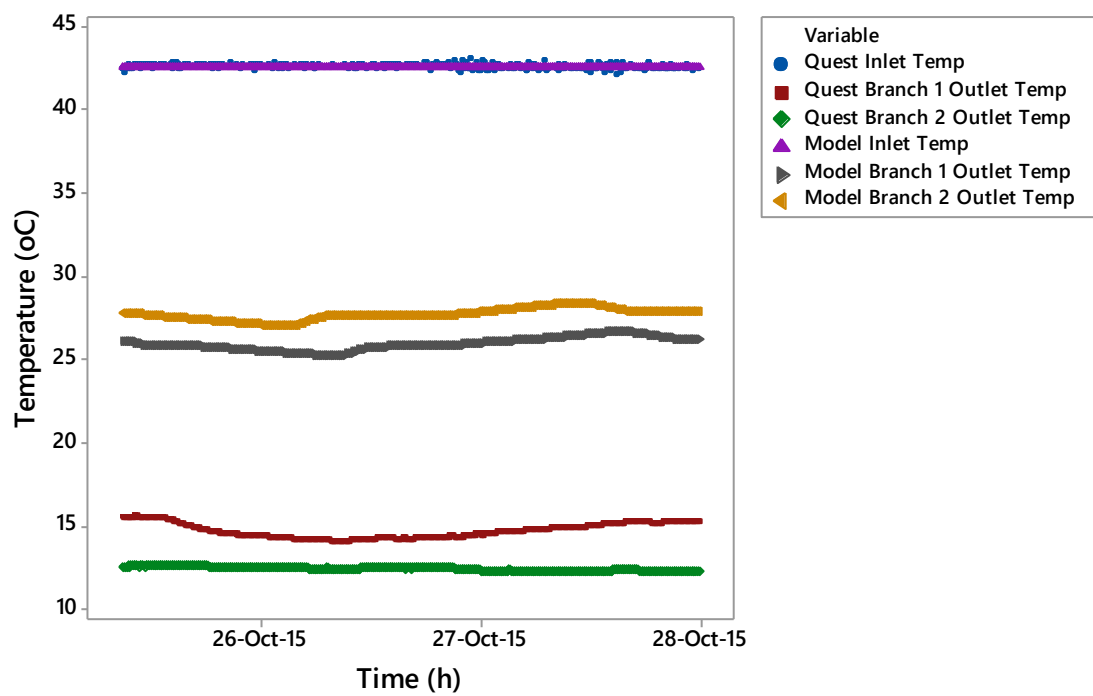


Figure 5-24: Model and QUEST pipeline inlet and outlet temperatures 24/10/15 – 28/10/15

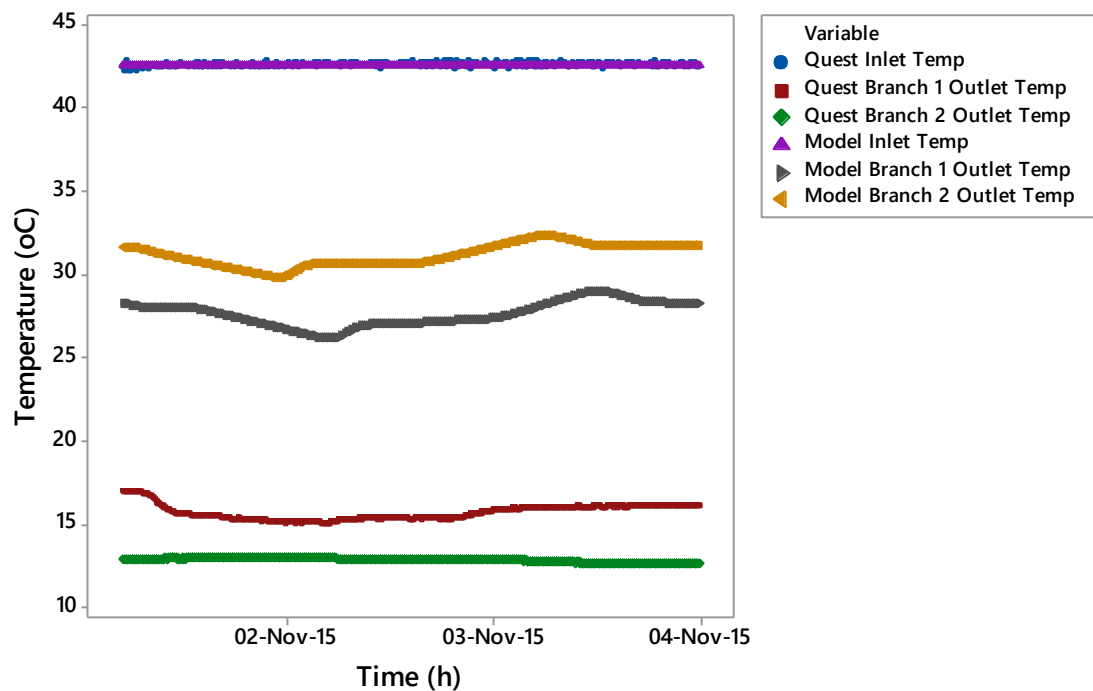


Figure 5-25: Model and QUEST pipeline inlet and outlet temperatures 31/10/15 – 04/11/15

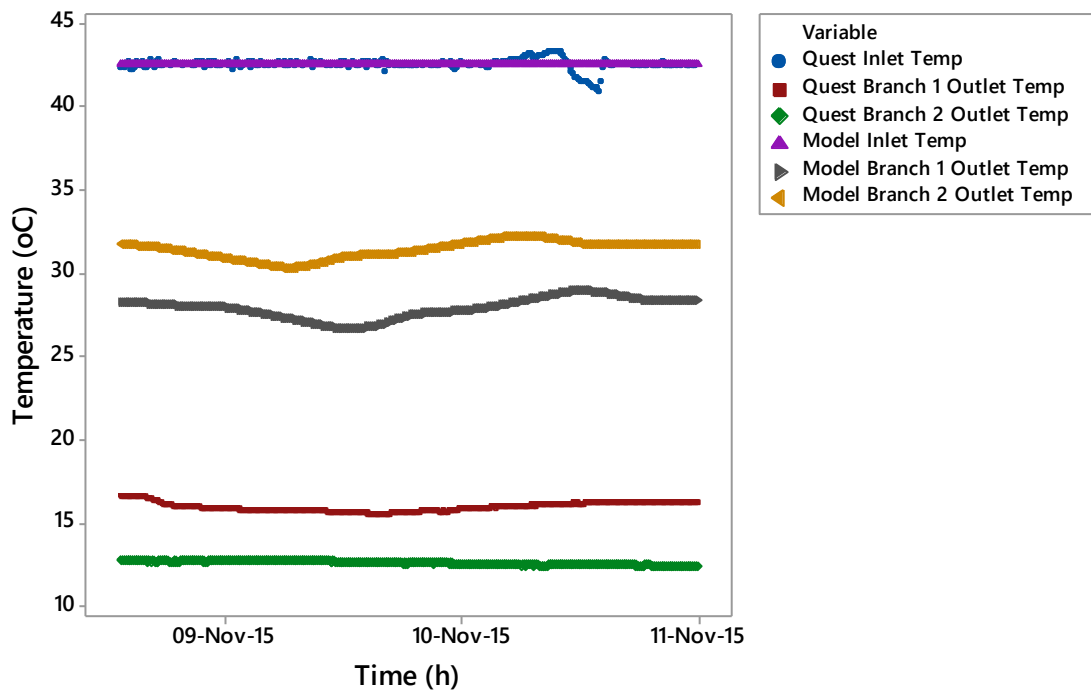


Figure 5-26: Model and QUEST pipeline inlet and outlet temperatures 08/11/15 – 11/11/15

## 5.5 Determining ‘Goodness of Fit’

Goodness of fit is a way in which the accuracy of models can be measured quantitatively. It compares how well the model is able to predict output values with changing input conditions. There are different methods to determine goodness of fit, each with their own benefits and limitations. An evaluation on different methods of ‘goodness of fit’ for time series data, shows that the coefficient of efficiency and the Index of agreement are both methods that are suitable to use to determine goodness of fit of the model. The parameters that will be tested for goodness of fit are those that are determined by the model and not those that have been user defined.

### 5.5.1 Coefficient of Efficiency

The coefficient of efficiency has a range between minus infinity to 1.0, with higher values indicating better agreement. The CoE is given by the following formulae:



$$E = 1.0 - \frac{\sum_{i=1}^N (O_i - P_i)^2}{\sum_{i=1}^N (O_i - \bar{O})^2}$$

*Equation 5-2: Coefficient of Efficiency*

The CoE is the ratio of the mean squared error to the ratio of the variance in the observed data minus unity. If the mean squared error is the same as the variability in the observed data then we get a value of E=0. A value of E < 0 indicates that the mean is a better predictor than the model. A limitation of this method is that it can be sensitive to outliers due to the square of the error.

### 5.5.2 Index of Agreement

The Index of Agreement (IoA) is given by the formula:

$$d = 1.0 - \frac{\sum_{i=1}^N (O_i - P_i)^2}{\sum_{i=1}^N (|P_i - \bar{O}| + |O_i - \bar{O}|)}$$

*Equation 5-3: Index of Agreement*

The IoA varies from 0 to 1 with higher values indicating better agreement between the model and the observations.

Table 5-7: Goodness of fit

	24 <sup>th</sup> Oct – 28 <sup>th</sup> Oct	31 <sup>st</sup> Oct – 3 <sup>rd</sup> Nov	7 <sup>th</sup> Nov – 11 <sup>th</sup> Nov	Mean
Outlet Flowrate 001	0.8761	0.9612	0.9631	0.9335
Inlet Pressure	0.9130	0.4559	0.7050	0.6913
LBV1 UP	0.8680	0.3858	0.7152	0.6563
LBV2 UP	0.8100	0.2717	0.5009	0.5275
LBV3 UP	0.7732	0.2314	0.4453	0.4833
LBV4 UP	0.6017	0.1818	0.3309	0.3715
LBV5 UP	0.5126	0.1215	0.2265	0.2869
Outlet Temperature 001	0.003788	0.007534	0.03211	0.01448

Table 5-7 shows the index of agreement values for the determined parameters in the model. The values for the outlet flowrate indicate that the model is able to determine the change in the flowrate with high accuracy given that the average index of agreement for the three time periods is 0.9335.

The goodness of fit for the inlet pressure shows that there is good agreement between the model and the data with an average index of agreement of 0.6913. The index of agreement for the pressures upstream of each valve show a decrease along the pipeline. This clearly indicates that the model is failing to predict the pressure drop along the pipeline. This discrepancy can be explained with the Darcy-Weisbach equation

$$\frac{\Delta p}{L} = f_D \times \frac{\rho}{2} \times \frac{v^2}{D}$$

*Equation 5-4: Darcy-Weisbach Equation*

The Darcy-Weisbach equation shows that the pressure drop along a pipeline is dependent on the density of the fluid. The density of the CO<sub>2</sub> is affected by the temperature of the fluid. The model determined outlet temperature is shown to have a low index of agreement which indicates that the density of the fluid in the model at this point would also show low agreement with the data and therefore explain why the pressure drop along the pipeline deviates from what is occurring.

## **5.6 Conclusion**

The development of the Shell Quest pipeline within gCCS has allowed for the specific gCCS CO<sub>2</sub> pipeline model to be compared to real industrial data. This has not been found in any of the current literature and is novel to this research. The pipeline was created in gCCS using the specific pipeline models, the use of historical pipeline data allowed for three scenarios to be simulated that covered three time periods in which the inlet flowrate of the CO<sub>2</sub> to the pipeline varied. The outputs from the model were then compared to the data, looking at temperature, pressure and flowrate. To analyse the differences between the model and the data a goodness of fit was determined through calculating the Index of Agreement. The Index of Agreement showed that the model was good at determining the outlet flowrate of the pipeline with a consistently high value across all three time periods that were modelled. The inlet pressure to the pipeline was also shown to have good agreement between the model and the data. The analysis did show that along the length of the pipeline the model deviates from the data with the Index of Agreement getting lower. There are two reasons for the model predictions of the pressure getting worse along the length of the pipeline, it could be either due to the temperature losses in the model along the pipeline being much lower than the real

data. This difference in fluid temperature effects the density of the CO<sub>2</sub> and therefore impacts on the pressure drop along the pipeline. The second possible reason for the pressure discrepancies is the difference between the friction factor in the model and the actual QUEST pipeline. Through this validation process it can be concluded that the gCCS model struggles to predict the temperature losses along the pipeline which has repercussions for determining the pressure drop. It has been argued that the reason behind this significant temperature difference between the model and the data is due to the thermal conductivity of the soil, as the model has predetermined values for each of the soil options. The accuracy of the model outputs could be improved by allowing the user to define the thermal conductivities of the soil which could be analytically determined for each case that is modelled.

## **Chapter 6 – Conclusions and Future Work**

## 6.1 Conclusions

The aims of the research presented in the thesis were to investigate the effects of changing the inlet flowrate of CO<sub>2</sub> into a pipeline for the purposes of carbon capture and storage, which would allow a greater understanding how a CCS transport system operates when attached to a load following power plant with CCS. The method to understand how the transport system responds when a step change occurs was carried out using the modelling tool gCCS, which was evaluated and concluded to be the most appropriate tool for the requirements of the research. The first stage of the modelling was to develop a base case scenario in which the outputs from more detailed scenarios could be compared. The second stage of the modelling was to look at the impacts of two important developments in the scenario; the first investigated the effects of impurities in the CO<sub>2</sub> on the dynamics of the model, the second scenario that was modelled examined the effects of a system with multiple sources of CO<sub>2</sub>. The final stage of the research was comparing the model outputs to the data from a real CCS pipeline in Canada, this allowed for a greater examination of the accuracy of the modelling tool.

### 6.1.1 Base case scenario

The base case scenario was set up in gCCS to investigate the effects of reducing the inlet flowrate from a single source of pure CO<sub>2</sub> on the pipeline dynamics. The following hypothesis was tested;

‘The gCCS model will show that the rate of change in the outlet flowrate of a CO<sub>2</sub> pipeline when the inlet flowrate is reduced, will be greater when the CO<sub>2</sub> is transported in the subcooled liquid phase compared to the supercritical phase’

Through analysis of the flowrate, temperature and pressure within the pipeline certain conclusions could be made about the modelling tools understanding of CO<sub>2</sub> pipeline transport:

- The effect of reducing the inlet flowrate to the pipeline was shown to have an impact on the pipeline outlet flowrate, with three distinct phases in the response being observed. The three phases have been referred to as the 'delayed response phase', the 'offset phase' and the 'final reduction phase'.
- The hypothesis was demonstrated to be correct and the phase of the CO<sub>2</sub> was shown to impact the response of the fluid within the pipeline when the inlet flowrate is reduced. CO<sub>2</sub> in the supercritical phase was shown to have a greater impact on the dynamics of the fluid in the pipeline when compared to CO<sub>2</sub> in the liquid phase.
- CO<sub>2</sub> in the supercritical phase was shown to cause a larger offset between the inlet and the outlet flowrate during the offset phase of the response to a change in the inlet flowrate.
- The modelling shows that there is a drop in the pressure of the CO<sub>2</sub> at the inlet and outlet of the pipeline when there is a reduction in the flowrate. The pressure change did not follow the same profile as the flowrate as there was no distinct phases during the fall in the flowrate with the outlet pressure drop following the same profile as the inlet pressure drop. When comparing the pressure profiles of supercritical and liquid phase CO<sub>2</sub> it was found that the inlet pipeline pressure for supercritical CO<sub>2</sub> was higher than when in the liquid phase. This was explained through the Darcy-Weisbach equation which shows that the flow velocity has a greater impact on the pressure drop than the density.

- The temperature at the outlet of the pipeline dropped sharply by 6°C when the flowrate was reduced but then increased during the ‘final reduction phase’ with a sharp gradient to the temperature before the flowrate change. The results from the simulation indicate that the temperature and flowrate are closely related and have been explained by the continuity equation however there is also the possibility that the results are a peculiarity of the modelling tool and the interactions between the underlying equations.

Overall the results from the simulations have shown that there should be no real technical difficulties between transporting CO<sub>2</sub> in the liquid phase or transporting it in the supercritical phase and that the decision on which phase would be preferred is down to economical considerations. However in cases where CO<sub>2</sub> is being bought or sold such as for enhanced oil recovery there may need to be some consideration given to the difference in flowrates between the inlet and the outlet of the pipeline when there is a step change in the flowrate as there may be discrepancies between the quantity of CO<sub>2</sub> that is thought to have been provided and what was actually provided .

#### 6.1.1 CO<sub>2</sub> with impurities scenario

Developing the scenario from the base case, the impact of different impurities in the CO<sub>2</sub> on the flow dynamics was investigated. Three impurities were studied, that are known to be present in the three main types of CO<sub>2</sub> capture technology. These impurities are; nitrogen, hydrogen and oxygen. To allow for a comparison with the base case results the composition of the fluid entering the pipeline was the only parameter that was changed, all other parameters in the model were kept constant. The hypothesis that was tested in this part of the research was as follows:



'The gCCS modelling tool will demonstrate that impurities within the carbon dioxide transported for CCS will cause a different response in the flowrate to changing the inlet flowrate compared to when transporting pure CO<sub>2</sub>'

Through the analysis of the results from the model the following conclusions were made regarding this scenario;

- The hypothesis was proven to be correct, in that the addition of any three of the impurities caused an observable difference in the response of the outlet flowrate when the inlet flowrate was reduced.
- The difference between the base case scenario and the scenario when impurities were introduced to the system was the size of the offset during the 'offset phase'. The addition of any of the impurities was shown to cause an increase in the offset between the inlet flowrate and the outlet flowrate. This phenomena could be explained with the effect of these impurities on the density of the CO<sub>2</sub> and therefore impacting on the flowrate at which the flow wave propagates through the pipeline. This is supported by the fact that there was a larger offset when CO<sub>2</sub> was transported in the supercritical phase, which also has a lower density than liquid CO<sub>2</sub>.
- When comparing the three impurities against each other it was found that hydrogen had the greatest impact on the offset, while oxygen had the least impact on the size of the offset when compared to the base case. It is believed that the reason for this difference is due to the difference in the molecular mass when compared to carbon dioxide. Hydrogen is the most different from carbon dioxide while oxygen is the most similar.

### 6.1.1 Multiple sources of CO<sub>2</sub> scenario

The final scenario that was modelled investigated the effects of two sources of CO<sub>2</sub> into a single pipeline. This scenario was investigated as it is expected that hubs of CO<sub>2</sub> sources will develop in the future which will eventually share transport infrastructure. If there is variability in the CO<sub>2</sub> output from any of these sources it is necessary to understand how this might impact on the entire transport infrastructure. For this scenario the following hypothesis was tested:

‘The gCCS modelling tool will show that that varying the flowrate of one of two sources of CO<sub>2</sub> will have a different effect on the flowrate of the CO<sub>2</sub> within the trunk pipeline, compared to when there is only a single source of CO<sub>2</sub>’

The analysis of the outputs from the modelling in gCCS resulted in the following conclusions regarding this scenario;

- The results from the modelling show that the hypothesis was incorrect and that there is no difference in the response of the flowrate when there are multiple sources of CO<sub>2</sub> then when there is a single source of CO<sub>2</sub> entering a pipeline.
- The flowrate profile at the inlet and the outlet of the trunk pipeline is the same as the base case scenario as the flowrate at the outlet of the branch pipeline has the same profile as the setpoint change. The difference in the flowrate profile of the branch pipeline and the trunk pipeline can be explained by the difference in either the pipeline diameter, pipeline length or the fluid flowrate.
- The change in the flowrate of one of the sources didn't cause any back flow in the branch pipeline of the other CO<sub>2</sub> source. However due to the method in which the software calculates the pressure, the pressure in the flowrate source was forced to reduce to ensure the reservoir pressure was stable. This is a limitation of the software

and is therefore knowledge gained about the use of gCCS rather than how the pipeline will actually respond when there are multiple sources of CO<sub>2</sub>.

#### 6.1.1 Modelling of the Shell QUEST CO<sub>2</sub> pipeline

Due to an arising opportunity during the research, real CO<sub>2</sub> pipeline data was able to be obtained from the Shell QUEST CCS pipeline. A flowsheet was developed in gCCS that represented the QUEST pipeline with the same pipeline dimensions, topology and fluid parameters. Historical data was then used to develop a simulation that could then be directly compared to the pipeline data. To evaluate how well the gCCS model predicts the variables of interest a statistical value known as the Index of Agreement was used. The index of agreement was determined for each variable of interest to understand the goodness of fit between the model and the industrial data. The following conclusions were developed;

- The model was able to predict with a high degree of accuracy the outlet flowrates of the pipeline with an average Index of agreement value of 0.9335. However, observation of the QUEST pipeline data indicated that the three separate phases that were predicted by the model do not occur.
- The model was able to predict the pressure at the inlet of the pipeline with a reasonable degree of accuracy with a mean index of agreement of 0.6913. However the further along the pipeline, the accuracy of the model got increasingly worse with a declining index of agreement along the length of the pipeline. This indicates that the model has difficulty in determining the pressure drop along the pipeline when there is a change in flowrate at the inlet of the pipeline. The reason behind this difference can be attributed the friction factor, from the Darcy-Weisbach equation the pressure drop

along the pipeline is a function of the friction factor and is the only parameter in the equation that there could be a discrepancy between the model and the actual pipeline.

- There was a significant difference between the pipeline data and the model predictions when determining the temperature loss along the pipeline. The mean value for the index of agreement was 0.01448, meaning that the model was not able to predict the temperature at the outlet of the pipeline with any degree of accuracy. The reasoning behind this discrepancy between the QUEST data and the model is that the thermal conductivity of the soil surrounding the pipeline is understood to be variable depending on the composition of the soil. Since the model does not allow the user to define the thermal conductivity of the surrounding soil the model is limited and therefore cannot take into account varying soil types, which can lead to differences in the heat loss between the model and the actual pipeline being modelled.

## **6.2 Future Work**

The research has shown that the phase of the CO<sub>2</sub> effects the way in which the CO<sub>2</sub> in the pipeline responds, that the presence of impurities effects the offset between the inlet and the outlet of the pipeline and that multiple sources of CO<sub>2</sub> does not impact on the way in which the outlet flowrate reacts to a change in the inlet flowrate. There are two areas in which further research needs to be conducted to improve the developments in CO<sub>2</sub> pipeline transportation. The first being the scenarios which are modelled and the second the improvements to the gCCS modelling tool.

### **6.2.1 Further scenarios analysis**

The research carried out investigated three scenarios of CO<sub>2</sub> pipeline transport. The first scenario was developed a base case scenario which other scenarios could be compared to. The second scenario investigated the effects of impurities in the CO<sub>2</sub> on the flowrate

dynamics and the third scenario examined how multiple sources of CO<sub>2</sub> effect the flowrate. Future work will take the scenarios further and investigate the impacts of other parameters on the flowrate of CO<sub>2</sub>. The areas which should be investigated are those that further represent real CO<sub>2</sub> pipeline infrastructures, such as;

- *Multiple sequestration sites.* Within this study, the impact of multiple sources of CO<sub>2</sub> on the flowrate within a pipeline were investigated however it is also anticipated that there will be multiple wells which the CO<sub>2</sub> is delivered to and is therefore an area of research that would further inform the operation of CCS transport infrastructures.
- *Varying pipeline diameters.* Within the modelling, certain parameters were kept constant throughout each scenario, this included the pipeline diameter. It is likely that for different CCS projects different pipeline diameters will be required based upon technical and economic factors. It is therefore necessary to develop a greater understanding of how the pipeline diameter effects the flow of CO<sub>2</sub> when there are variable inlet flows.
- *Offshore pipelines.* For all scenarios investigated the modelling looked specifically at onshore pipelines. Given that offshore storage of CO<sub>2</sub> is most likely to be used within the U.K. it will be essential to understand how CO<sub>2</sub> flows within offshore pipelines given that the surrounding material of the pipeline will be significantly different to onshore pipelines which may affect the heat transfer of the CO<sub>2</sub>.

#### 6.2.1 gCCS model development

From the validation work carried out with the support of the Shell QUEST project, suggestions for improvements to the modelling tool gCCS are able to be made. Throughout the research the temperature profile in the pipeline reacted the least intuitive and had the greatest disagreement with the data from the QUEST pipeline compared to all other variables. It has been suggested that the reason behind this is due to the thermal conductivity of the surrounding material of the pipeline, which is pre-defined within the model. Allowing an extra degree of freedom so that the user can define the thermal conductivity of the surrounding material would allow for greater accuracy when the model attempts to determine the heat loss or gain of the CO<sub>2</sub>. This could significantly improve the model in determining the temperature of the CO<sub>2</sub> for real CCS pipeline projects.

## **Appendix A      Simulation Code**

### **A.1 Code for Base Case and Impurities Case**

SEQUENCE

CONTINUE FOR 30

REASSIGN

Flowsheet.Source\_CO2001.F:=OLD(Flowsheet.Source\_CO2001.F)-50\*(Time-30)/750;

END

CONTINUE FOR 750

REASSIGN

Flowsheet.Source\_CO2001.F:=OLD(Flowsheet.Source\_CO2001.F);

END

CONTINUE FOR 500000

REASSIGN

Flowsheet.Source\_CO2001.F:=OLD(Flowsheet.Source\_CO2001.F);

END

## **Appendix B                      Simulation Code**

### **B.1 Code for Multiple CO<sub>2</sub> Sources Case**

SEQUENCE

CONTINUE FOR 30

REASSIGN

Flowsheet.Source\_CO2001.F:=OLD(Flowsheet.Source\_CO2001.F)-25\*(Time-30)/375;

END

CONTINUE FOR 375

REASSIGN

Flowsheet.Source\_CO2001.F:=OLD(Flowsheet.Source\_CO2001.F);

END

CONTINUE FOR 500000

REASSIGN

Flowsheet.Source\_CO2001.F:=OLD(Flowsheet.Source\_CO2001.F);

END



## Appendix C                      Simulation Code

### C.1 Code for Shell QUEST Simulation for Time Period 24/10/15 – 28/10/15

SCHEDULE

SEQUENCE

CONTINUE FOR 30

REASSIGN

Flowsheet.Source\_CO2001.F := OLD(Flowsheet.Source\_CO2001.F) - 7.6\*(TIME - 30)/9960;

END

CONTINUE FOR 9960

REASSIGN

Flowsheet.Source\_CO2001.F := OLD(Flowsheet.Source\_CO2001.F) ;

END

CONTINUE FOR 122400

REASSIGN

Flowsheet.Source\_CO2001.F := OLD(Flowsheet.Source\_CO2001.F) + 8.4\*(TIME - 132390)/23880;

END

CONTINUE FOR 23880

REASSIGN

Flowsheet.Source\_CO2001.F := OLD(Flowsheet.Source\_CO2001.F) ;

END

CONTINUE FOR 200000

END

## C.2 Code for Shell QUEST Simulation for Time Period 31/10/15 – 04/11/15

### SCHEDULE

#### SEQUENCE

CONTINUE FOR 30

REASSIGN

Flowsheet.Source\_CO2001.F := OLD(Flowsheet.Source\_CO2001.F) - 8\*(TIME - 30)/7200;

END

CONTINUE FOR 7200

REASSIGN

Flowsheet.Source\_CO2001.F := OLD(Flowsheet.Source\_CO2001.F) ;

END

CONTINUE FOR 109728

REASSIGN

Flowsheet.Source\_CO2001.F := OLD(Flowsheet.Source\_CO2001.F) + 8\*(TIME - 116958)/21600;

END

CONTINUE FOR 21600

REASSIGN

Flowsheet.Source\_CO2001.F := OLD(Flowsheet.Source\_CO2001.F) ;

END

CONTINUE FOR 200000

END

### **C.3 Code for Shell QUEST Simulation for Time Period 08/11/15 – 11/11/15**

SEQUENCE

CONTINUE FOR 30

REASSIGN

Flowsheet.Source\_CO2001.F := OLD(Flowsheet.Source\_CO2001.F) - 8.25\*(TIME - 30)/18900;

END

CONTINUE FOR 18900

REASSIGN

Flowsheet.Source\_CO2001.F := OLD(Flowsheet.Source\_CO2001.F) ;

END

CONTINUE FOR 68640

REASSIGN

Flowsheet.Source\_CO2001.F := OLD(Flowsheet.Source\_CO2001.F) + 7.0024\*(TIME - 87570)/25740;

END

CONTINUE FOR 24740

REASSIGN

Flowsheet.Source\_CO2001.F := OLD(Flowsheet.Source\_CO2001.F) ;

END

CONTINUE FOR 200000

END

## References

1. Agency, I.E., *Technology Roadmap: Carbon capture and storage*. 2013.
2. Day, G., *Building the UK carbon capture and storage sector by 2030 - Scenarios and actions*. 2015, Energy Technologies Institute.
3. J.T. Houton, G.J.J., J. J. Ephraums, *Climate Change: The IPCC Scientific Assessment*. 1990.
4. IPCC, *Climate Change 2007: Synthesis Report*. 2007, IPCC: Geneva, Switzerland.
5. Anderson, T.R., E. Hawkins, and P.D. Jones, *CO<sub>2</sub>, the greenhouse effect and global warming: from the pioneering work of Arrhenius and Callendar to today's Earth System Models*. Endeavour, 2016. **40**(3): p. 178-187.
6. *2015 UK greenhouse gas emissions: final figures - statistical summary*, E.I.S. Department for Business, Editor. 2017.
7. Milne, S., *Options Choices Actions - UK scenarios for a low carbon energy system*. 2015, Energy Technologies Institute.
8. Newton-Cross, G. and D. Gammer, *The evidence for deploying bioenergy with CCS (BECCS) in the UK*. 2016, Energy Technologies Institute.
9. Leung, D.Y.C., G. Caramanna, and M.M. Maroto-Valer, *An overview of current status of carbon dioxide capture and storage technologies*. Renewable and Sustainable Energy Reviews, 2014. **39**: p. 426-443.
10. Association, C.C.a.S. *What is CCS?* [cited 2016 5th November]; Available from: <http://www.ccsassociation.org/what-is-ccs/>.
11. Intergovernmental Panel on Climate Change, *Special Report on Carbon Dioxide Capture and Storage*. 2005: Cambridge, UK.
12. Liang, Z., et al., *Review on current advances, future challenges and consideration issues for post-combustion CO<sub>2</sub> capture using amine-based absorbents*. Chinese Journal of Chemical Engineering, 2016. **24**(2): p. 278-288.
13. IEAGHG, *Assessment of Emerging CO<sub>2</sub> Capture Technologies and their Potential to Reduce Costs*. 2014.
14. Global CCS Institute, *The Global Status of CCS: 2011*. 2011: Canberra, Australia.
15. Wang, M., et al., *Post-combustion CO<sub>2</sub> capture with chemical absorption: A state-of-the-art review*. Chemical Engineering Research and Design, 2011. **89**(9): p. 1609-1624.
16. Jansen, D., et al., *Pre-combustion CO<sub>2</sub> capture*. International Journal of Greenhouse Gas Control, 2015. **40**: p. 167-187.
17. Uchida, T., et al., *Oxyfuel Combustion as CO<sub>2</sub> Capture Technology Advancing for Practical use - callide Oxyfuel Project*. Energy Procedia, 2013. **37**: p. 1471-1479.
18. Modekurti, S., et al., *Design, dynamic modeling, and control of a multistage CO<sub>2</sub> compression system*. International Journal of Greenhouse Gas Control, 2017. **62**: p. 31-45.
19. Pei, P., et al., *Waste heat recovery in CO<sub>2</sub> compression*. International Journal of Greenhouse Gas Control, 2014. **30**: p. 86-96.
20. Institute, G.C. *Large-scale CCS facilities*. [cited 2016 10th July]; Available from: <https://www.globalccsinstitute.com/projects/large-scale-ccs-projects>.
21. SaskPower. *Boundary Dam Carbon Capture Project*. [cited 2016 23rd July]; Available from: <http://www.saskpower.com/our-power-future/carbon-capture-and-storage/boundary-dam-carbon-capture-project/>.
22. Energy, O.o.F. *Petra Nova - W.A. Parish Project*. [cited 2016 23rd July]; Available from: <https://energy.gov/fe/petra-nova-wa-parish-project>.
23. Paul, S., R. Shepherd, and P. Woolin, *Selection of materials for high pressure CO<sub>2</sub> transport*, in *Third International Forum on the Transportation of CO<sub>2</sub> by Pipeline*. 2012: Newcastle, UK.
24. Aspelund, A., M.J. Møltnvik, and G. De Koeijer, *Ship Transport of CO<sub>2</sub>*. Chemical Engineering Research and Design, 2006. **84**(9): p. 847-855.
25. platform, Z.e., *The Costs of CO<sub>2</sub> Capture, Transport and Storage*.

26. Svensson, R., et al., *Transportation systems for CO<sub>2</sub>—application to carbon capture and storage*. Energy Conversion and Management, 2004. **45**(15): p. 2343-2353.
27. Technology, M.I.o. *Peterhead Project Fact Sheet: Carbon Capture and Storage Project*. [cited 2016 28th July]; Available from: <https://sequestration.mit.edu/tools/projects/peterhead.html>.
28. McCoy, S.T. and E.S. Rubin, *An engineering-economic model of pipeline transport of CO<sub>2</sub> with application to carbon capture and storage*. International Journal of Greenhouse Gas Control, 2008. **2**(2): p. 219-229.
29. GHG), I.G.G.R.D.P.I., *Upgraded calculator for CO<sub>2</sub> pipeline systems*. 2009.
30. Noothout, P., et al., *CO<sub>2</sub> Pipeline Infrastructure – Lessons Learnt*. Energy Procedia, 2014. **63**: p. 2481-2492.
31. Ghazi, N. and J.M. Race, *Techno-economic modelling and analysis of CO<sub>2</sub> pipelines*. The Journal of Pipeline Engineering, 2013. **12**(2): p. 83-92.
32. Institute, G.C., *IEAGHG, Building the cost curves for CO<sub>2</sub> storage; European Sector*. 2005.
33. Ecofys, *Global carbon dioxide storage potential and costs*. 2004.
34. IEAGHG, *Transmission of CO<sub>2</sub> and Energy*. 2002.
35. Brown, S., et al., *Modelling the non-equilibrium two-phase flow during depressurisation of CO<sub>2</sub> pipelines*. International Journal of Greenhouse Gas Control, 2014. **30**: p. 9-18.
36. Martynov, S., et al., *Modelling three-phase releases of carbon dioxide from high-pressure pipelines*. Process Safety and Environmental Protection, 2014. **92**(1): p. 36-46.
37. M. Bilio, S.B., M. Fairweather, H Mahgerefteh, *CO<sub>2</sub> pipelines material and safety considerations*, in *IChemE Symposium*. 2009, Institute of Chemical Engineers.
38. Ibrahim, M. and I.S. Ertesvåg, *PVTx Modeling of CO<sub>2</sub> Pipeline at Depressurization Conditions Using SPUNG Equation of State (EoS) with a Comparison to SRK*. Energy Procedia, 2014. **63**: p. 2467-2474.
39. Clausen, S., A. Oosterkamp, and K.L. Strøm, *Depressurization of a 50 km Long 24 inches CO<sub>2</sub> Pipeline*. Energy Procedia, 2012. **23**: p. 256-265.
40. Kaufmann, D.K.-D., *Carbon Dioxide Transport in Pipelines - Under Special Consideration of Safety-Related Aspects*, in *3rd Pipeline Technology Conference 2008*. 2008: Hannover, Germany.
41. Zhang, Z.X., et al., *Optimization of pipeline transport for CO<sub>2</sub> sequestration*. Energy Conversion and Management, 2006. **47**(6): p. 702-715.
42. Witkowski, A, R.A., Majkut, M, Stolecka, K, *The Analysis of Pipeline Transportation Process for CO<sub>2</sub> Captured From Reference Coal-Fired 900 MW Power Plant to Sequestration Region*. Chemical and Process Engineering, 2014. **35**: p. 497-514.
43. Witkowski, A. and M. Majkut, *Analysis of Transportation Systems for CO<sub>2</sub> Sequestration*, in *Advances in Carbon Dioxide Compression and Pipeline Transportation Processes*. 2015, Springer International Publishing: Cham. p. 73-93.
44. Nimtz, M., et al., *Modelling of the CO<sub>2</sub> process- and transport chain in CCS systems—Examination of transport and storage processes*. Chemie der Erde - Geochemistry, 2010. **70**: p. 185-192.
45. Kunz, O. and G. Groupe Européen de Recherches, *The GERG-2004 wide-range equation of state for natural gases and other mixtures*. 2007, Düsseldorf: VDI Verlag.
46. Liljemark, S., et al., *Dynamic simulation of a carbon dioxide transfer pipeline for analysis of normal operation and failure modes*. Energy Procedia, 2011. **4**: p. 3040-3047.
47. Luo, X., et al., *Simulation-based techno-economic evaluation for optimal design of CO<sub>2</sub> transport pipeline network*. Applied Energy, 2014. **132**: p. 610-620.
48. Technology, M.I.o. *Don Valley Power Project Fact Sheet: Carbon Dioxide Capture and Storage Project*. [cited 2016 9th August]; Available from: [https://sequestration.mit.edu/tools/projects/don\\_valley.html](https://sequestration.mit.edu/tools/projects/don_valley.html).
49. Technology, M.I.o. *White Rose\* Project Fact Sheet: Carbon Dioxide Capture and Storage Project* (\*Formerly UK Oxy CCS Project). Available from: [https://sequestration.mit.edu/tools/projects/white\\_rose.html](https://sequestration.mit.edu/tools/projects/white_rose.html).
50. Chapoy, A., et al., *Effect of impurities on thermophysical properties and phase behaviour of a CO<sub>2</sub>-rich system in CCS*. International Journal of Greenhouse Gas Control, 2013. **19**: p. 92-100.

51. Cole, I.S., et al., *Corrosion of pipelines used for CO<sub>2</sub> transport in CCS: Is it a real problem?* International Journal of Greenhouse Gas Control, 2011. **5**(4): p. 749-756.
52. Dugstad, A., M. Halseid, and B. Morland, *Experimental Techniques used for Corrosion Testing in Dense Phase CO<sub>2</sub> with Flue Gas Impurities*, in *CORROSION 2014*. 2014, NACE International: San Antonio, Texas, USA.
53. Technology, I.f.E. *The history of OLGA*. [cited 2016 9th August]; Available from: [https://www.ife.no/en/ife/departments/process\\_and\\_fluid\\_flow\\_tech/historienomolga](https://www.ife.no/en/ife/departments/process_and_fluid_flow_tech/historienomolga).
54. Schlumberger. *OLGA Dynamic Multiphase Flow Simulator*. [cited 2016 11th August]; Available from: <https://www.software.slb.com/products/olga>.
55. Schlumberger. *Case Study: BP Saves 12 Days of Downtime and 6,000-m<sup>3</sup> Diesel Managing Deepwater Pipeline with the OLGA Simulator*. [cited 2016 16th August]; Available from: [http://www.slb.com/resources/case\\_studies/software/cs\\_bp\\_olga\\_deepwater\\_pipeline.aspx](http://www.slb.com/resources/case_studies/software/cs_bp_olga_deepwater_pipeline.aspx).
56. Span, R. and W. Wagner, *A New Equation of State for Carbon Dioxide Covering the Fluid Region from the Triple-Point Temperature to 1100 K at Pressures up to 800 MPa*. Journal of Physical and Chemical Reference Data, 1996: p. Medium: X; Size: pp. 1509-1596.
57. Giljarhus, K.E.T., S.T. Munkejord, and G. Skaugen, *Solution of the Span–Wagner Equation of State Using a Density–Energy State Function for Fluid-Dynamic Simulation of Carbon Dioxide*. Industrial & Engineering Chemistry Research, 2012. **51**(2): p. 1006-1014.
58. Leachman, J., et al., *Thermodynamic Properties of Cryogenic Fluids*. 2 ed. International Cryogenics Monograph Series. 2017: Springer International Publishing. 213.
59. Witkowski, A. M.M., Rulik, S, *Analysis of pipeline transportation systems for carbon dioxide sequestration*. Archives of Thermodynamics 2014. **35**(1): p. 117-140.
60. L, R., *CO<sub>2</sub> Transportation with Pipelines - Model Analysis for Steady, Dynamic and Relief Simulation*. The Italian Association of Chemical Engineering, 2014. **36**: p. 619-624.
61. Demetriades, T.A. and R.S. Graham, *A new equation of state for CCS pipeline transport: Calibration of mixing rules for binary mixtures of CO<sub>2</sub> with N<sub>2</sub>, O<sub>2</sub> and H<sub>2</sub>*. The Journal of Chemical Thermodynamics, 2016. **93**: p. 294-304.
62. Fandiño, O., J.P.M. Trusler, and D. Vega-Maza, *Phase behavior of (CO<sub>2</sub>+H<sub>2</sub>) and (CO<sub>2</sub>+N<sub>2</sub>) at temperatures between (218.15 and 303.15)K at pressures up to 15MPa*. International Journal of Greenhouse Gas Control, 2015. **36**: p. 78-92.
63. Economou, I.G., *Statistical Associating Fluid Theory: A Successful Model for the Calculation of Thermodynamic and Phase Equilibrium Properties of Complex Fluid Mixtures*. Industrial & Engineering Chemistry Research, 2002. **41**(5): p. 953-962.
64. Diamantonis, N. E.I., *Evaluation of SAFT and PC-SAFT EoS for the calculation of thermodynamic derivative properties of fluids related to carbon capture and sequestration*, CO<sub>2</sub>PipeHaz, Editor. 2011: Energy & Fuels.
65. Islam, A.W. and E.S. Carlson, *Application of SAFT equation for CO<sub>2</sub>+H<sub>2</sub>O phase equilibrium calculations over a wide temperature and pressure range*. Fluid Phase Equilibria, 2012. **321**: p. 17-24.
66. Diamantonis, N.I., et al., *Evaluation of Cubic, SAFT, and PC-SAFT Equations of State for the Vapor–Liquid Equilibrium Modeling of CO<sub>2</sub> Mixtures with Other Gases*. Industrial & Engineering Chemistry Research 2013. **52**(10): p. 3933-3942.
67. Florides, G. and S. Kalogirou, *Measurements of Ground Temperatures at Various Depths*. 2004.
68. Johansen, O., *Thermal Conductivity of Soils*. 1977, U.S. Army Cold Regions Research and Engineering Laboratory.
69. Bratland, O., *Single-phase Flow Assurance*. 2009. 341.
70. Institute, E., *Good Plant Design And Operation For Onshore Carbon Capture Installations And Onshore Pipelines*. 2010, Energy Institute London.
71. Peplinski, S. *QUEST CCS PROJECT*. in *PCCC2 Conference*. 2013. Bergen, Norway.
72. Peters, D., *Pipelines Flow and Flow Assurance Report - Final*. 2014.
73. *Climate: FORT SASKATCHEWAN*. 2015 [cited 2015 November 19]; Available from: <https://en.climate-data.org/location/949/>.

74. Endress+Hauser. *Absolute and gauge pressure Cerabar PMP71*. [cited 2016 March 23]; Available from: <https://www.uk.endress.com/en/Field-instruments-overview/pressure/Absolute-Gauge-Cerabar-PMP71>.
75. Farouki, O.T., *Thermal properties of soil*. 1981, U.S. Army Cold Regions Research and Engineering Laboratory.